INTERACTIONS VIA ELECTRICAL COUPLING IN AXIAL AND APPENDICULAR MOTOR NETWORKS DURING METAMORPHOSIS IN XENOPUS LAEVIS

Monica Anne Wagner

A Thesis Submitted for the Degree of MPhil
at the
University of St Andrews

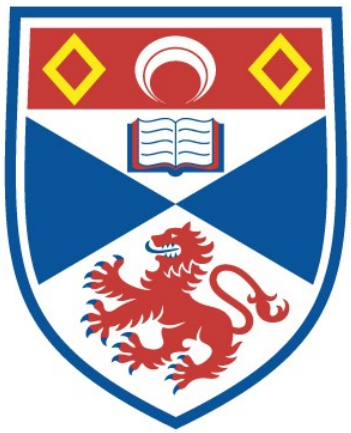

2017

Interactions via electrical coupling in axial and appendicular motor networks during metamorphosis in *Xenopus laevis* tadpoles

Monica Anne Wagner

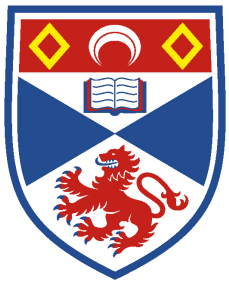

University of
St Andrews

This thesis is submitted for the degree of Master of Philosophy in Neuroscience at the University of St Andrews

School of Psychology and Neuroscience
University of St Andrews
Fife
KY16 9JP

September 2016

1. CANDIDATE'S DECLARATIONS:

I, Monica Anne Wagner, hereby certify that this thesis, which is approximately 19,300 words in length, has been written by me, and that it is the record of work carried out by me, or principally by myself in collaboration with others as acknowledged, and that it has not been submitted in any previous application for a higher degree.

I was admitted as a research student in September 2013 and as a candidate for the degree of MPhil in September 2015; the higher study for which this is a record that was carried out in the University of St Andrews between 2013 and 2016.

Date …… signature of candidate ……

2. Supervisor's declaration:

I hereby certify that the candidate has fulfilled the conditions of the Resolution and Regulations appropriate for the degree of MPhil in the University of St Andrews and that the candidate is qualified to submit this thesis in application for that degree.

Date …… signature of supervisor ……

3. Permission for publication: (*to be signed by both candidate and supervisor*)

In submitting this thesis to the University of St Andrews I understand that I am giving permission for it to be made available for use in accordance with the regulations of the University Library for the time being in force, subject to any copyright vested in the work not being affected thereby. I also understand that the title and the abstract will be published, and that a copy of the work may be made and supplied to any bona fide library or research worker, that my thesis will be electronically accessible for personal or research use unless exempt by award of an embargo as requested below, and that the library has the right to migrate my thesis into new electronic forms as required to ensure continued access to the thesis. I have obtained any third-party copyright permissions that may be required in order to allow such access and migration, or have requested by the appropriate embargo below.

The following is an agreed request by candidate and supervisor regarding the publication of this thesis:

PRINTED COPY

Embargo on all of the print copy for a period of 1 year on the following grounds:

- Publication would preclude future publication

ELECTRONIC COPY

Embargo on all of the electronic copy for a period of 1 year on the following grounds:

- Publication would preclude future publication

Date…… signature of candidate ……

signature of supervisor ……

Please note initial embargos can be requested for a maximum of five years. An embargo on a thesis submitted to the Faculty of Science or Medicine is rarely granted for more than two years in the first instance, without good justification. The Library will not lift an embargo before confirming with the student and supervisor that they do not intend to request a continuation. In the absence of an agreed response from both student and supervisor, the Head of School will be consulted. Please note that the total period of an embargo, including any continuation, is not expected to exceed ten years.
Where part of a thesis is to be embargoed, please specify the part and the reason.

Dedicated to and in loving memory of
Eberhard Henry Uhlenhuth

15 September 1927 - 7 June 2016

Physician, Scientist, Grandfather, Mentor, Friend

Thank you for fostering my scientific curiosity and encouraging critical thinking in all aspects of my life.

ACKNOWLEDGEMENTS

First and foremost, I would like to thank my supervisor, Professor Keith Sillar, without whom this project would not have been possible. I have the utmost respect for his vast wisdom and technical prowess, and I can always count on his sage advice and the fact that he makes his students feel like they are a priority. Keith: you have truly pushed me to be a better version of myself whilst simultaneously showing unwavering support through various personal challenges that were thrown my way; and for this, I am grateful.

I would also like to thank present and past members of the Sillar Lab for their instruction, patience, and support. Laurence: thank you for always being there to answer all of my questions, no matter how trivial; you were definitely a rock throughout this entire graduate experience. Whenever I listen to the weekly BBC Travelling Folk radio programme, I will always remember how much I appreciate the time we spent together in lab. And no matter where I end up in the world, Scotland will always feel a little bit closer! I cannot forget to thank HongYan, Stephen, and our collaborator from Bordeaux, Denis (aka the magician): I am indebted to your kindness and the time you spent teaching me dissections, discussing concepts and showing me around the lab. Also a big thanks to everyone in the B15 office and SCAM – your enthusiasm for your own work kept me focussed and driven.

It is also necessary to express my appreciation to the animal house and workshop technicians. In particular, Isobel has always been a hard-working ally, keeping the tadpoles healthy and ready to go. And this experience was made more enjoyable as it was punctuated by her holiday cheer and birthday-cake-baking magic.

And last but certainly not least, I would like to express gratitude to my family and friends, especially: mom, dad, Rebecca, Alonzo, Pam, Dan and Riho. Your encouragement and support has been integral to my success. Thank you for being happy with me through the good times, and keeping me sane when things seemed impossible. Your high value of knowledge and its acquisition has strengthened my own.

TABLE OF CONTENTS

LIST OF FIGURES

I. INTRODUCTION

II. METHODS

III. RESULTS

ABBREVIATIONS

18-B-GA 18-β-glycerrhetinic acid
5-HT Serotonin
5-HTP 5-Hydroxytryptophan
ACH Acetylcholine
AIN Ascending Inhibitory Interneuron
CA^{2+} Calcium
CBNX Carbenoxolone disodium salt
CINS Commissural Reciprocal Inhibitory Interneuron
CNS Central Nervous System
CPG Central Pattern Generator
CX Connexin
DA Dopamine
DIA Dorsolateral Sensory Interneuron
DIC Dorsolateral Commissural Sensory Interneuron
DIN Descending Excitatory Interneuron
DINR Descending Repetitive Excitatory Interneuron
DMSO Dimethylsulfoxide
ECIN Excitatory Commisural Sensory Interneuron
ECIN Flufenamic Acid
HCG Human Chorionic Gonadotropin
HRP Horseradish Peroxidase
IPSP Inhibitory Postsynaptic Potential
GJ Gap Junction
KA Kolmer-Agdjur Neuron
KDA Kilodalton
LMC Lateral Motor Column
MLR Mesencephalic Locomotor Region
MMC Medial Motor Column
MN Motoneuron
MW Molecular Weight
NA Noradrenaline
NF Nieuwkoop & Faber
NMJ Neuromuscular Junction
NO Nitric Oxide
NOS Nitric Oxide Synthase
OPN5 Opsin 5
PBS Phosphate Buffered Saline
PMN Primary Motoneuron
PFA Paraformaldehyde
SEM Standard Error of the Mean
SK1 Schedule I Kill
SMN Secondary Motoneuron
RA Retinoid Acid
RANAS RANA saline
RB Rohan Beard Cell
T3 Triiodothyronine
T4 Thyroxine
TH Thyroid Hormone
USAHP Ultraslow Afterhyperpolarisation
VR Ventral Root

ABSTRACT

The spinal locomotor networks in *Xenopus laevis* frog tadpoles undergo a remarkable transformation during metamorphosis to accommodate a switch from axial-based swimming to a limb-based kicking locomotor strategy. For a brief period during ontogeny, both the axial- and limb-based systems are present and functional, but reliant on different central pattern generators (CPGs) that are simultaneously active. However, the mechanisms controlling the functional coupling both within and between these locomotor networks are unknown. At metamorphosing larval stages (52-58), retrograde motoneuron (MN) backfilling from both axial (11^{th}-12^{th} post-otic segments) and hindlimb muscles with fluorescent rhodamine- and fluorescein-conjugated dextran dyes revealed two discrete MN populations (axial and appendicular) within the spinal cord. The co-labelling of both axial and appendicular cells provides evidence that the two MN pools in the lumbar enlargement are coupled. Electrophysiological data from animals at the same larval stages suggest that axial CPG excitability is modified as burst durations were increased by gap junction (GJ) blockers (18-β-glycyrrhetinic **(**18-β-GA**)** acid 100μM; CBNX 200μM), however, limb CPG burst parameters were not altered by GJ block. For spontaneous fictive locomotor bouts, the number of axial episodes initially increased, but then sharply decreased from control levels ~15-30 minutes after drug application. Coordinated and simultaneous axial and limb CPG output was observed with electrical stimulation to the optic tectum, an axial ventral root (VR), and a limb VR; GJ block did not affect the coordinated output from optic tectum stimulation, however, it decreased simultaneous output when the axial VR was stimulated. This novel finding that antidromic stimulation of an axial VR is sufficient to activate a different CPG for the limbs suggests there is synaptic coupling in the direction of axial to limb. These data suggest that axial CPG output is in part regulated by GJs. The anatomical data also suggest a connection exists between the axial and limb MN pools, and may be involved in the initial cycle-by-cycle coupling of the two CPG outputs. Thus the rhythm of the appendicular CPG is initially highly dependent on that of the axial CPG, which in turn is dependent on its own GJ connections within the spinal circuit. It appears that the immature limb MN pools in the lumbar spinal cord possess functional connections via electrical synapses to the axial locomotor system, which are presumably "pruned" as metamorphosis proceeds, and eventually lost completely by the adult stages when the limb network has become completely independent.

I. Introduction

Ia. Amphibian Metamorphosis: the emergence of the appencidular locmotor network

The development of anuran amphibians, such as in the South African clawed frog, *Xenopus laevis*, takes place in three main phases: the first being embryogenesis, which occurs prior to a free-feeding existence and before the formation of a functional thyroid gland. The second, larval, phase includes metamorphosis; and this is the transformation of a larval tadpole into the third adult (frog) phase. This transition from larva to juvenile adult is wholly dependent on adequate levels of thyroid hormone (TH) in the plasma (Dodd & Dodd, 1976; Shi, 2000; Shi, 2001). *Xenopus* tadpoles undergo an extensive and dramatic transformation of virtually all bodily systems from larval to adult forms during metamorphosis (Shi, 2000). The metamorphic transition is directed by THs triggering a restructuring of the musculoskeletal system with the resorption of its tail and its transfiguration into a quadruped (Galton, 1992; Bishop and Brandhorst, 2003). Specifically, thyroxine (T4) and triiodothyronine (T3), both produced by the thyroid gland, are in control of triggering metamorphosis; and the concentration of these THs increases as metamorphosis advances until stage 66 at metamorphic climax, when a sharp decrease in TH levels is seen (Shi, 2000; Leloup & Buscaglia, 1977). Although metamorphosis is not unique to anurans such as *Xenopus*, it occurs whilst the animal is continually exposed to the environment (as opposed to metamorphoses undergone by, for example, insects isolated in cocoons (Blossman-Myer & Burggren, 2010)). *Xenopus* tadpoles must therefore mature gradually, as the animal is required to remain fully functional in its environment throughout this process. This is a physiologically demanding period, which includes the emergence and reconfiguration of locomotor neural circuitry.

To develop to maturity, the tadpole must be able to adapt its behaviour constantly to changes encountered in its environment, and this requires changes to the underlying neural control systems. This high degree of plasticity in the nervous system must involve not only the development of new networks to serve new or altered structures (e.g., limbs and their neuromuscular circuitry), but also the re-wiring of pre-existing ones (e.g., axial circuitry) (Rauscent, 2008). The appearance and control of limb buds during metamorphosis adds an extra dimension of spinal circuit complexity than just the need to control the main axial muscles required for anguilliform swimming in younger larvae (Roberts, 2012). The metamorphic transition in *Xenopus* necessarily therefore requires a fundamental change in locomotor strategy; as the tail regresses in adult animals, the trunk undulations which propelled the larvae are superseded by coordinated and rhythmic bilateral hindlimb kicks from successive flexor-extensor activation cycles (Combes et al., 2004; Rauscent, 2008; Sillar et al., 2008). *Xenopus* is exceptional as, for a short time during maturation, both the axial and limb motor systems are present and have the ability to function simultaneously (Combes et al., 2004).

Combes et al. (2004) and Sillar et al. (2008) have suggested how the coexistence and functionality of these axial and appendicular systems in the spinal cord during this period might be accommodated. The axial neuronal circuit responsible for rhythmic swimming output is called a central pattern generator (CPG). In the pre-metamorphic and pro-metamorphic *Xenopus* tadpole, there is circumstantial electrophysiological evidence of electrical coupling between the axial and appendicular systems, whereby the emergent limb-kicking CPG rises from the established tail CPG, providing anguilliform movement with rostrocaudal delay (Combes et al., 2004) (Fig. 1). In the midst of metamorphosis (from

Nieuwkoop & Faber (NF) stage ~58), ventral root (VR) recordings of lumbar activity show that appendicular motor bursts are rhythmically modulated during ongoing tail-root bursting, with ipsilateral flexor and extensor motoneuron (MN) activity bursting alternating with contralateral limb and tail-root bursting. Flexor-extensor co-activation and left-right limb alternation are the opposite to how the limbs will eventually be coordinated in the juvenile adult. One possible explanation for this unusual interim mode of coordination is that emerging limb network neurons are electrically coupled to the axial system via gap junctions (GJs; reviewed below in Section 1b, below). Initially this would provide coincident rhythmic output, as metamorphosis progresses, the rhythms generated by the axial and appendicular CPGs then gradually diverge, such that they are completely separate by metamorphic climax. Indeed, the appendicular CPG then supersedes that of the axial, as adult *Xenopus* no longer locomote via undulatory propulsions of the tail, but instead use the hindlimbs to drive successive flexion-extension kick cycles. Although it is known that the mature axial system (corresponding to postural muscles in the adult) interacts with the mature appendicular system in the adult (Beyeler et al., 2008), the cellular and inter-system bases for this change in locomotor strategy have yet to be fully elucidated, both on functional and anatomical levels. Whilst the axial CPG and the neurons comprising it have been well characterised in younger larval stages (discussed in section Ic i), these are less well understood during metamorphosing stages, including the precise roles of GJ within the axial CPG circuit. Since the axial system appears to provide an initial functional scaffold for the appendicular CPG in terms of synchronising its rhythmic output, connections both within the axial CPG itself and also between the axial and limb CPGs need to be explored at various timepoints throughout metamorphosis, from initial limb CPG emergence when its rhythm is dependent on the axial system, to climax, when its rhythm generation is independent.

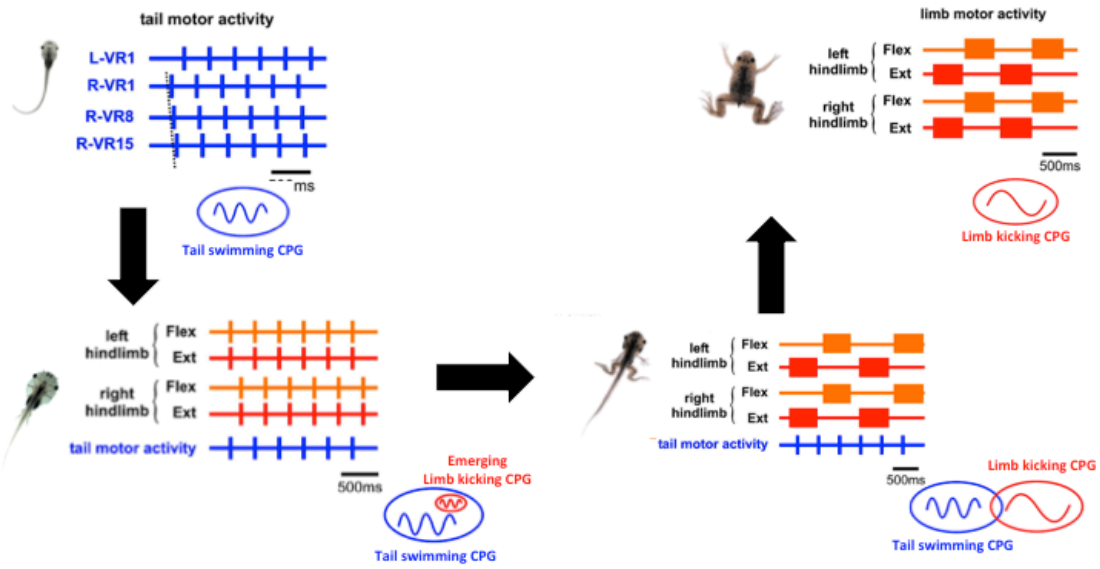

Fig 1. During metamorphosis, Xenopus laevis abandons tail-based undulations in favour of appendicular-based flexor-extensor hopping cycles. Circumstantial evidence of pre-metamorphic (< stage 53) animals employ tail-based swimming, with the rhythm provided by the tail swimming CPG. Pro-metamorphic or late pre-metamorphic animals (stages 54-58) show an emerging limb kicking CPG that is completely dependent on the rhythm of the axial CPG for its own output. As metamorphosis progresses, at metamorphic climax, the tail and limb CPG have to separate rhythms, while in adulthood the limb kicking CPG generates the locomotor output. *Figure adapted from Sillar et al., 2008.*

There are, of course, other possible types of linking connections within and between the axial and hindlimb networks, aside from electrical coupling. It is known, for example, that normally inhibitory connections in the adult mediated at $GABA_A$ receptors can be depolarizing and excitatory early in development due to high intracellular chloride ion concentrations that are rectified during development by incorporation of the potassium-choloride co-transporter KCC-2 (reviewed in Ben-Ari et al., 2007). To start with, GABA and glycine are excitatory in early development due to the high intracellular chloride concentration. However, as development progresses, KCC-2 potassium-chloride co-transporters are inserted into the neuronal membrane, such that potassium is imported and chloride is extruded, causing a low intracellular chloride concentration in mature animals; thus, GABA and glycine become inhibitory (reviewed in Kaila et al., 2014). This can cause major changes in the motor output of an animal over the course of ontogeny: for example,

before this inhibitory signalling which causes left-right as well as flexor-extensor alternation is set up, the hindlimb muscles of prenatal rats are active synchronously (Kudo, Nishimaru & Nakayama, 2004). Therefore, the relationships between groups of neurons projecting to different muscle groups, and hence the way that an animal locomotes (e.g., synchronously active versus alternating muscle groups), are modified over the course of development.

A plethora of synaptic connection types are often expressed initially during development, but as an organism matures, more heavily used pathways are strengthened while unused or aberrant connections are "pruned" (e.g., Personius et al., 2007). However, the synchronization between the axial and appendicular locomotor systems during early metamorphosis and the fact that extensor and flexor limb MN pools are initially co-active, provides circumstantial evidence that GJs and electrical coupling may play a role at specific stages of *Xenopus* motor system development. Many vertebrate central nervous system (CNS) neurons are coupled by electrical synapses (reviewed in Connors & Long, 2004), and these often synchronise activity in neuronal populations with comparable roles (Fuentealba at al., 2004; Leznik & Llinas, 2005; Sinfield & Collins, 2006; Hinckley & Ziskind-Conhaim, 2006; Wilson et al., 2007). Motor activity often requires such synchrony for rapid and smooth movements, and electrical coupling has also been reported within spinal motor networks in a variety of different species (Perrins & Roberts, 1995a,b; Kiehn & Tresch, 2002; Hinckley & Ziskind-Conhaim, 2006; Wilson et al., 2007; Li et al., 2009). Of specific relevance to this study, electrical coupling in *Xenopus* motor networks has also been described, albeit in younger hatching stage animals (Zhang et al., 2009; Li et al., 2009). Thus, it was deemed worthwhile to explore GJs as a possible point of connection both between and within the axial and appendicular rhythm-generating networks of the metamorphosing tadpole,

particularly since the hindlimb motor system is initially functionally coupled to the pre-existing axial system.

1B. Neuronal gap junctions in vertebrates: expression, function and location

There are two main modalities of synaptic transmission: chemical and electrical. In chemical transmission, neurotransmitters are released from vesicles that fuse with the presynaptic cell membrane; these transmitters are released, traverse the synaptic cleft, and dock on receptors on the postsynaptic cell membrane where they exert their effects. In contrast to chemical synaptic transmission, electrical synaptic transmission via GJ coupling allows for both rapid communication and the synchronisation of electrical activity between coupled cells. Rapid response times and synchronisation are achieved because the GJ machinery is inherently different to that in chemical signalling; there is no need to mobilise vesicles and release their contents for transmission as the gap junctions directly connect the cytoplasms of connected cells. Thus, electrical signals can pass directly through coupled cells as opposed to the need for transmitter-receptor docking and ion channel opening which is required to generate a post-synaptic response with chemical synapses (reviewed in Söhl et al., 2005). Electrical transmission plays an important role in different neuronal network types, especially those that require fast, synchronised activity such as escape circuitry. For example, the Mauthner neuron pathway that mediates both the tadpole and teleost fish startle response contains a large number of electrical synapses to ensure a fast, reliable and synchronised escape response (Robertson et al., 1963; Hackett, Cochran & Brown, 1979; Eaton, Bombardieri & Meyer, 1977).

GJs are pores formed by two hemichannels (connexons), each belonging to a neighbouring cell, which are in turn comprised of connexin proteins in vertebrates. The connexin (Cx) gene family in mammals contains approximately 20 types of subunits, but only a few of these are actually expressed in neural tissue, predominantly Cx36, Cx40, Cx45 and Cx57, with the number referring to the protein weight in kilodaltons (kDa) (Rozental et al, 2000; Söhl et al., 2005). Other gene families include pannexins in vertebrates and innexins in invertebrates, but these are outwith the scope of this review. Cx proteins combine to form 6-subunit 4-transmembrane hemichannels, which in turn, come together with a neighbouring cell's hemichannel to form a fully functional GJ (Fig 2; Söhl et al., 2005). These subunits can take homomeric/homotypical, heteromeric, or heterotypical combinatorial forms, with the central pores being roughly 1.5kDa in diameter. There can be thousands of GJs per electrical synapse. In this way, signalling molecules can pass between cells with ease (either charged ions such as K^+ or small chemical signals such as cAMP), provided the ions or molecules are below approximately 1.5kDa (16-20Å) (Söhl et al., 2005).

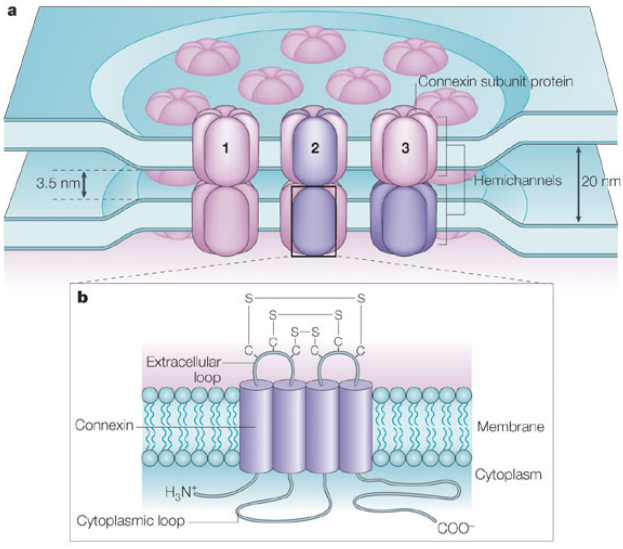

Fig 2. Schematic of connexin and gap junction composition. a) hemichannels in adjacent cells dock onto each other to form gap junction channels. These are made up of six connexin subunit proteins, which can be of three compositions: (1) homomeric/homotypic, (2) heteromeric, (3) heterotypic. b) a single connexin subunit contains four transmembrane proteins, which have three extracellular cysteine residues that are conserved and essential for docking to other connexin subunits in the adjacent cell. *Figure from Söhl et al., 2005.*

GJs have been implicated in a variety of developing vertebrate neural systems involved in motor output, and the formation of transient GJ networks during development is not uncommon in vertebrate nervous systems. Cx40, for example, is particularly relevant in mice as a developmentally-regulated gap junction protein expressed in spinal motor neurons; genetically-modified $Cx40^{-/-}$ mice display enhanced synapse elimination during development, converting multiply- to singly-innervated neuromuscular synapses as in the adult stages more quickly, as shown by immunohistochemistry and whole-cell recordings (Personius et al., 2007). In addition, electrical coupling (presumably via GJs) in early larval *Xenopus* (stage 37/38) is present in both the axial rhythm-generating CPG neurons and also between MNs innervating synergistic myotomes, serving to synchronise axial activity to each muscle segment during swimming when MNs fire together and only once per swim cycle (Zhang et al., 2009). This electrical coupling has been proposed to reduce dramatically or disappear completely by stage 42, when MNs are able to discharge more than one spike per burst to sustain left-fight alternating rhythmic swimming activity with rostrocaudal delay (Zhang et al., 2009) (discussed in further detail in section Ic iii). Thus, electrical synaptic strength within the motor system itself may be regulated during development.

More recently, Song et al. (2016) have found GJs can control the locomotor circuit function in adult zebrafish. MNs have traditionally been viewed as the "final common pathway" passively conveying a motor programme to muscles (Liddell & Sherrington, 1925). However, Song et al. (2016) have found gap junctions allow voltage fluctuations to be retrogradely propagated from MNs to upstream V2a interneurons (INs); this allows MNs to recruit these V2a INs, which drive locomotion. Therefore, GJs allow MNs to play a more active role in the motor programmes propagated to muscles than previously thought.

GJs can be subject to modulation both intrinsically and extrinsically. As GJs are found in either the open or the closed states (either maximum conductance or zero conductance), modulation changes the open probability of a given channel, rather than altering the rate of its conductance (Qu & Dahl, 2002; reviewed in Oshima, 2014). Intrinsic modulation relies primarily on voltage-dependency, to ensure the directionality of transmission is preserved (reviewed in Goodenough & Paul, 2009). Although the majority of GJ connections are not rectifying, a minority display asymmetrical current flow due to either heterotypic hemichannels or post-translational modifications of individual Cxs, such that the conductivity of forward transmission relies on one side of the synapse being positive relative to the other; if it is negative, the voltage-dependent channel closes and no communication occurs (reviewed in Marder, 2009; Goodenough & Paul, 2009; Pereda, 2014). Extrinsic modulation of GJs can be mediated by substances such as calcium (Ca^{2+}), dopamine (DA), nitric oxide (NO) or retinoic acid (RA), all of which cause a reduced channel open probability either directly or via second messenger pathways (Söhl et al., 2005).

The role of DA's inhibitory effects on GJs was made known first by the seminal work on electrical coupling between cone horizontal cells in teleost fish retinal receptive fields, whereby the spread of the fluorescent dye Lucifer Yellow was reduced in the network either during prolonged darkness or when DA was applied (Tornqvist et al, 1988, as cited in Katz, 1999). That is, the dye was restricted to the injected cell or injected cell and just a few neighbouring cells in prolonged darkness or in the presence of DA, which is the presumed mechanism by which this dark adaptation takes effect. The same effect of dark adaptation can also be seen very clearly in the turtle H1AT horizontal cell retinal network both in the presence of DA and also in the presence of forskolin, an adenylyl cyclase activator (Piccolino,

Neyton & Gerschenfeld, 1984) (Fig 3). In addition, GJs in the previously-described Mauthner escape system are also modulated by DA: DA enhances the electrotonic coupling potential via a cAMP-dependent phosphorylation pathway (Pereda et al., 1992; Pereda et al., 1994). Based on the studies mentioned in the previous paragraph employing either gap junction blockade (e.g., Zhang et al., 2009; Li et al., 2009) or specific gap junction knock-out (e.g., Personius et al., 2007), it is clear that developing locomotor systems rely to varying degrees on GJs for well-coordinated locomotor output, however the mechanisms by which they are "pruned" or modified, intrinsically or extrinsically, throughout ontogeny and into adulthood remains unclear.

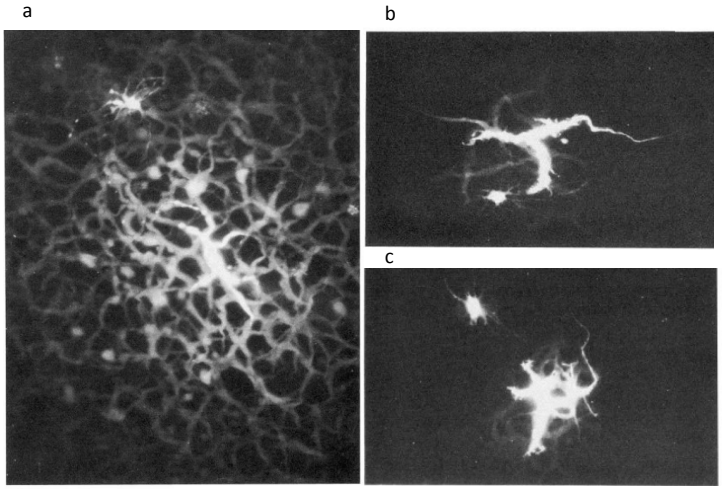

Fig 3. Diffusion of Lucifer yellow through gap junctions in the H1 horizontal cell network of the turtle retina. a) Control – the intracellularly injected dye diffuses, labelling many adjacent H1 cell bodies. Note that the central and brightest cell was the one injected with the dye initially. b) the presence of bath-applied extracellular 10uM dopamine restricts dye diffusion. c) the presence of bath-applied extracellular 10uM forskolin restricts dye diffusion. *Figure adapted from Piccolino et al., 1984.*

IC. DEVELOPMENT AND MODULATION OF THE XENOPUS LOCOMOTOR SYSTEM

IC I. THE AXIAL CPG

The *Xenopus* locomotor system has been particularly well characterised at early larval stages, specifically the hatching stage, 37/38. At this stage of development, with the use of whole-cell electrophysiology in conjunction with horseradish peroxidase (HRP), Lucifer Yellow and neurobiotin anatomical staining, 10 neuron classes which contribute to sensory integration, rhythm generation and motor output have been described (simplified in Fig 4):

(1) Rohon-Beard skin sensory neurons (RB); (2) dorsolateral commissural sensory interneurons (dlc); (3) dorsolateral sensory interneurons (dla); (4) excitatory commissural sensory interneurons (ecINs); (5) commissural reciprocal inhibitory interneurons (cINs); (6) ascending inhibitory interneurons (aINs); (7) descending excitatory interneurons (dINs); (8) descending repetitive excitatory interneurons (dINrs); (9) motoneurons (MNs) and (10) Kolmer-Agdjur cells (KAs) (Roberts & Clarke, 1982; Roberts, 1989; Li et al., 2001 & 2003; Roberts et al., 2010; Roberts, Li & Soffe, 2012; Li, Soffe & Roberts, 2004; Sautois et al., 2007). Nine similar and probably homologous classes exist in Zebrafish (*Danio rerio)* embryos defined using similar functionally relevant criteria (reviewed in Roberts, 2000). CPG circuitry in the spinal cord and hindbrain involves four major classes of neuron (aINs, cINs, dINs and MNs) and can produce rhythmic activity even in the absence of sensory input (Roberts, Li & Soffe, 2010; Li et al, 2014; Figure 4). The CPG coordinates rhythmic contractions required for *Xenopus* embryo and larval swimming, moderating the intensity, phasing and timing of locomotor output (e.g., Sillar et al., 1991). CPG interneurons provide ipsilateral glutamatergic excitatory input which is both tonic and phasic, and they also provide reciprocal glycinergic mid-cycle inhibition; MNs innervate muscles but also supply excitatory positive feedback to premotor interneurons as well as themselves (Roberts and Perrins, 1995).

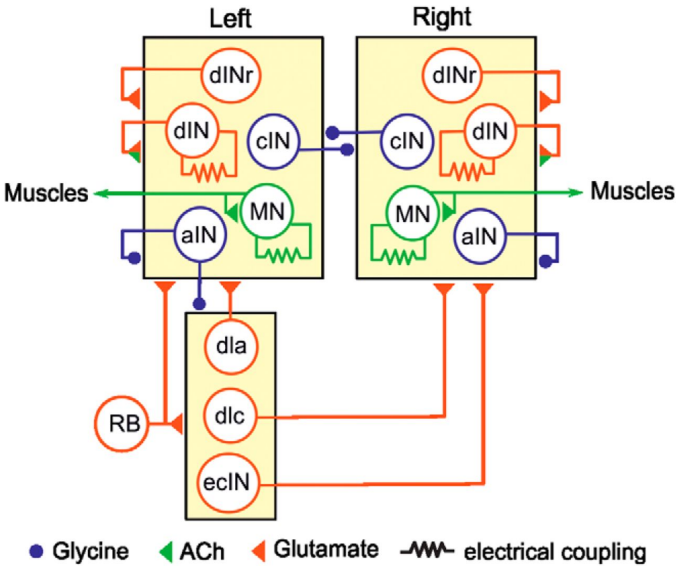

Fig 4. Simplified schematic of the axial CPG in a stage 37/38 Xenopus tadpole: neurons and their connections. Cell types are described in the main text. The triangle indicates an excitatory synapse, whilst the circle indicates an inhibitory synapse. *Figure taken from Li et al., 2014.*

In developing tadpoles, descending excitatory glutamatergic interneurons (dINs) are the source of the primary, rhythmic excitation driving firing of spinal cord neurons during swimming (Soffe 2009). These descending inputs, along with incoming sensory inputs, orchestrate the CPG's control of MN output as Sherrington's "final common pathway" for muscle activation, although sensory input is not required for CPG rhythmogenesis (Brown, 1914; Grillner & Zangger, 1979). In *Xenopus* tadpoles, this produces a rhythmic, rostrocaudally-propagated motor pattern involving 10 to 20Hz alternating contractions of left and right trunk muscles with a brief delay between muscle segments, that creates side-to-side oscillations of the torso and tail as it alternates across the body (Kahn, Roberts & Kashin, 1982). MNs exit through the ventral roots and release acetylcholine (ACh) at the neuromuscular junction (NMJ) to produce movement via muscle contraction; within the spinal cord MNs are extensively electrically interconnected locally within their segment of origin, helping to generate a phase-delayed rostrocaudally travelling body wave by sequentially activating body wall muscles (Roberts et al., 1999).

IC II. DEVELOPMENT OF MOTONEURON INNERVATION FIELDS

Adult musculature involved in generating vertebrate locomotion has primitive myomeric origins as a set of rostrocaudally-repeating myotomes; this is both evolutionarily derived and is also recapitulated to a certain extent during ontogeny. Myomeres can be divided into two functionally distinct fibre types: (1) deep white muscle fibres, specialised for fast burst swimming (these are at rest most of the time) and (2) superficial red fibres, specialised for the generation of sustained and slower swimming (Fetcho, 1986).

To execute efficient locomotor activity, appropriate synaptic connections must be formed between neurons and their target muscle fibres; the goal during development being that adult motoneuronal electrical characteristics eventually match the contractile properties of the fast or slow fibres they innervate (Eisen, 1991). For example, in zebrafish, differential dorsal and ventral cues exist, which dictate cell-specific and stereotyped motor axon pathways along axial muscle: in the *topped* zebrafish mutant, *topped* acts on ventromedial fast muscle, promoting axon outgrowth (Rodino-Klapac & Beattie, 2004).

In vertebrates such as fish and amphibians, the organisation of the medial motor and lateral motor columns (MMC, LMC) involves two classes of MN: primary MNs (pMNs), which are typically born earlier and have larger cell bodies, and secondary MNs (sMNs), which are typically born later and exhibit smaller cell bodies (Fetcho, 1986). It is important to note that the terms pMN and sMN have slightly different meanings amongst aquatic vertebrates. In limbless animals, such as zebrafish, pMNs innervate the more medial deep fast twitch white muscle fibres, whilst the sMNs innervate the more lateral slow twitch superficial red fibres. This is in contrast to quadrupedal amphibians such as *Xenopus*, whereby pMNs

found ventromedially and ventrolaterally in the spinal column innervate the axial musculature, but sMNs found predominantly dorsolaterally or ventromedially innervate the appendicular limb musculature, which contains a mixture of fibre types (Eisen, 1991; van Mier, 1986).

Thus, a topographic relationship exists between the dorsoventral and rostrocaudal positioning of a given pMN or sMN and the muscle it innervates, both embryonically and in the adult. This organisation is related to the functional segregation of white and red muscles, or axial and appendicular muscles in the developing and adult *Xenopus*. For example, axial MNs occupying adjacent positions in the MMC innervate neighbouring myotomes in both developing and adult musculature (Fetcho, 1986). Similar stereotyped projection patterns have also been observed in other vertebrate systems, such as innervations of the quail and chick hindlimb (Tyrrell et al., 1990; Rafus et al., 1996). Thus, the vertebrate spinal cord is comprised of discrete MN groupings, which innervate skeletal muscles in discrete locations with specific contractile properties. This precision in motor systems is replicated during development reliably between individuals, with disparate physiological roles of pMNs and sMNs being reflected by the dissimilarities in the roles of the muscle fibre types they innervate (Eisen, 1991; Westerfeld et al., 1986; Fetcho, 1986).

IC III. INCREASED FLEXIBILITY OF THE *XENOPUS* LOCOMOTOR SYSTEM DURING MULTIPLE SPECIFIED PERIODS OF DEVELOPMENT

The locomotor output of larval *Xenopus* at the stage that has been studied in detail (stage 37/38) is characteristically simple and relatively inflexible, with all MNs firing one action potential in each and every cycle of swimming, contributing to a very brief 5-7 millisecond

ventral root burst in each cycle (Sillar et al., 1991). This lack of neurobehavioural flexibility may be partly because the swimming CPG develops before locomotion in possible, so behavioural flexibility is not so necessary (discussed in Section Ic i). However, flexibility is rapidly gained in the locomotor circuitry so that even by stage 42, one day later and prior to free-swimming behaviour, MNs can now fire multiply and more variably (Sillar et al., 1991). This means they can contribute to longer and more variable ventral root bursts of around 20 milliseconds, and this versatility can develop even in the absence of movement (Bender 2009; Zhang et al., 2011). During this relatively brief period of time, the animal's MN innervation fields also change; at stage 37/38 each MN innervates all or most of the dorsoventral extent of the myotome, but this becomes more restricted by stage 42 to a more limited section of each muscle block (dorsal, medial, or ventral regions) (Zhang et al., 2011). Zhang et al. (2009) have found a role for GJs in the transition from stage 37/38 to stage 42 CPG output: when bath applied to stage 37/38, GJ blockers (18-β-glycerrhetinic acid (18-β-GA) or carbenoxolone (CBNX)) increased the duration of ventral root bursts similar to those seen in stage 42. This finding implies that GJs assist in phase-locking the firing of electrically-coupled MNs. By stage 42, however, there was no effect of GJ blocker application, suggesting that at least part of the mechanism by which flexibility increases by stage 42 to sustain longer and more variable burst durations is via a decrease in GJ coupling during normal development. Thus a pre-patterned motor rhythm precursor acquires flexibility, allowing it to be modified by descending brain and sensory inputs to the CPG; however, these inputs are not required for these physiological and anatomical transformations (rhythmic CPG output; restriction of MN innervation fields) leading to increased flexibility taking place.

Flexibility in motor output is also required at a second time point, later in *Xenopus* ontogeny, during metamorphosis with the emergence of the limb network. As discussed earlier in Section Ia, the appendicular CPG is initially coupled to the axial CPG and shares the same rhythmic frequency until approximately stage 54. However, later on in larval development by stage 60/61 and into adulthood, the axial and limb CPGs do not share the same rhythm frequency; in fact, the axial musculature plays primarily a postural role as the limbs become the main generators of thrust, although the adult axial postural muscle CPG still communicates with the appendicular CPG (Combes et al., 2004; Sillar et al., 2008; Beyeler et al., 2008). Thus some form connection must exist between these two rhythmogenic systems that is progressively eliminated or at least drastically diminished, with a plausible candidate being GJs (see Section Ia). As axial and limb CPGs during metamorphosis are much less well characterised than in stages 37/38 and 42, this forms the basis of the current study, whereby the roles of GJs both within the axial system and between the axial and limb systems during metamorphosis are explored, with a particular focus on their relationship and potential coordination.

Ic iv. The role of neuromodulation and descending inputs on the development and output of CPGs

Although the locomotor output of CPGs does not require neuromodulation for the basic production of movement, neuromodulation does play a crucial role in shaping short-term behavioural output *in vivo*. In addition, neuromodulators can confer more long-lasting changes in neuronal electrical properties and synaptic strengths, often via second messenger pathways. They can do so by regulating the types, number and properties of neurons in maturing motor networks, which dictates certain properties of adult network

output (reviewed in Sillar et al, 2014). In particular, biogenic amines such as noradrenaline (NA), serotonin (5-HT) and DA, as well as the gaseous modulator nitric oxide (NO) play key roles in the modulation of CPG output. These will now be discussed in terms of development either in young larvae or during the metamorphic period.

In young, hatchling *Xenopus* tadpoles (stages 37/38), descending supraspinal control pathways from the brainstem, most notably those using 5-HT and NA as neurotransmitters, are important in the modulation and maturation of spinal locomotor networks (McLean et al., 2000). In young embryos, both amines target the strength of cross-cord glycinergic inhibitory synaptic connections that are responsible for reciprocal mid-cycle inhibition producing left-right alternation. In this way the two amines control the temporal organisation of burst activity within swim episodes: NA enhances the amplitude of mid-cycle glycinergic inhibitory post-synaptic potentials (IPSPs) during fictive swimming by increasing the probability of presynaptic glycine release, while 5-HT decreases them by inhibiting presynaptic glycine release (McDearmid et al., 1997). This results in NA ultimately reducing swimming frequency, while 5-HT increases motor burst durations. Another biogenic amine, DA, affects the occurrence of swim episodes at later stages, in contrast to NA and 5-HT which regulate the temporal organisation of burst activity within a swim episode in pre-metamorphic *Xenopus* (Clemens et al., 2012). A concentration-dependent effect of DA application on D1-like and D2-like receptors enables DA itself to produce opposing effects on the system: low concentration of exogenous DA application affects the D2 receptor which has an inhibitory effect on occurrence of swim episodes, however high concentration of exogenous DA application affects the D1 receptor which has an excitatory effect on occurrence of swim episodes (Clemens et al., 2012).

The maturation of motor networks from stage 37/38 to stage 42 occurs in a rostrocaudal direction (Sillar et al., 1991), the same interval over which serotonergic raphespinal axons begin to establish synapses within the spinal cord (van Mier, 1986). 5-HT from raphespinal interneurons of the brainstem contributes to larval locomotor maturation by enhancing developmental acquisition of more flexible and efficient axial swimming; the embryonic pattern of discharge is seen as short biphasic ventral root impulses at each activity cycle, whereas the more complex larval pattern comprises bursts of discharge, which can also be induced by applying 5-HT or precursor 5-hydroxytryptophan (5-HTP) (Sillar et al., 1991, 1992a,b, 1995). Furthermore, exposure to a neurotoxin (5,7 dihydroxytryptamine) which destroys serotonergic raphespinal projections inhibits normal swimming maturation in these young animals, whilst the rhythm of more mature animals which experience a block of 5-HT receptors reverts back to an embryo-like rhythm. This demonstrates not only the requirement of developing 5-HT axons in the spinal cord for the maturation of locomotor rhythm, but also that the axial neural circuitry is flexible because it is amenable to changes during ontogeny (Sillar et al., 1995).

During various key stages of the switch in locomotor strategy during metamorphosis from tadpole to frog, the same aminergic neuromodulatory inputs are known to play an active role in shaping the final adult axial and appendicular CPG networks and the interconnections between the two. Although some axial circuitry is lost with the regression of the tail, new appendicular adult limb-kick circuitry with accompanying sensory inputs is gained (Combes et al., 2004). During *Xenopus* metamorphosis, supra- and intra-spinal modulatory inputs probably play a critical role in maturation as well as functional flexibility (Rauscent et al.,

2006). As during the younger stages, NA and 5-HT exert opposing effects, this time on short-term adaptive control of both inter-network coordination and within-circuit activity. This parallels long-term changes in network development. Specifically, at metamorphic climax when coexisting tail-based and limb-based systems can operate independently (Combes et al., 2004; Sillar et al., 2008), bath-applied NA decouples axial and appendicular rhythms, whereas 5-HT couples them into a single unified rhythm (Rauscent et al., 2009) (Fig 5). Presumably this allows for rapid coupling or decoupling of the two rhythms in accordance with the animal's propulsive requirements at any given time, as dictated perhaps by a change in the animal's environment.

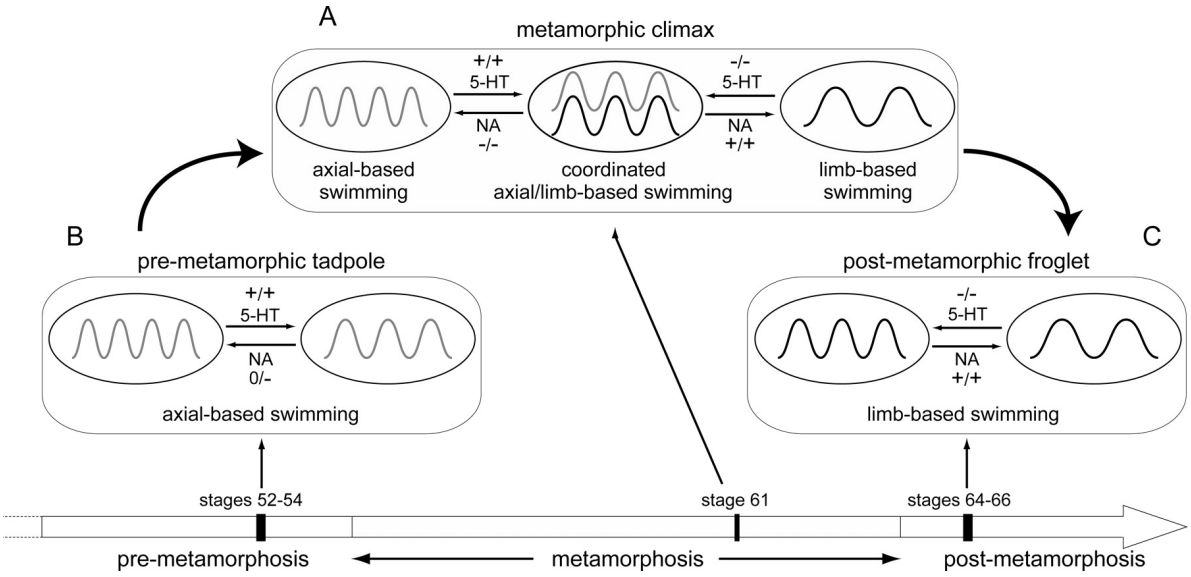

Fig 5. Summary of neuromodulation of the bioamines, noradrenaline (NA) and serotonin (5-HT) on the locomotor output at different stages in Xenopus development from pre-metamorphosis to post-metamorphosis. During all stages, 5-HT and NA exert opposing effects; + signifies enhancement, - signifies reduction, 0 signifies no effect of the monoamine on cycle period and burst duration of axial or limb output. The main text describes the change in effect over the course of development. *Figure taken from Rauscent et al., 2009.*

The neuromodulator nitric oxide (NO) also plays a role in maturing limb locomotor networks. Nitric oxide synthase (NOS) expression is increased in the brainstem and spinal cord during metamorphosis, specifically in time with limb bud development, while in pre-

metamorphic tadpoles it appears restricted to the brainstem (Ramanathan et al., 2006; McLean and Sillar 2000, 2001). It is likely that NO plays a multifaceted role in spinal cord locomotor development; in younger animals, it has an inhibitory effect on cell proliferation. Its absence from the cervical and lumbar areas of early pro-metamorphic *Xenopus* could be responsible for neuronal proliferation required during preliminary assembly of fore- and hindlimb locomotor networks, respectively (Rauscent et al., 2006; Ramanathan et al., 2006).

Some of the modulators that influence locomotor CPGs in general have also been shown to modulate electrical coupling, albeit in different systems (e.g., DA decreases GJ open probability in cone horizontal retinal cells, discussed in Section Ib). Thus it is conceivable that these or other substances are employed in a whole animal system during development to modulate GJs in CPGs to achieve both short- and long-term effects. This could form the basis for future experiments exploring potential modulators of GJs within and between CPG networks during metamorphosis.

II. Materials and Methods

IIA. Animal Husbandry

All experiments were performed on free-feeding and metamorphosing *Xenopus laevis* tadpoles (stages 54-58; Nieuwkoop & Faber (NF), 1956) and complied with UK Home Office regulations (Animals Scientific Procedures Act, 1986) as well being approved by the local Animal Welfare Ethics Committee (AWEC).

IIB. Breeding and Rearing

Mating of sexually mature pairs of adult *Xenopus laevis* frogs selected from an in-house breeding colony was achieved by subcutaneous human chorionic gonadotropin (hCG) injections on average twice per week by personal license holders. The resulting fertilised ova were collected and reared in aerated dechlorinated tap water in enamel-coated or glass trays at 17-24°C to stagger tadpole larval development. Once over stage NF 42 and free-feeding, tadpoles were transferred to standard glass aquarium tanks (room temperature 24°C or on a heat mat) to mature further and undergo metamorphosis. Water in these tanks was treated with AquaSafe (Tetra), and Canadian Pondweed plants were added to aid water quality and to simulate a more authentic environment, also providing the necessary iodine for metamorphosis. Animals experienced a 12-hour light/dark cycle (light 7am-7pm).

IIC. Sacrificing

Free-feeding tadpoles are covered by the Animals (Scientific Procedures) Act (1986), and thus were sacrificed using a Schedule I Kill (SK1) method: first, the animal was immersed in 0.017g/L) of the anaesthetic tricane methanesulphate (MS-222; Sigma Aldrich) in RANA saline (RANAs; 112mM NaCl, 2mM KCl, 20mM $NaHCO_3$, 17mM glucose, +100µl 1M $MgCl_2$

and 280µl 1M $CaCl_2$ per 100ml saline) for 2-10 minutes, until they ceased responding to tactile stimulation. Then in pure RANAs, death was confirmed first via destruction of the circulatory system (removal of heart), then removal and destruction of the forebrain.

IID. EXPERIMENTS

IID I. RETROGRADE MOTONEURON BACKFILLING (STAINING) FROM MUSCLE TARGETS IN VIVO

IID IA. CONTROL CONDITION

Animals ranging from NF stages 54-58 were sacrificed via SK1 as before, and the remaining liquid was siphoned out of the dish after confirmation of death. Dye was applied exclusively to the right-hand side of the animals, however it is possible that on occasion the needle punctured through to the left-hand side. The hindlimb bud (flexor and extensor) and post-otic axial myotomes 11 and 12 were punctured several times with a sharp tungsten needle (~0.125mm diameter) to damage the tissue and thus make it more amenable to dye uptake, and then dried with a paper towel before depositing either Lucifer Yellow (Sigma), fluorescein-conjugated dextran dye (lysine-fixable, maximum 3000 MW; Invitrogen) or tetramethylrhodamine-conjugated dextran dye (lysine-fixable, maximum 3000 MW; Invitrogen) crystals into the damaged muscle tissue (Fig 6). One set of experiments exclusively used the two dextran-conjugated dyes. In this case, one colour dye was applied to the appendicular tissue, whilst the other was applied to the axial tissue; with colours periodically reversed to ensure the effect was not due to an intrinsic property of the dyes themselves. Another set of experiments used Lucifer Yellow on the axial tissue and the rhodamine dextran on the appendicular tissue, as it was found the appendicular tissue was not amenable to Lucifer Yellow uptake. Following dye deposition, the tissue was left for ~45-60 minutes to facilitate dye uptake (retrograde transport of the dye to the motoneuron

cell bodies in the spinal cord projecting to the various muscle tissues) before being placed in a light-impermeable container for 4-6 hours in carbogen-aerated RANAs (pH ~7.4) at room temperature ~24°C, and then for 20-24 hours in 4°C without aeration in the dark. Spinal cords were then dissected in the same liquid and placed in 4% paraformaldehyde (PFA) overnight in the dark before histological processing.

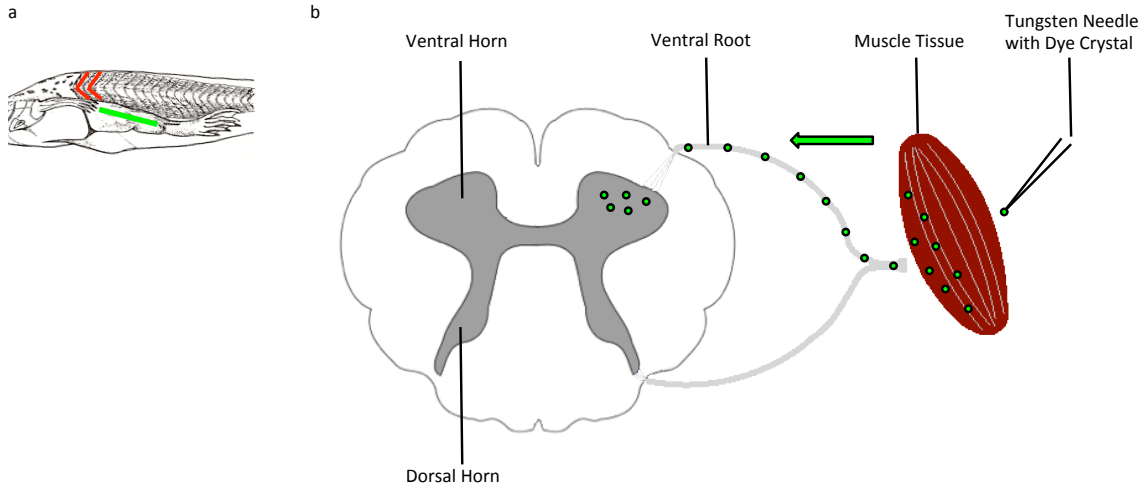

Fig 6. Motoneuron dye backfilling technique. a. Dyes conjugated to different fluorophores were crushed into the 11th & 12th post-otic axial myotomes and the hindlimb. This example shows a NF stage 58 animal after SK1. b. The dye was retrogradely transported to the somas in the ventral horn of the muscles they innervate. *Fig a adapted from Nieuwkoop & Faber, 1956; Fig b based on Rauscent, 2008.*

IID IB. DRUG CONDITIONS: GAP JUNCTION BLOCKERS

Animals underwent the same treatment as in Control (above), however, either 200µM CBNX (in RANAs) or 100µM 18-β-GA (in 100µl DMSO) (Li et al., 2009; Zhang et al., 2009) were added to RANAs and used throughout the entire process: during the SK1 confirmation of death, during room temperature aeration and at 4°C. Both control and drug conditions were performed on the same day to eliminate any confounding variables. Spinal cords were then dissected in the same solution and pinned in a Sylgard-lined petri dish to be placed in 4% PFA overnight in the dark before histological processing.

IID IC. HISTOLOGICAL PROCESSING

Fixed dissected spinal cords pinned in a dish were washed first in Phosphate Buffered Saline (PBS) for 30-90 minutes before being put through a dehydration and clearing series of 100% ethanol (Sigma) thrice, methylbenzoate (Sigma) once and xylene (Sigma) twice, each for a duration of three minutes. Each cord was then mounted on its own metal slide with DePeX or HistoMount and a glass coverslip. These custom-made metal slides had a circular cavity lined with glass, and the preparation was placed in this cavity with a small amount of DePeX or HistoMount, before placing a circular glass coverslip overtop; after trial and error, imaging was found to be much more successful if the preparation was placed on the slide before the mounting medium. Slides were left overnight in the fume hood unexposed to light, then placed in a light-impermeable box in 4°C. Cords were imaged within 72 hours of being mounted.

IID IE. QUANTIFICATION OF MOTONEURON BACKFILLING DATA

All imaging and raw data quantification were performed using a Zeiss confocal-like AxioImager.M2 microscope with ApoTome.2 optical sectioning capability, on a PC equipped with Zen2012 software: through Lucifer Yellow, FITC, and Rhodamine filters, optical sectioning of z-stacks at the optimal suggested intervals (usually 3.8-4.2µM) by Zen2012 were taken of each spinal cord at 10x magnification. MNs were identified based on the following criteria: depth of a round soma in all three planes X, Y and Z; rostrocaudal columnar distribution; and, where possible, axonal processes and/or dendritic arbours (most commonly for axial as opposed to appendicular MNs). For experiments where both conjugated dextran dyes were used, MN parameters (e.g., diameter) were quantified manually using the circle tool (i.e., drawing a circle over the cell, which was the same size as the cell itself) and line tool (to measure clusters), which measured diameter and length.

IID II. EXTRACELLULAR VENTRAL ROOT ELECTROPHYSIOLOGY

IID IIA. CONTROL PERIOD

Animals ranging from NF stages 54 to 58 were sacrificed via SK1, and the spinal cord and hindbrain were dissected free from the remaining carcass. This part of the CNS was pinned to the Sylgard surface of a glass petri dish through the optic nerves, and left to recover for at least one hour. Temperature-controlled (Peltier (built in-house), ~16.3-17.3°C) and carbogen-aerated RANAs (pH ~7.4) was re-circulated in the dish via a peristaltic pump at a rate of ~19ml/s. During recovery, at least one VR was suctioned in a glass extracellular recording electrode on the left or right side of the body: to monitor axial CPG output, a recording electrode was placed on axial VR 17-20, with a stimulating electrode on the optic tectum. VRs were counted rostrocaudally, with VR 10 being the caudal-most output of the lumbar enlargement. Electrodes were fabricated from glass capillary tubes which were heated in the flame of a Bunsen burner and pulled by hand. The larger end of the tube was flamed and the smaller tip end was broken to approximately the same diameter as the VR to which it was attached, which reduced electrical noise. When experiments measuring limb output were performed, an additional recording electrode was placed on limb VR 9 or 10, and additional stimulating electrodes were placed on limb VR 8 or 9 and axial VR 12-15, allowing for simultaneous recording.

To obtain elicited fictive locomotion, a train of current pulses (usually one to two in control, but sometimes more in the drug and wash conditions) at a threshold of 0.1-9.9V for 1-20ms via a Digitimer Ltd. isolated stimulator (model DS2A) was delivered to the optic tectum (Currie, 2013), axial VR, or limb VR via a copper wire coiled around a glass suction stimulating electrode; only the optic tectum was stimulated during axial-only output

experiments, whereas all three areas were stimulated at different points in the experiments where limb and coupling were measured. During limb experiments, axial recording and stimulating electrodes were placed on the left side of the preparation, whilst limb recording and stimulating electrodes were placed on the right side of the preparation. The order of the three stimulated regions was switched in different experiments, to ensure no order effect. Schematics detailing electrode placement are included in each results figure for clarification. All experiments were performed in a modified Faraday cage covered with tin foil. The light source remained on for the duration of the entire experiment, as light is a known source which evokes fictive locomotion (Currie et al., 2016); in instances where the light source contributed too much electrical noise, it was simply turned off for the duration of all control, drug, and wash conditions.

This signal was passed through a grounded cable to an A-M Systems model 1700 differential AC amplifier with 10000x gain and finally connected via a 1401 model analogue-to-digital acquisition system CED (Cambridge Electronic Design) to Spike2 software on a PC (sampling rate 8-10kHz). If the preparation exhibited spontaneous fictive locomotor bursts from spinal ventral roots, a 20-minute period from the start of the first episode was considered the spontaneous control period.

IID IIB. DRUG PERIODS (GAP JUNCTION BLOCKERS)

Following the control period, 100ml temperature-controlled and carbogen-aerated RANAs with either 10µM 18β-Glycyrrhetinic acid (18-β-GA) in dimethylsulfoxide (in 100µl DMSO; Sigma), 20µM 18-β-GA (in 100µl DMSO), or 200µM carbenoxolone (CBNX) (in RANAs) (pH ~7.4) were bath applied, with the loop closed after 50-60ml of the drug solution was in the

bath (max bath volume 50-60ml). (Please note that a sample axial output only experiment timecourse can be seen in Fig 7. A typical experiment measuring solely axial output measured lasted ~8 hours, and a typical experiment measuring both axial and limb output lasted ~11 hours, including dissection.) During spontaneous fictive locomotion, the first drug period was calculated in a 20-minute period from when the drug hit the bath; the second drug period began when the first spontaneous episode occurred after ~35-40 minutes of drug exposure, when the drug had taken full effect (Li et al., 2009; Zhang et al, 2009). In the instance of elicited fictive locomotion, the drug was always allowed to take effect for ~35-40 minutes before evoked swimming was stimulated. In both spontaneous and elicited conditions, the drug was then washed after an additional ~30-45 minutes.

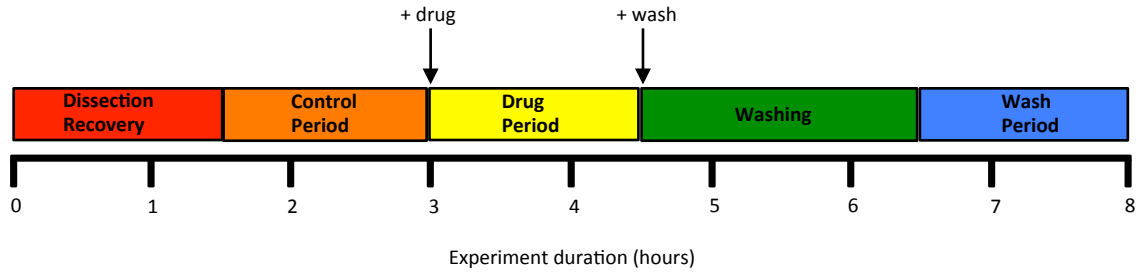

Fig 7. Sample timecourse of an axial-only output experiment. This depicts all major sections of the experiment from when the recording started. The addition of the drug and the beginning of the wash are denoted by their respective arrows.

IID IIC. WASH PERIOD

Evoked locomotor activity was started after ~60-120 minutes of washing with temperature-controlled and carbogen-aerated RANAs (pH 7.4). Spontaneous activity was calculated as a 20-minute period from the start of the first episode after ~60-120 minutes of washing. No recirculation was employed during the wash period, such that a continuous supply of fresh RANAs was pumped across the prep, and no build-up of drug occurred in the bath.

IID IID. ELIMINATING POSSIBLE CONFOUNDING VARIABLES

-LIGHT

It is known that the episode frequency of locomotor activity is sensitive to changes in ambient light levels, but that the burst parameters are unaffected (Currie, 2013; Currie et al., 2016). Therefore, in my experiments the light source was kept either on or off for the entirety the periods of the experiment that were to be analysed (control, drug, wash); ideally, it was kept *on* the entire experiment, but in instances where the light source gave off too much electrical noise, it was shut off at the start. Occasionally, the light was turned on (e.g., during the beginning of the wash, 2 hours before the period to be analysed began) to shed enough light to ensure, for example, that the recording and stimulating electrodes were still in the same position; it was then shut off immediately. In these instances when the light was turned on, it was noted that this elicited a bout of activity (personal observation, no data); this is consistent with findings from Currie et al. (2016) that light is a sufficient stimulus to evoke activity, and that there is a significant decrease in the time a preparation spent active in the dark versus the light. This is thought to be due to a physiologically relevant luminance-detection-to-motor-output pathway involving activation of light-sensitive proteins (opsin 5 (OPN5) and cryptochrome 1) in nonvisual photoreceptors intrinsic to the tadpole brain (Currie et al., 2016). However, since the light was kept either on or off during the control, drug and wash periods within a single experiment, it can be assumed that the findings reported here were not due to any photostimulation.

-TEMPERATURE

It is also known that locomotor activity in *Xenopus* is sensitive to changes in temperature (Sillar & Robertson, 2009), and that the optimal temperature to record fictive locomotion of pro-metamorphic *Xenopus* tadpole brainstem/spinal cord preparations is between 16 and

17°C (Currie, 2013). Any confounding effect of temperature was excluded in two ways: first, all experiments were carried out in a recording bath connected to a Peltier cooler, and this kept the saline at 16.5°C ± 1°C. Second, two light pipes were connected to the light source, and the ends of these both generated a trivial amount of heat and were also placed sufficiently far enough from the recording bath (~10cm). These experiments were therefore designed to reduce any effect of temperature on the preparation.

-SHORT-TERM MEMORY OF NEURAL SYSTEMS

The *Xenopus* tadpole locomotor system at younger stages (37/38 – 42) also retains a short-term memory for neural network function via the Na^+/K^+ pump (Zhang & Sillar, 2012): swim episode duration is dependent on the amount of time between evoked episodes (inter-swim interval), meaning that the system requires at least one minute to recover back to baseline after an elicited episode in these younger animals (Zhang & Sillar, 2012). In the older stage animals used in this study, Currie (2013) found the pro-metamorphic preparations required a minimum of two minutes for episode durations to return back to baseline; this is thought to be due to the ultra-slow afterhyperpolarisation (usAHP) underlying short-term memory in these old animals, which necessitates introducing an interval between successive bouts of stimulation such that each episode would not be influenced by the preceding one (Currie, 2013). In the present study, evoked episodes were first attempted at two-minute intervals, however, this frequently resulted in failure or much shorter episodes. Therefore the interval was increased between three to five minutes; each preparation was tested before the control period for the optimum interval to elicit, and this was kept constant throughout the control, drug and wash periods of each preparation.

IID IIE. QUANTIFICATION OF ELECTROPHYSIOLOGICAL DATA

Raw data files obtained in Spike2 were analysed on a PC equipped with the semi-automated DataView software (courtesy of Dr William Heitler, University of St Andrews, versions 9.3.1 and 9.3.7). For all *evoked* control, drug, and wash conditions, the three most representative episodes were selected for data analysis; however, occasionally there were only one or two successful elicited episodes per condition, in which case just these were used for analysis. In the instances where more than one episode followed an electrical stimulus, only the first episode was analysed. For all *spontaneous* conditions, a 20-minute period was selected from the first spontaneous episode occurring in: (1) (control) after the recovery from dissection period, (2) (drug period 1) as soon as the drug reached the bath, (3) (drug period 2) ~35-40 minutes after the drug hit the bath and the drug had taken full effect, and (4) (wash) after washing with RANAs for at least 60-120 minutes. Whenever possible, spontaneous and evoked experiments were performed on the same preparation. Specific burst and episode parameters were analysed for possible differences between conditions: burst amplitude, burst duration, cycle period, burst proportion (burst duration ÷ cycle period), and episode duration.

Bursts were quantified using the threshold technique in Dataview: in a quiescent segment of recording, a cursor was placed at the voltage level of maximum noise, and all periods when the voltage was greater than the threshold level were considered events. Minimum off and on durations were set to approximate burst durations more accurately and minimise outliers; thereafter the occasional outlier was manually detected and removed. The cycle period was defined as the beginning of one burst to the beginning of the subsequent burst (Fig. 12). Any burst at the start or end of an episode with a duration over 130ms was

excluded, and activity was only considered an episode when it was rhythmic and contained more than three bursts to ensure alternating activity.

To indicate left-right alternation and rostrocaudal delay, simultaneous activity from three recording electrodes at different tail VRs (13-21) on one preparation were processed in DataView using the de-mean, rectify, and smooth option. This yielded three transformed waveform traces, which could be compared with each other showing left-right alternation and rostrocaudal delay (Figs. 11 and 16).

IID III. STATISTICAL ANALYIS OF BOTH MOTONEURON BACKFILLING AND ELECTROPHYSIOLOGICAL DATA

All statistical analyses were performed using the GraphPad Prism 7 statistical software package. Normal distribution was determined using the Kolmogorov-Smirnov test, and repeated measures one-way ANOVAs with the post-hoc Bonferroni correction as well as paired t-tests were used. For all tests, differences were considered significant at $p<0.05$; in the following figures, * = $p<0.05$ and ** = $p<0.01$. MS Excel 2010 and 2011 were used to plot graphs, with error bars representing standard error of the mean (SEM).

III. Results

IIIa. Anatomy

IIIa i. Metamorphic Axial- and Hindlimb-Motoneuron Networks Coexist and Interact in the Lumbar Spinal Cord

As *Xenopus* metamorphose and the limbs emerge, tadpoles switch locomotor strategy from one exclusively employing the axial musculature for undulatory propulsion to another strategy relying primarily on appendicular hindlimb musculature (at the expense of axial postural muscles) for bilaterally symmetrical flexor-extensor kick cycles. MN somas controlling these different muscle groups are located in the spinal cord in different spatial locations. MNs of tadpoles in the early metamorphic period (stages 52-58) were investigated to determine the development and potential coupling between the axial- and limb-based systems during this critical period, when extensive re-wiring takes place.

Axial- and hindlimb-MNs were backfilled via the muscles to which they project (axial post-otic segments 11 and 12; hindlimb flexors and extensors), with the use of low-molecular weight (MW) fluorescent rhodamine and fluorescein dextran conjugates (refer to Methods section II). Each conjugate (red or green) primarily stained one of two distinct subsets of MNs positioned in distinct clusters in a columnar fashion (Fig. 8 a-c) in the vicinity of the lumbar enlargement. Additionally, 6/8 cords exhibited a proportion of MNs of both the axial and limb varieties, which were clearly co-labelled (axial 5.33 cells ±0.76SEM, appendicular 2.83 cells ±0.65SEM) (Fig. 8 b-c, d-f). A paired t-test found the mean number of co-labelled axial cells to be significantly higher than the appendicular cells ($t=2.52$, $p=0.05$, $n=6$). The appendicular CPG rhythm is initially entrained by the axial system before diverging, thus it was considered plausible that the co-labelling occurred via dye coupling through gap junctions between axial and appendicular MNs.

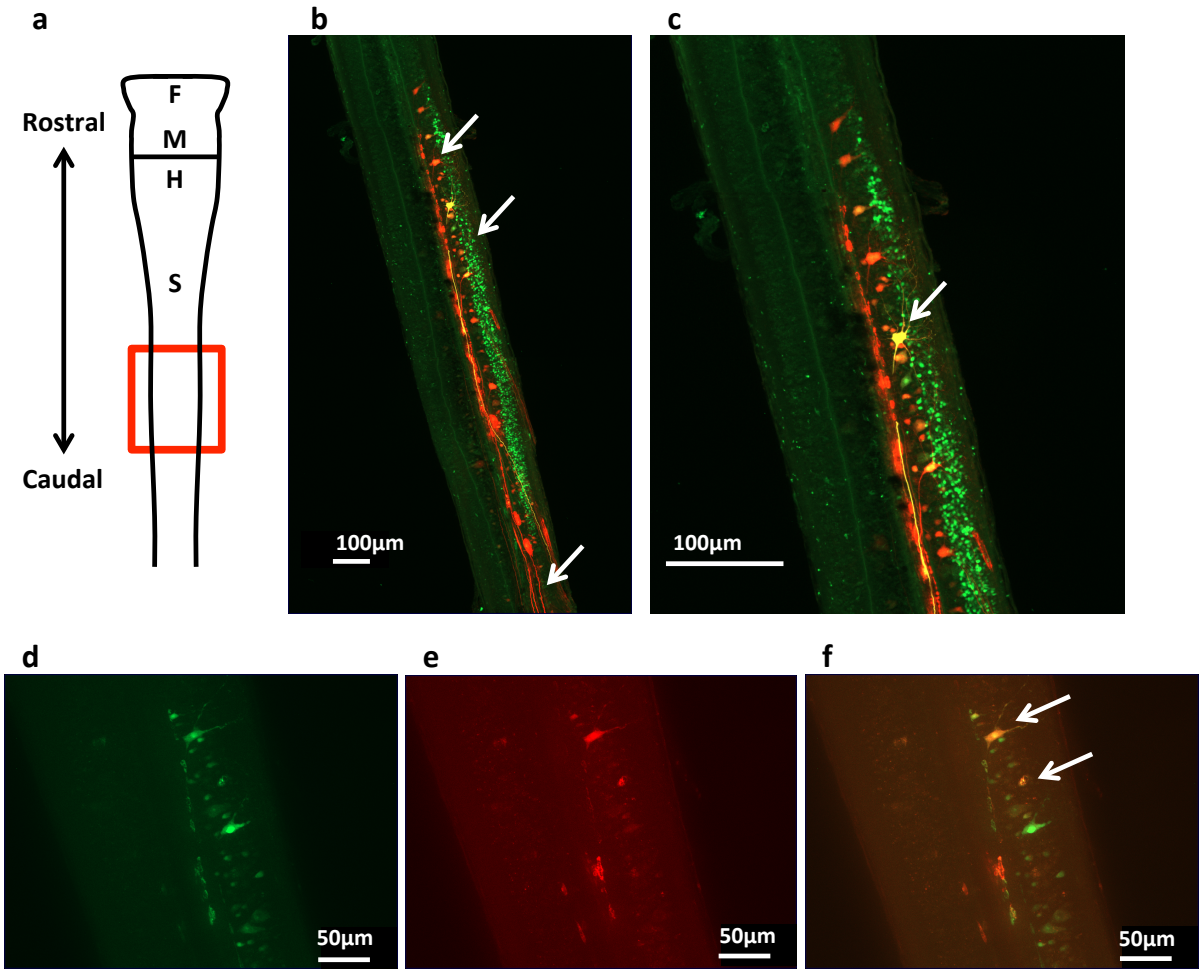

Fig. 8 Axial and appendicular MN networks coexist in the lumbar spinal cord during pro-metamorphic stages (control conditions). a. Schematic of the *Xenopus* spinal cord, with a red box around the lumbar region, where the staining was found (F = forebrain, M = midbrain, H = hindbrain, S = spinal cord). b. Orthogonal view of a maximum intensity projection of a cord labelled with rhodamine (11^{th} & 12^{th} post-otic segments) and fluorescein (hindlimb) dextran dyes at 10x magnification. Top arrrow points to the medial axial MN cluster (red), and middle arrow points to the lateral hindlimb MN cluster (green). Clusters are similar in length. Bottom arrow points to a ventral root where the axial (red) dye travelled retrogradely to the somas. c. Expanded view of (b), with the arrow pointing to a co-labelled axial MN (yellow). d-f. Photos of the lumbar region at 20x exhibiting co-labelling in both axial (top arrow) and appendicular (bottom arrow) MNs; fluorescein and rhodamine channels have been separated (d, e) to show the co-labelling more clearly.

IIIA II. ANATOMICAL DIFFERENCES BETWEEN METAMORPHIC LUMBAR AXIAL AND HINDLIMB MOTONEURONS

Several morphological parameters of the axial- and limb-MNs and their clusters were explored (Fig. 9).

IIIA IIA. SOMA SIZE AND CELL NUMBER

The mean number of axial MN somas per cord was 16.25 ±4.2SEM, while appendicular somas per cord were 173.63 ±48.85SEM, which were significantly different using a paired t-test (t=3.42, df 7, p=0.01, n=8). Additionally, axial MN soma diameter averaged 20.79µm ± 0.63SEM, whereas hindlimb soma diameter averaged 7.40µm ±0.043SEM, which were deemed significantly different using a paired t-test (t=9.19, df=7, p<0.01, n=8) (Fig. 9 a, b). This indicates the hindlimb somas are more numerous but smaller in diameter, whereas the axial somas are less numerous but larger in diameter.

IIIA IIB. CLUSTER LENGTH

The average axial MN cluster length of cells projecting to post-otic myotomes 11 and 12 rostrocaudally was 769.70µm ±108.70SEM, while the average appendicular MN cluster length of cells projecting to the whole of the hindlimb was 1008.94µm ±90.78SEM. These were not significantly different using a paired t-test (t =1.81, df 7, p>0.05, n=8).

IIIA IIC. LATEROMEDIAL DISTANCE

The distance to the spinal cord midline for each of the axial- and appendicular-MN clusters was assessed. Axial clusters averaged 58.10µm ±9.22SEM from the midline, whereas hindlimb clusters averaged 101.74µm ±18.09SEM (Fig. 9 c). This was significantly different,

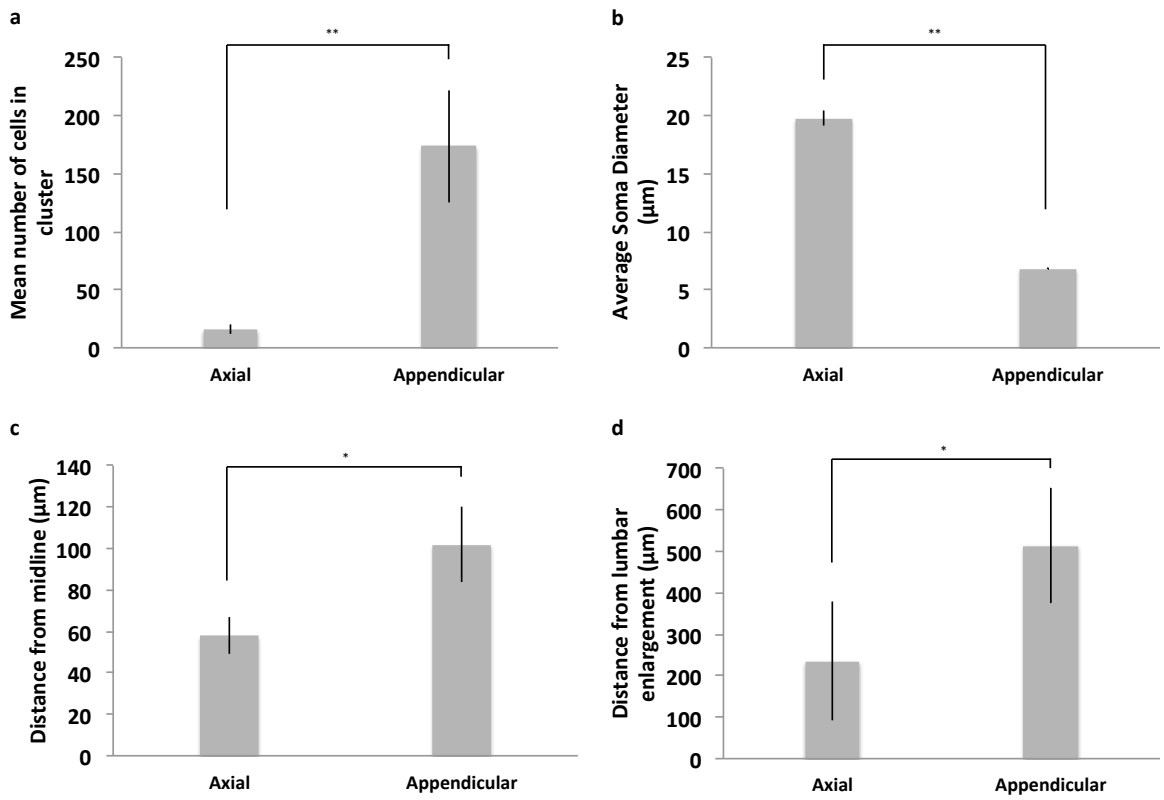

Fig. 9 Lumbar axial and appendicular soma parameter quantification for pro-metamorphic *Xenopus* after staining of MNs innervating axial post-otic segments 11 & 12, as well as the hindlimb. a. The mean number of cells in each cluster is significantly greater in appendicular clusters (t=3.42, df 7, p=0.01, n=8). b. The average soma diameter is significantly greater in axial cells (t=9.19, df=7, p<0.01, n=8). c. The distance of the middle of the cluster from the cord midline is significantly greater in appendicular clusters (t =3.86, df 4, p<0.05, n=5). d. The distance from the lumbar enlargement to the rostral-most tip of the cluster is significantly greater in appendicular clusters (t =2.81; df 8; p<0.05, n=8). Values are means, and error bars represent ±SEM; paired t-test used, with ** = p<0.01, * = p<0.05.

as determined by a paired t-test ($t = 3.86$, df 4, $p<0.05$, $n=5$), meaning that the axial clusters are positioned medially to the hindlimb clusters in the cord.

IIIA IID. ROSTROCAUDAL DISTANCE

The distance from the widest part of the lumbar enlargement to each of the axial- and appendicular-MN clusters was assessed (Fig. 9 d). The rostral-most tip of the axial clusters averaged 253.13µm ± 142.85SEM, while hindlimb clusters averaged 513.63µm ± 138.12SEM from the widest part of the lumbar enlargement. A paired t-test found a significant difference in the rostrocaudal positioning of axial and hindlimb MN clusters along the spinal cord, with the axial MN clusters occupying a more rostral space in the cord than the hindlimb MN clusters ($t = 2.81$; df 8; $p<0.05$, $n=8$).

IIIA III. LUCIFER YELLOW CAN BE USED TO BACKFILL MNS WITH LIMITED SUCCESS

Attempts were made to use Lucifer Yellow as a backfilling agent, both alone and in conjunction with dextran-rhodamine in differential application to the axial and hindlimb musculature as outlined above with the two fluorescent dextran conjugates (Fig. 6, 8). This is due to the fact that Lucifer Yellow is known to pass freely through GJs (Piccolino, Neyton & Gerschenfeld, 1984), whereas the fluorescently-conjugated dextran particles were on the upper limit of what could pass through in terms of particle size. While it is possible for Lucifer Yellow to backfill MNs in the spinal cord (examples of successful attempts in Fig. 10), this technique was not successful enough to have sufficient sample sizes in order to run appropriate statistical analyses. First of all, the Lucifer Yellow only backfilled MNs when applied to the axial tissue, not the hindlimb tissue. In total, 26 cords were backfilled with Lucifer Yellow applied to the axial tissue and dextran-rhodamine to the appendicular tissue

across all three conditions: control, 100µM 18-β-GA, and 200µM CBNX. Under the confocal-like microscope, only five of these cords appeared to have been successfully backfilled with both populations labelled across all three of these conditions (Fig. 10 b-d). The idea behind this experiment was that there should be a reduction in the number of co-labelled cells in the presence of gap junction blocker; this was found with a small sample size in an undergraduate project using 200µM CBNX only. This experiment needed to be repeated with a higher sample size and more drugs, namely the less "dirty" 100µM 18-β-GA in addition to 200µM CBNX again. However, these drug conditions were attempted with the Lucifer Yellow/dextran-rhodamine preparations which yielded a low success rate. Therefore, although it is evident from the double dextran-fluorophore conjugate labelling that these two MN pools have different cell properties, exist adjacent to each other in the spinal cord and interact to a limited extent as evidenced by cell co-labelling, more backfilling experiments will need to be performed with the addition of gap junction blockers in the future to assess the role of GJs in connectivity between the axial and limb MN networks.

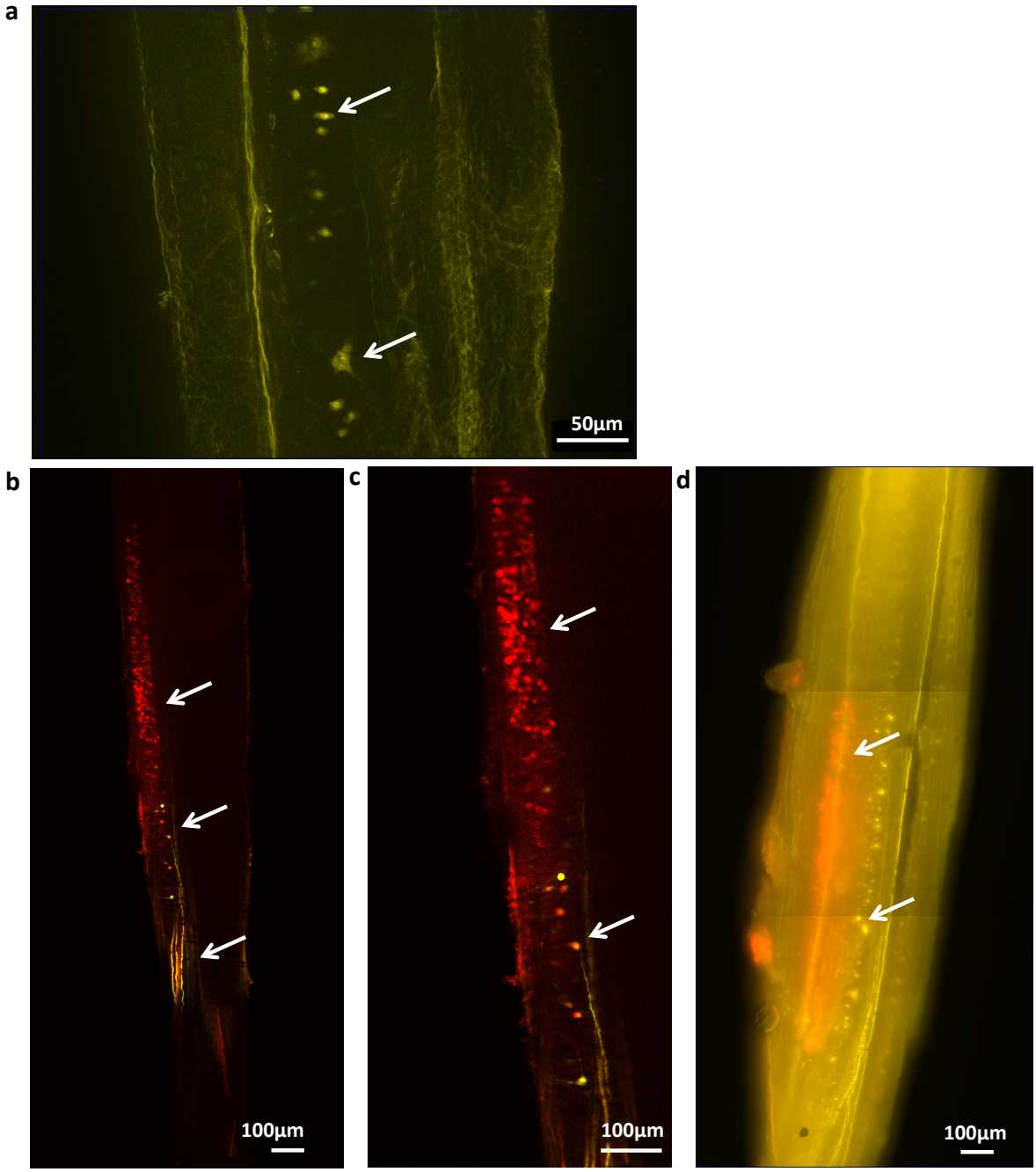

Fig. 10 Lucifer Yellow labels axial MNs in the lumbar spinal cord during pre- and early metamorphic stages with limited success. a. Orthogonal view of a maximum intensity projection of a cord labelled via axial muscles exclusively with Lucifer Yellow at 10x magnification; top arrow points to a smaller MN, bottom arrow points to a larger MN. b. Orthogonal view of a maximum intensity projection cord labelled with Lucifer Yellow (11^{th} - 12^{th} axial post-otic segments) and dextran-rhodamine (hindlimb, red) dyes at 10x. Top arrow points to a cluster of hindlimb MNs (red), middle arrow points to a cluster of axial MNs (yellow), and bottom arrow points to the ventral root through which the dye was retrogradely transported. c. Enlarged view of (b), top arrow points to a hindlimb MN cluster (red), bottom arrow points to an axial MN which appears to be co-labelled (red with yellow). d. Orthogonal view of a maximum intensity projection cord labelled with Lucifer Yellow (11^{th} - 12^{th} axial post-otic segments) and dextran-rhodamine (hindlimb, red) dyes at 10x in the presence of gap junction blocker 100µM 18-β-GA. Top arrow points to a cluster of hindlimb MNs (red), and bottom arrow points to a cluster of axial MNs (yellow).

IIIB. ELECTROPHYSIOLOGY

IIIB I. A ROLE OF GAP JUNCTIONS IN THE AXIAL SWIMMING CPG: ELECTRICAL COUPLING AFFECTS EVOKED FICTIVE LOCOMOTOR OUTPUT

Rhythmic rostrocaudally-propagated waves of locomotor activity which alternate across the spinal cord and propagate with an intersegmental delay are generated by the axial CPG, and have been described *in vitro* in the late pre-metamorphic (stages 50-54) and early metamorphic stages (55-58) (e.g., Combes et al., 2004). This motor pattern recorded *in vitro* would normally propel the animal forward in an aqueous environment. During metamorphosis, at the onset of limb bud development, the lumbar enlargement emerges. It contains the developing appendicular pattern-generating circuitry, however recordings made caudally to VR projections from the lumbar enlargement (after VR 10) represent fictive locomotor activity in the tail-swimming axial system.

In the present study, a possible role for coupling via gap junctions was first tested within the axial tail-swimming CPG in preparations where fictive locomotion was evoked electrically via stimulation to the optic tectum (Currie, 2013)(Fig. 11). Extracellular ventral root (VR) recordings were made from VR 17-20 in stage 53-58 animals to examine the effect of GJ block on fictive locomotor output of this axial system. This should elucidate any role for GJs within the axial system itself in metamorphosing animals, which will enable comparison with their role in younger stages (Li et al., 2009; Zhang et al., 2009).

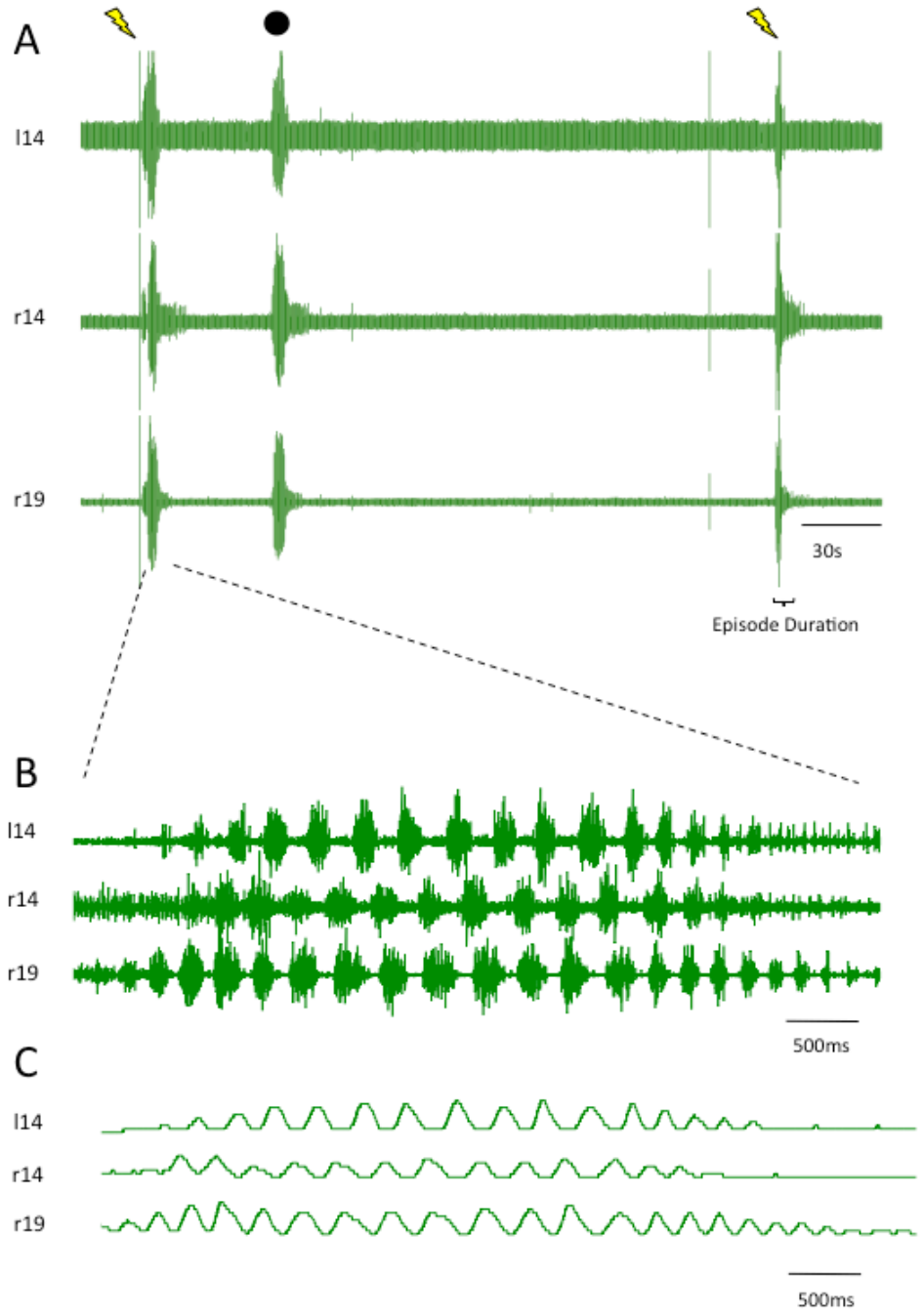

Fig. 11 The electrically elicited fictive locomotor response of the pro-metamorphic *Xenopus laevis* axial spinal cord exhibits left-right alternation and rostrocaudal delay. (A) A representative extracellular recording showing the coordination of *elicited* fictive locomotor ventral root rhythm in the control condition, with (B) an expanded timebase showing a sample episode and (C) corresponding rectified integrated traces for clarity. The lighting bolt represents electrically stimulated episodes, and the circle represents a spontaneous episode. The episode duration parameter is also denoted in (A).

IIIB II. Electrical Stimulation via the Optic Tectum is Sufficient to Evoke Fictive Locomotor Output

In the control condition, electrical stimulation of the optic tectum (delivered via a glass suction electrode; Currie, 2013; refer to Methods in section II) elicits episodes of fictive swimming activity (Fig. 11 A; evoked episodes denoted by the lightning bolt). These were elicited at 2, 3, or 4-minute intervals. This varied by preparation, depending on the amount of time each individual preparation required to recover fully from a preceding bout of activity; however, the stimulation interval was constant within any given single preparation in all control, drug, and wash conditions. Occasionally, preparations exhibited spontaneous activity in addition to the evoked episodes (Fig. 11 A; spontaneous episode denoted by the circle). Using three recording electrodes, an expanded timebase (Fig. 11 B and C) illustrates the left-right alternation and rostrocaudal delay in both raw and rectified/integrated traces, which is characteristic of fictive locomotor output in the pro-metamorphic *Xenopus* preparation (e.g., Combes et al., 2004; Currie, 2013).

IIIB III. Gap Junction Blockade Alters Axial Swimming Parameters in Electrically Stimulated Preparations

To test the extent and role of electrical coupling within the axial CPG, two gap junction blockers (18-β-GA (100µM; 200µM) or CBNX (200µM)) were bath applied. Drug concentrations were selected based on what has been previously published on this preparation, albeit at earlier stages of development (Li et al., 2009; Zhang et al., 2009) (Figs. 12-15). The drug period was selected after a minimum of 35 minutes, as these drugs require at least 35 minutes to reach the full gap junction blocking effect (Li et al., 2009; Zhang et al., 2009). Addition of 100µM 18-β-GA yielded several significant changes in swimming burst parameters (Fig. 12 Bi-Biv; Fig. 13 A-F). The mean burst duration increased

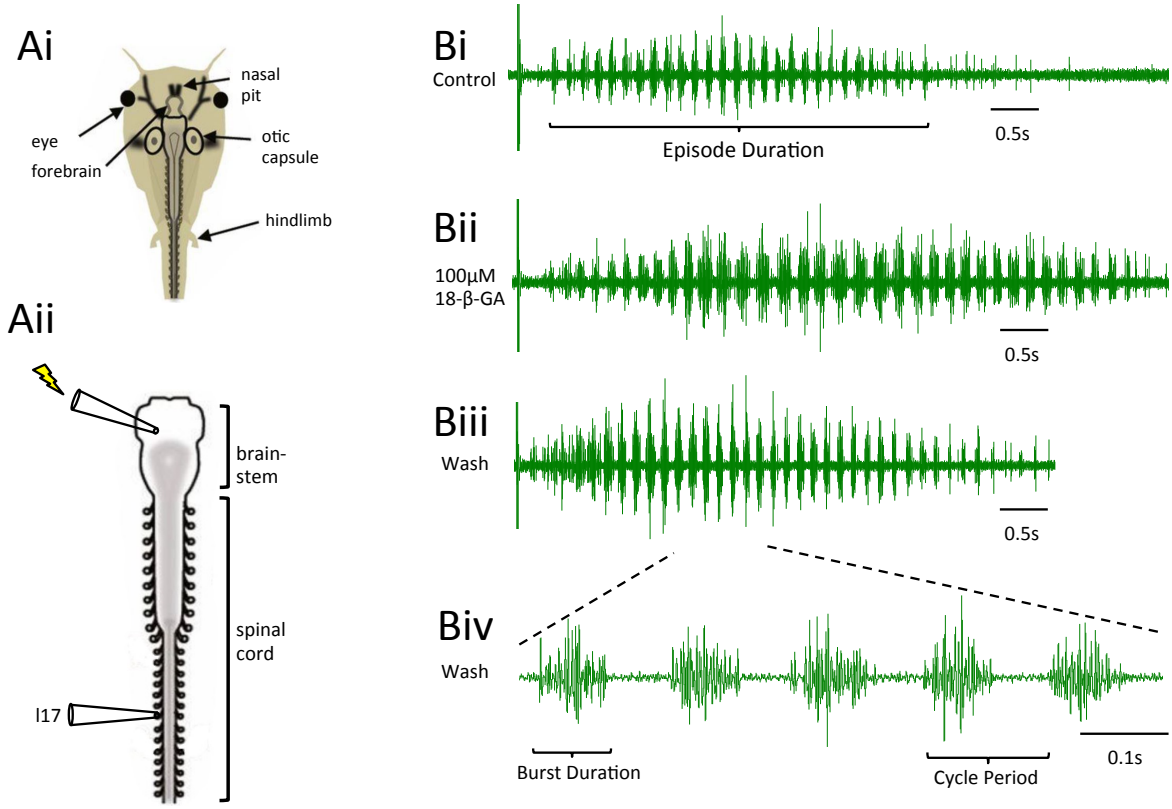

Fig. 12 Electrical stimulation of the optic tectum is sufficient to evoke rhythmic elicited fictive locomotor output from the pro-metamorphic *Xenopus laevis* axial spinal cord in the presence of the gap junction blocker 18-β-glycyrrhetinic acid (18-β-GA; 100µM). (Ai) Schematic of stage 56 larva, showing the approximate location of the central nervous system (taken from Currie et al., 2016; also used in subsequent figures). (Aii) Schematic of the isolated brainstem/spinal cord preparation with a glass suction stimulating electrode (denoted by the lightning bolt) on the optic tectum and a glass suction recording electrode on a tail VR (adapted from Currie et al., 2016; also used in subsequent figures). (Bi-iii) Representative extracellular VR recordings of fictive locomotor episodes in control, drug and wash conditions; the episode duration parameter is depicted. (Biv) Expanded time base of the wash condition depicting swim parameters burst duration and cycle period.

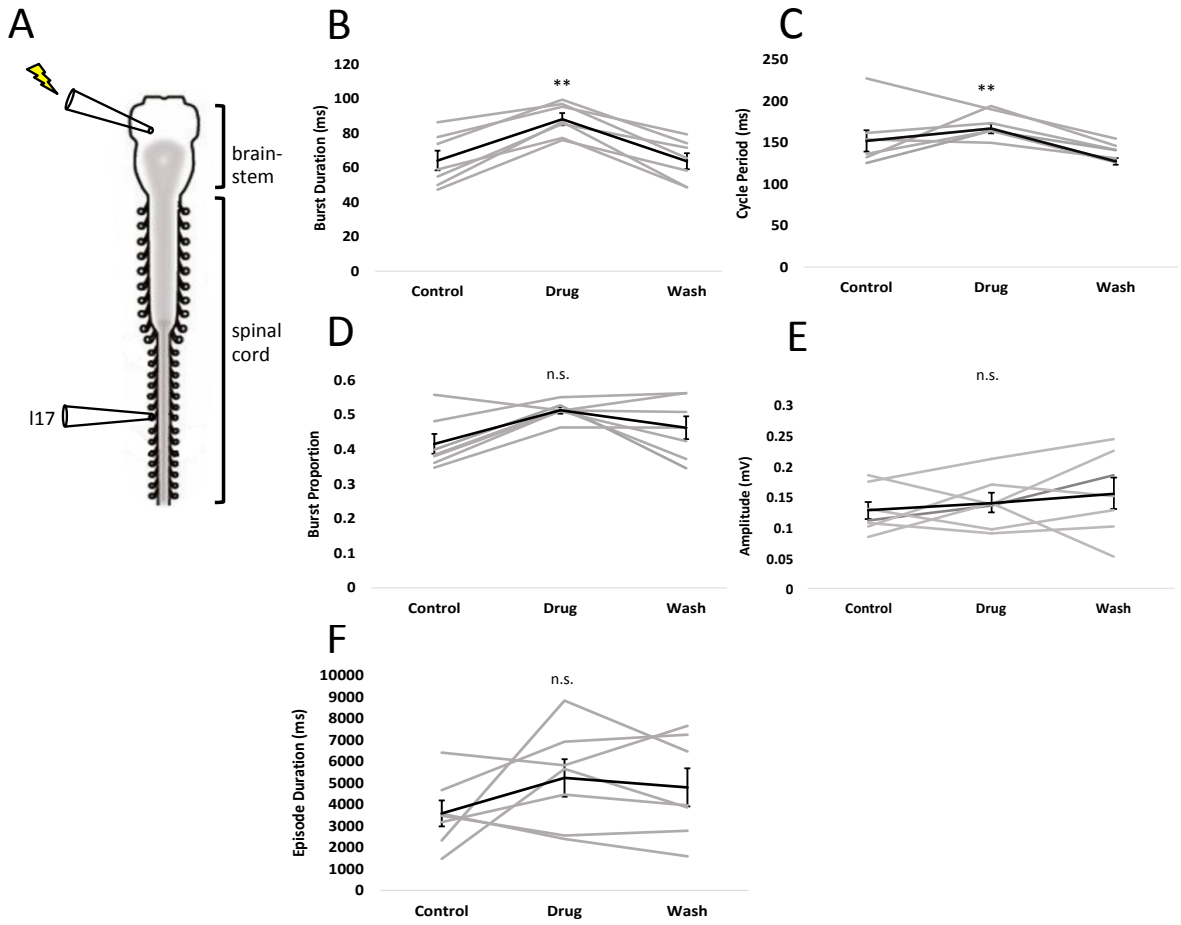

Fig. 13 Analysis of electrically elicited fictive axial locomotor responses of the pro-metamorphic *Xenopus laevis* axial spinal cord in the presence of the gap junction blocker 18-β-glycyrrhetinic acid (18-β-GA; 100µM). (A) Schematic of the pro-metamorphic isolated brainstem/spinal cord preparation with a glass suction stimulating electrode (denoted by the lightning bolt) on the optic tectum and a glass suction recording electrode on a tail ventral motor root. (B-F) Burst and episode parameters: grey lines represent individual preparations, and black lines represent the average of all preparations. (B) Burst duration increases following gap junction blockade ($F=8.7$, $p<0.01$, $n=7$). (C) Cycle period increases with gap junction blockade ($F=11.16$, $p<0.01$, $n=6$). (D) Burst proportion (burst duration/cycle period) increases (but not significantly) with gap junction blockade ($n=7$). (E) Burst amplitude is unaffected by gap junction blockade ($n=7$). (F) Episode duration do not change significantly with gap junction blockade but does not reach statistical significance ($n=7$). Repeated measures ANOVA with Bonferroni correction; error bars represent ±SEM. ** = $p<0.01$.

significantly from control (64.2ms ± 5.7SEM) to drug (88.2ms ± 3.6SEM) ($F=8.7$, $p<0.01$, $n=7$) (Fig. 12 B), and the mean cycle period also increased significantly (control 155.5ms ±12.9SEM; drug 171.8ms ±5.9SEM) ($F=11.16$, $p<0.01$, $n=6$) (Fig. 13 C). However, the burst proportion (burst duration/cycle period), burst amplitude, and episode duration were not significantly affected by the gap junction blocker (Fig. 13 D-F).

As 18-β-GA is considered a more selective gap junction blocker with fewer off-target side effects than CBNX (Li et al., 2009), a higher dose of 200μM 18-β-GA was applied to explore the dose dependency of the effect (Fig. 14). However, the effect was so severe that eventually no activity could be elicited. This effect was measured both by the sheer number of episodes in a 20-minute period (control 6.2 episodes ±0.6SEM; drug 0 episodes ±0SEM) ($F=18.22$, $p<0.01$, $n=5$) (Fig. 14 C), as well as the percent success in eliciting an episode in each condition (control 96% success ±4SEM; drug 0 % success ±0SEM) ($F=18.5$, $p<0.01$, $n=5$) (Fig. 14 D). As activity was completely abolished in the drug condition, burst and episode parameters could not be quantified to compare with control. Partial wash indicates that the preparation was not killed by the drug. Therefore, at a high enough concentration, gap junction block abolishes evoked axial output.

Similar to 100μM 18-β-GA, the addition of a different gap junction blocker, 200μM CBNX, also affected locomotor activity (Fig. 15). Specifically, as in 100μM 18-β-GA, the burst duration was also significantly increased (control 45.8ms ±1.9SEM; drug 60.3ms ±3.9SEM) ($F=4.03$, $p<0.05$, $n=10$) (Fig. 15 C). Similarly, the burst proportion, burst amplitude, and episode duration were also unaffected by the gap junction block (Fig. 15 E-G). However,

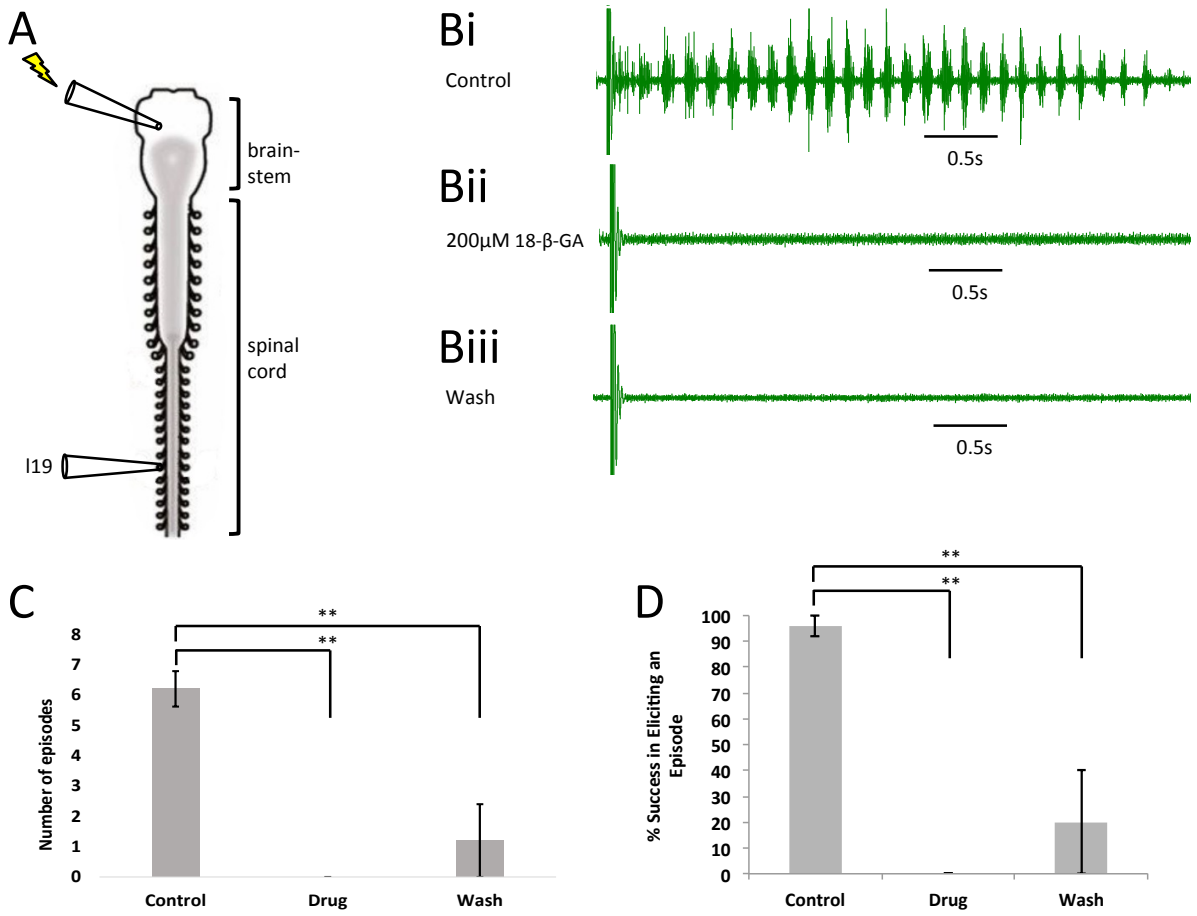

Fig. 14 Electrically elicited fictive axial locomotor response of the pro-metamorphic *Xenopus laevis* axial spinal cord is blocked by the gap junction blocker 18-β-glycyrrhetinic acid (18-β-GA; 200µM). (A) Schematic of the pro-metamorphic isolated brainstem/spinal cord preparation with a glass suction stimulating electrode (denoted by the lightning bolt) on the optic tectum and a glass suction recording electrode on a tail ventral motor root. (Bi-iii) Representative extracellular recordings of a fictive locomotor ventral root bursting episode from a single preparation in control, drug and wash conditions. (C) Number of elicited episodes in a 20 minute period decreases with gap junction blockade; rhythmic activity is abolished ($F=18.22$, $p<0.01$, $n=5$). (D) Percent success in eliciting an episode decreases to zero with gap junction blockade ($F=18.5$, $p<0.01$, $n=5$). Repeated measures ANOVA with Bonferroni correction; error bars represent ±SEM. ** = $p<0.01$.

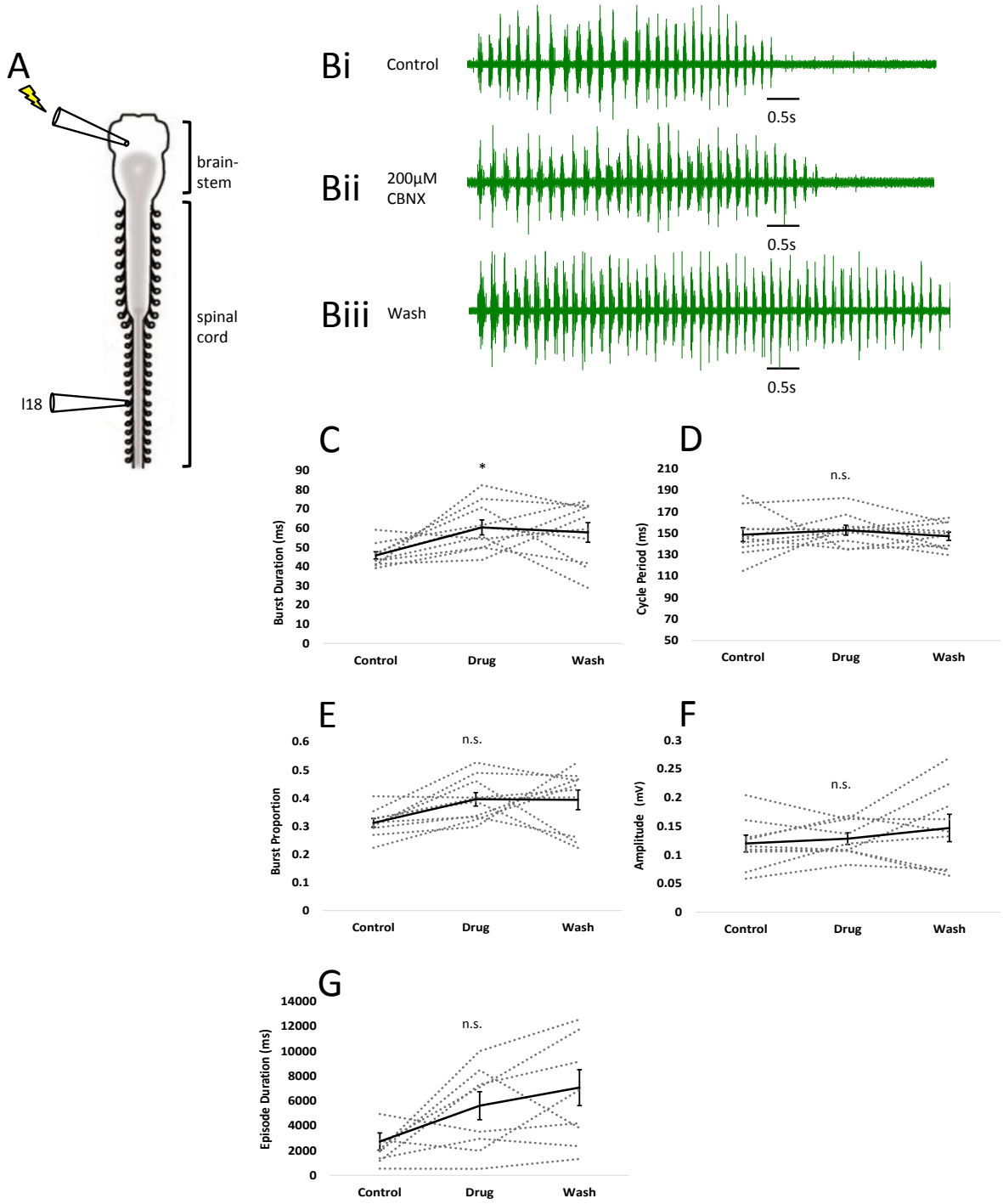

Fig. 15 Electrically elicited fictive axial locomotor response of the pro-metamorphic *Xenopus laevis* axial spinal cord in the presence of the gap junction blocker Carbenoxolone (CBNX; 200µM). (A) Schematic of the pro-metamorphic isolated brainstem/spinal cord preparation with a glass suction stimulating electrode (denoted by the lightning bolt) on the optic tectum and a glass suction recording electrode on a tail ventral motor root. (Bi-iii) Representative extracellular recordings of a fictive locomotor ventral root bursting episode from a single preparation in control, drug and wash conditions. (C-G) Burst and episode parameters: grey lines represent individual preparations, and black lines represent the average of all preparations. (C) Burst duration increases with gap junction blockade ($F=4.03$, $p<0.05$, $n=10$). (D) Cycle period is unaffected by gap junction blockade ($n=10$). (E) Burst proportion (burst duration/cycle period) is unaffected by gap junction blockade ($n=10$). (F) Burst amplitude is unaffected by gap junction blockade ($n=10$). (G) Episode duration is unaffected by gap junction blockade ($n=10$). Repeated measures ANOVA with Bonferroni correction; error bars represent ±SEM. * = $p<0.05$.

whereas 100µM 18-β-GA yielded a significant increase in cycle period, this was not the case in 200µM CBNX (Fig. 15 D). Taken together, these results suggest gap junction block slows the axial rhthm.

IIIB IV. SPONTANEOUS FICTIVE LOCOMOTOR OUTPUT OCCURS IN PRE-METAMORPHIC TADPOLES WITH THE SAME RHYTHMIC PATTERN SEEN IN EVOKED OUTPUT

As indicated by the occasional bouts of spontaneous locomotor activity in (Fig. 11 A; denoted by the circle), it is possible for pre-metamorphic *Xenopus laevis* tadpoles to exhibit activity without the need for stimulation (electrical, tactile; Combes et al., 2004; Currie et al, 2016). This is also illustrated by an excerpt of activity from an experiment from the control condition (Fig. 16 A; spontaneous episodes denoted by circles). Similar to activity in evoked preparations, this spontaneous activity also occurs in episodes, with bursts exhibiting left-right alternation and rostrocaudal delay. This is evident both in raw and rectified/integrated traces (Fig. 16 B and C), and it corresponds to ventral root output necessary for alternating contractions required for propulsive swimming in an aqueous environment. Thus, the locomotor output occurring spontaneously is effectively the same as that evoked by electrically stimulating the optic tectum.

IIIB V. GAP JUNCTION BLOCKADE ALTERS AXIAL SWIMMING PARAMETERS IN PREPARATIONS WITH SPONTANEOUS OUTPUT

Again, to test the extent of electrical coupling within the axial CPG, the same gap junction blockers: 18-β-GA (100µM; 200µM) CBNX (200µM) were bath applied (Figs. 17, 18, 19). However, two drug periods were tested, as it was noted that a spike in spontaneous episode frequency occurred shortly after the addition of drug. Therefore, the first drug period comprised the first 20 minutes after the first episode immediately following drug

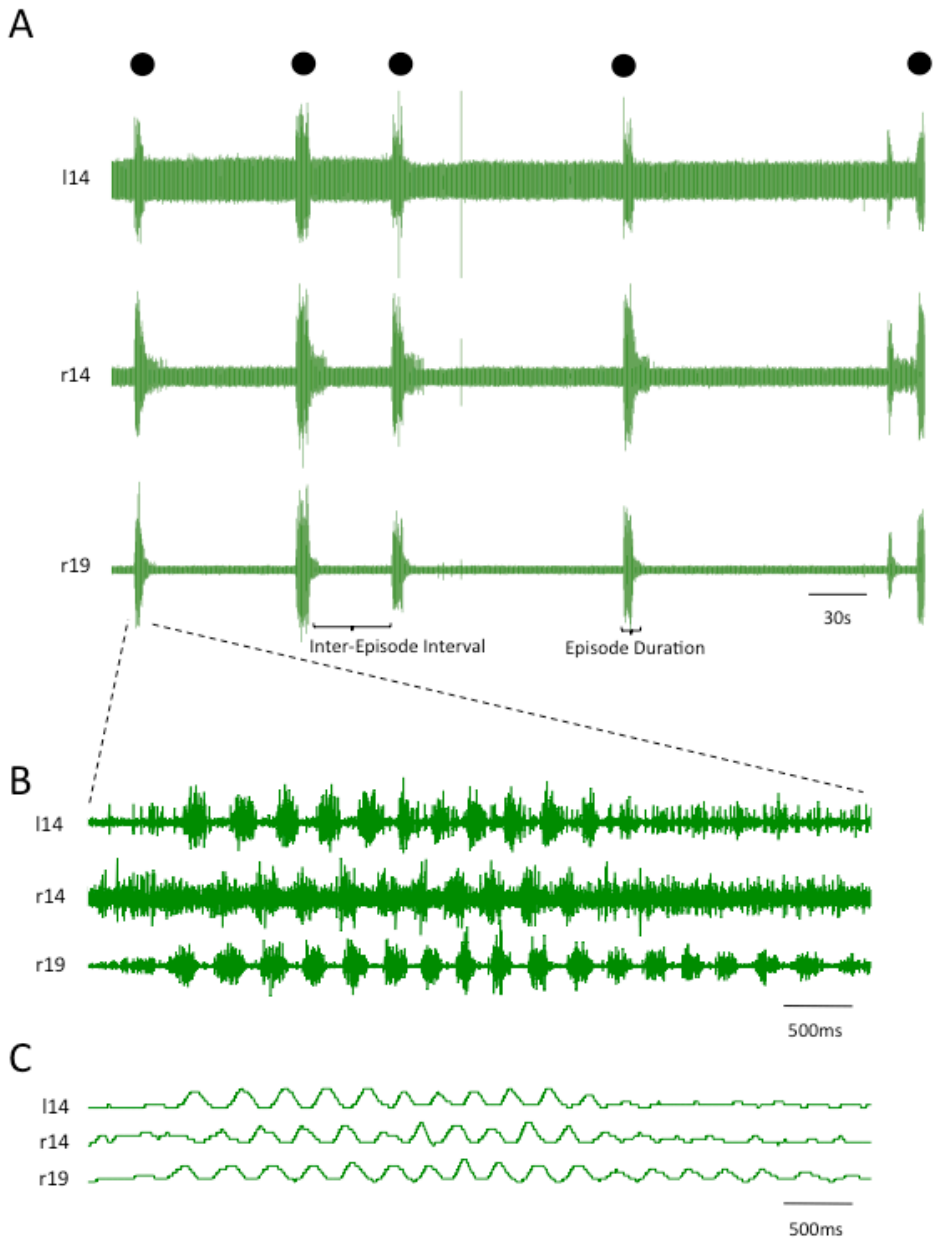

Fig. 16 The spontaneous fictive locomotor activity of the pro-metamorphic *Xenopus laevis* axial spinal cord exhibits left-right alternation and rostrocaudal delay. (A) Representative extracellular recording showing the coordination of spontaneous fictive locomotor ventral root episodes in the control condition, with (B) an expanded timebase showing a sample episode and (C) corresponding rectified integrated traces for clarity (n=5). In (A), the circle represents spontaneous episodes, and the episode duration and inter-episode interval parameters are also denoted.

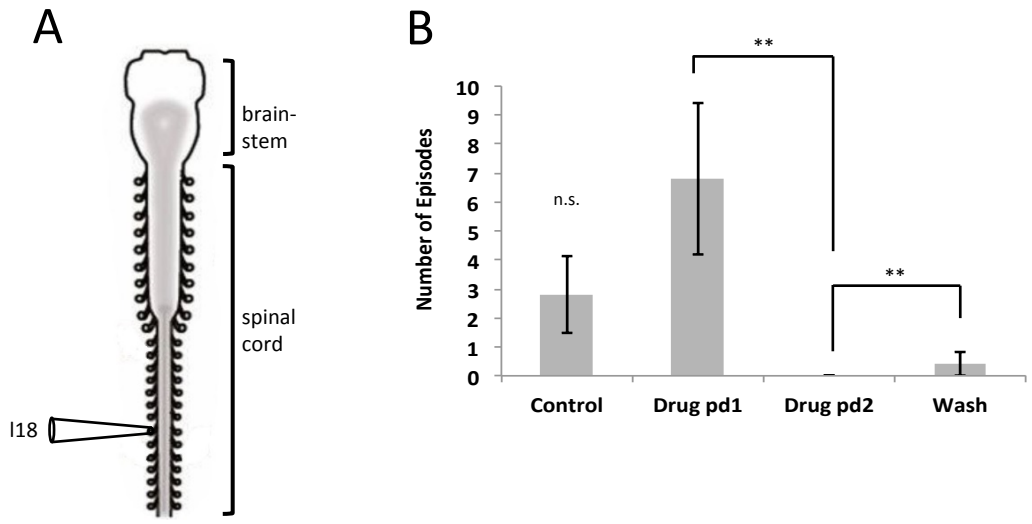

Fig. 17 Spontaneous fictive axial locomotor response of the pro-metamorphic *Xenopus laevis* axial spinal cord in the presence of the gap junction blocker 18-β-glycyrrhetinic acid (18-β-GA; 100µM). (A) Schematic of the pro-metamorphic isolated brainstem/spinal cord preparation with a glass suction recording electrode on a tail ventral motor root. (B) The number of episodes in a 20 minute period decreases significantly with prolonged gap junction blockade, with a partial wash ($F=5.57$, $p<0.01$, $n=5$). Repeated measures ANOVA with Bonferroni correction; error bars represent ±SEM. ** = $p<0.01$.

application, and the second drug period comprised 20 minutes after a minimum of 35 minutes drug exposure. With exposure of both 18-β-GA concentrations, activity was abolished in the second drug period; and with exposure to CBNX, the number of episodes in the second period was also dramatically reduced from the first drug period (Figs. 17, 18, 19). This suggests that gap junction block reduces or abolishes axial CPG output.

Addition of 100μM 18-β-GA produced only a significant increase from drug period one to drug period two, and there was a significant partial wash from drug period two to wash (control: 2.8 episodes ±1.3SEM; drug period one: 6.8 episodes ±2.6SEM; drug period two: 0 episodes ±0SEM; wash: 0.4 episodes ±0.4SEM) ($F=5.57$, $p<0.01$, $n=5$) (Fig. 17). The number of episodes in any 20-minute period is related to the inter-episode interval, or frequency. However, as it was not uncommon to have zero spontaneous episodes in certain conditions (control: 2/5 preps exhibited no episodes; drug period two: all preps exhibited zero episodes; wash: 4/5 preps exhibited no episodes), this made it impossible to calculate inter-episode interval on these occasions as there was insufficient data to do so. An attempt was made also to analyse any difference in episode duration; but, due to the same fact that many conditions contained periods of no activity, this parameter was also unable to be calculated across all conditions.

Addition of 200μM CBNX produced a very similar temporal profile of effects to that of 100μM 18-β-GA, in terms of number of episodes across conditions (Fig. 18). Again, the decrease in number of episodes between drug period one and drug period two was

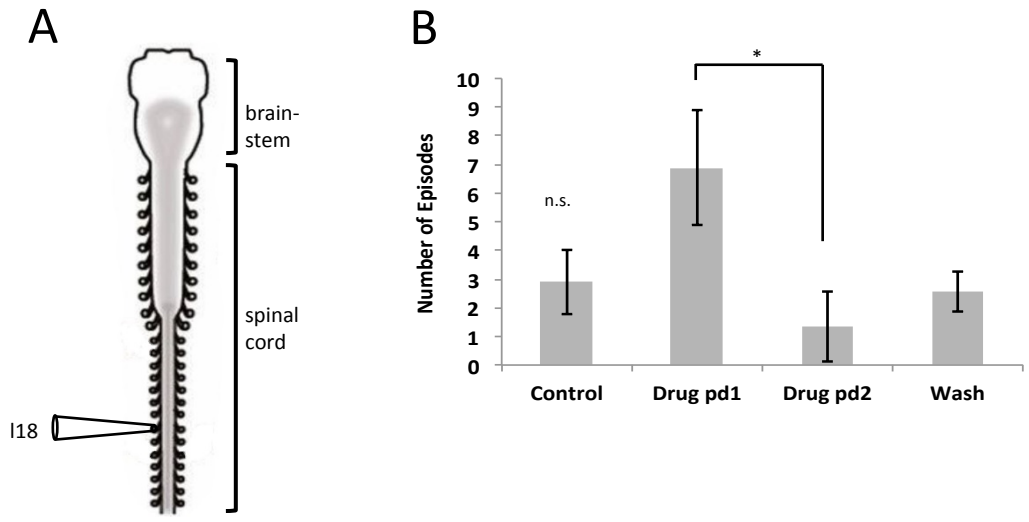

Fig. 18 Spontaneous fictive axial locomotor response of the pro-metamorphic *Xenopus laevis* axial spinal cord in the presence of the gap junction blocker Carbenoxolone (CBNX; 200µM). (A) Schematic of the pro-metamorphic isolated brainstem/spinal cord preparation with a glass suction recording electrode on a tail ventral motor root. (B) The number of episodes in a 20 minute period decreases significantly with prolonged gap junction blockade ($F=3.18$; $p<0.05$; $n=9$). Repeated measures ANOVA with Bonferroni correction; error bars represent ±SEM. * = $p<0.05$.

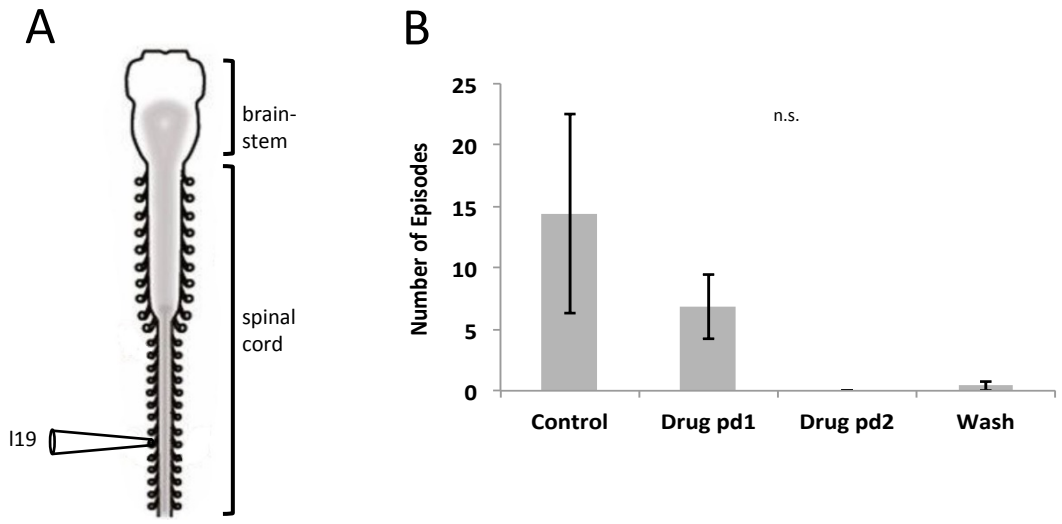

Fig. 19 Spontaneous fictive axial locomotor response of the pro-metamorphic *Xenopus laevis* axial spinal cord in the presence of the gap junction blocker 18-β-glycyrrhetinic acid (18-β-GA; 200µM). (A) Schematic of the pro-metamorphic isolated brainstem/spinal cord preparation with a glass suction recording electrode on a tail ventral motor root. (B) The number of episodes is not affected by gap junction blockade (n=5). Repeated measures ANOVA with Bonferroni correction.

significant. However, the wash was unsuccessful in this condition (control: 2.9 episodes ±1.1SEM; drug period one: 6.9 episodes ±2.0SEM; drug period two: 1.3 episodes ±1.2SEM; wash: 2.6 episodes ±0.7SEM) ($F=3.18$; $p<0.05$; $n=9$). Again, episode duration was calculated with an incomplete set of data: 6/9 preparations exhibited episodes in both control and the first drug period. In this instance, there was still no significant difference between the episode durations of control and the first drug period (data not shown). However, the significant decrease in number of episodes between drug periods one and two suggests gap junction block reduces excitability of the axial CPG.

Application of 200µM 18-β-GA created a different episode profile to both 100µM 18-β-GA and 200µM CBNX across conditions, however none of the values proved to be significantly different across conditions (control: 14.4 episodes ±8.0SEM; drug period one: 7.2 episodes ±2.9SEM; drug period two: 0 episodes ±0SEM; wash: 0.4 episodes ±0.4SEM) ($F=2.51$; $p=0.18$; $n=5$) (Fig. 19). As seen with the evoked experiments (Results section IIIB iii), it is likely that 200µM 18-β-GA is too high a concentration for this particular preparation, and therefore results from 100µM 18-β-GA should be trusted instead.

IIIB VI. A ROLE OF GAP JUNCTIONS BETWEEN THE AXIAL AND LIMB CPGS: ELECTRICAL COUPLING AFFECTS EVOKED FICTIVE LOCOMOTOR OUTPUT

During the transitional period of metamorphosis, *Xenopus laevis* tadpoles develop limbs that gain function while the tail still plays an active role in locomotion for one to two weeks before it is resorbed (Combes et al., 2004; Nieuwkoop and Faber, 1956). In pro-metamorphic stages 55-59, the limbs are present, but not yet fully functional on their own, as they rely on the rhythm provided by the axial CPG (Combes et al., 2004; also refer to Introduction Section Ia). Since the appendicular system initially adopts the rhythm of the

axial system before developing its own divergent rhythm during these critical developmental stages, it is important to tease apart the interconnectivity between these two systems in terms of how they interact and the mechanism(s) by which their rhythms are first coupled and then segregate; in this instance, the potential mechanism of gap junctions was probed. To this end, the rhythmic output of the limb VRs was recorded in animals from stages 55/56 to 58; these VRs (rostrocaudally 8^{th}-10^{th}) project from the emerging lumbar enlargement, which contains the developing appendicular CPG. The limb output shown here is first characterised on its own in terms of burst and episode parameters in control and in the presence of a gap junction blocker. Additionally, simultaneous recordings of axial and limb VR output were recorded and analysed to investigate the role of gap junctions in coupling these two systems. 18-β-GA is known to have fewer off-target effects than CBNX (Li et al., 2009, and refer to Results section IIIB iii) and the appropriate dose for this preparation in the axial experiments (Results section IIIB iii) was found to be 100µM. Therefore only this drug at this concentration (100µM 18-β-GA) was used in the following limb and coupling experiments. Again, the drug period was selected after a minimum of 35 minutes, as these drugs require at least 35 minutes to reach the full gap junction blocking effect (Li et al., 2009; Zhang et al., 2009).

IIIB VII. OPTIC TECTUM SIMULATION PRODUCES SIMULTANEOUS AXIAL AND APPENDICULAR LOCOMOTOR OUTPUT

Stimulation of the optic tectum not only produces a reliable response of the axial system (refer to Results section IIIB ii), but it also produces a simultaneous response of the limb

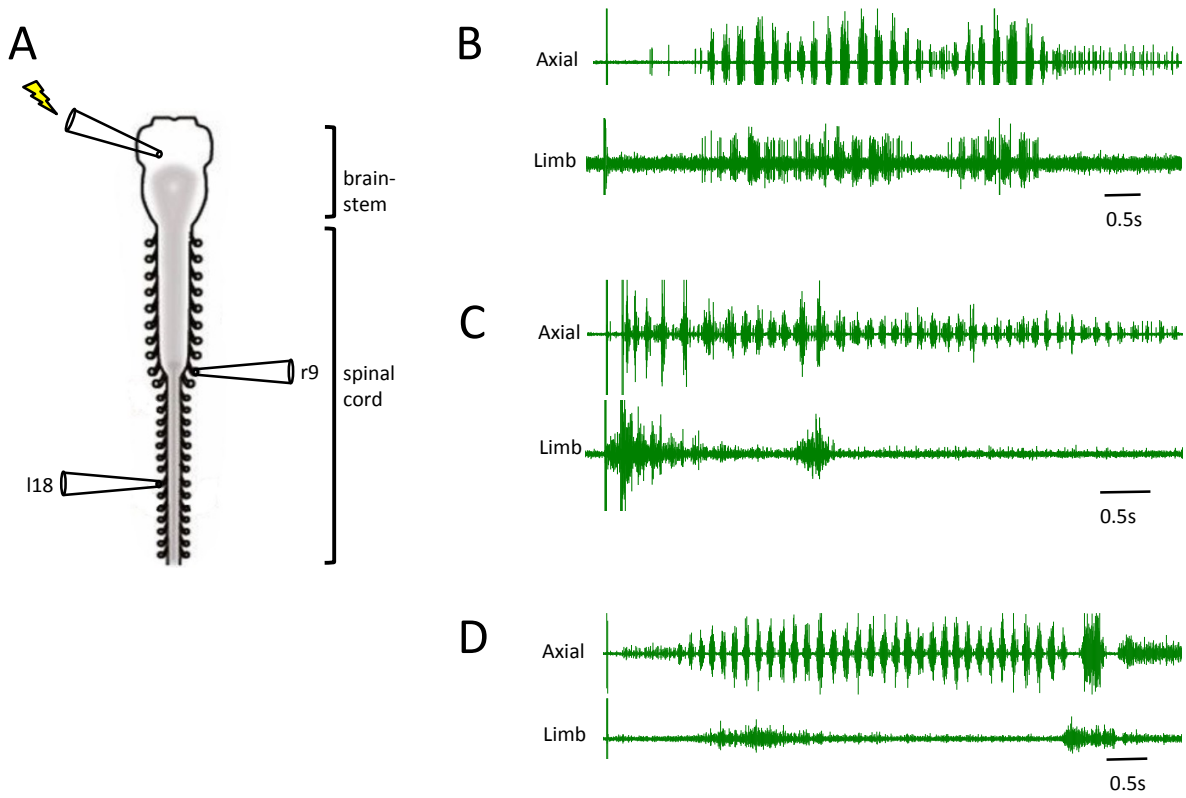

Fig. 20 Electrical stimulation of the optic tectum is sufficient to evoke simultaneous axial and limb rhythmic fictive locomotor output from the pro-metamorphic *Xenopus laevis* spinal cord. (A) Schematic of the isolated brainstem/spinal cord preparation with a glass suction stimulating electrode (denoted by the lightning bolt) on the optic tectum and a glass suction recording electrode on a tail VR and limb VR. (B) Representative extracellular VR recording of a fictive locomotor episode from a stage 55/56 animal. (C) Representative extracellular VR recording of a fictive locomotor episode from a different stage 55/56 animal. (D) Representative extracellular VR recording of a fictive locomotor episode from a stage 58 animal.

system (Fig. 20) (quantification of limb burst parameters in Results section IIIB viii below). Fig. 20 shows the output of three different preparations at two different stages: 55/56 and 58. Preparations at stages 57 or 58 did not display axial involvement in the limb response, however those at stage 55/56 did to varying degrees (Fig. 20 B-D). This confirms findings in Combes et al. (2004) that, at younger metamorphic stages, the limb CPG uses the axial CPG as a slave oscillator, whilst as metamorphosis progresses, the limb CPG develops its own slower rhythm and segregates completely from the axial CPG rhythm. And during this time there is a gradual transition until the segregation is complete, with slight inter-animal variation (Fig. 20 B and C).

IIIB VIII. EVOKED APPENDICULAR LOCOMOTOR OUTPUT PARAMETERS ARE UNAFFECTED BY GAP JUNCTION BLOCKADE

First, optic tectum stimulation was used to elicit limb fictive locomotor responses (Fig. 21 A, Bi-Biii). While the average axial burst duration described previously (Results section IIIB iii) was 64.2ms ±5.7SEM (n=7), the average limb burst duration was considerably longer at 416.5ms ±90.3SEM. These two values are significantly different ($t=4.69$, $df=10$, $p<0.01$) (Fig. 21 F). A longer limb versus axial burst duration is consistent with findings from Combes et al. (2004). Additionally, each episode mostly contained only one (or occasionally two) limb VR bursts, therefore cycle period and burst proportion could not be quantified. The addition of 100µM 18-β-GA yielded no significant difference between conditions for the remaining parameters: burst duration, amplitude, and episode duration (Fig. 21 C-E), despite the fact that the amplitude of limb bursts appeared to decrease in many preparations (Fig. 21 Bi-Biii). Although the burst parameters, most notably burst duration increased in the axial system in the presence of both 100uM 18BGA and 200uM CBNX (refer

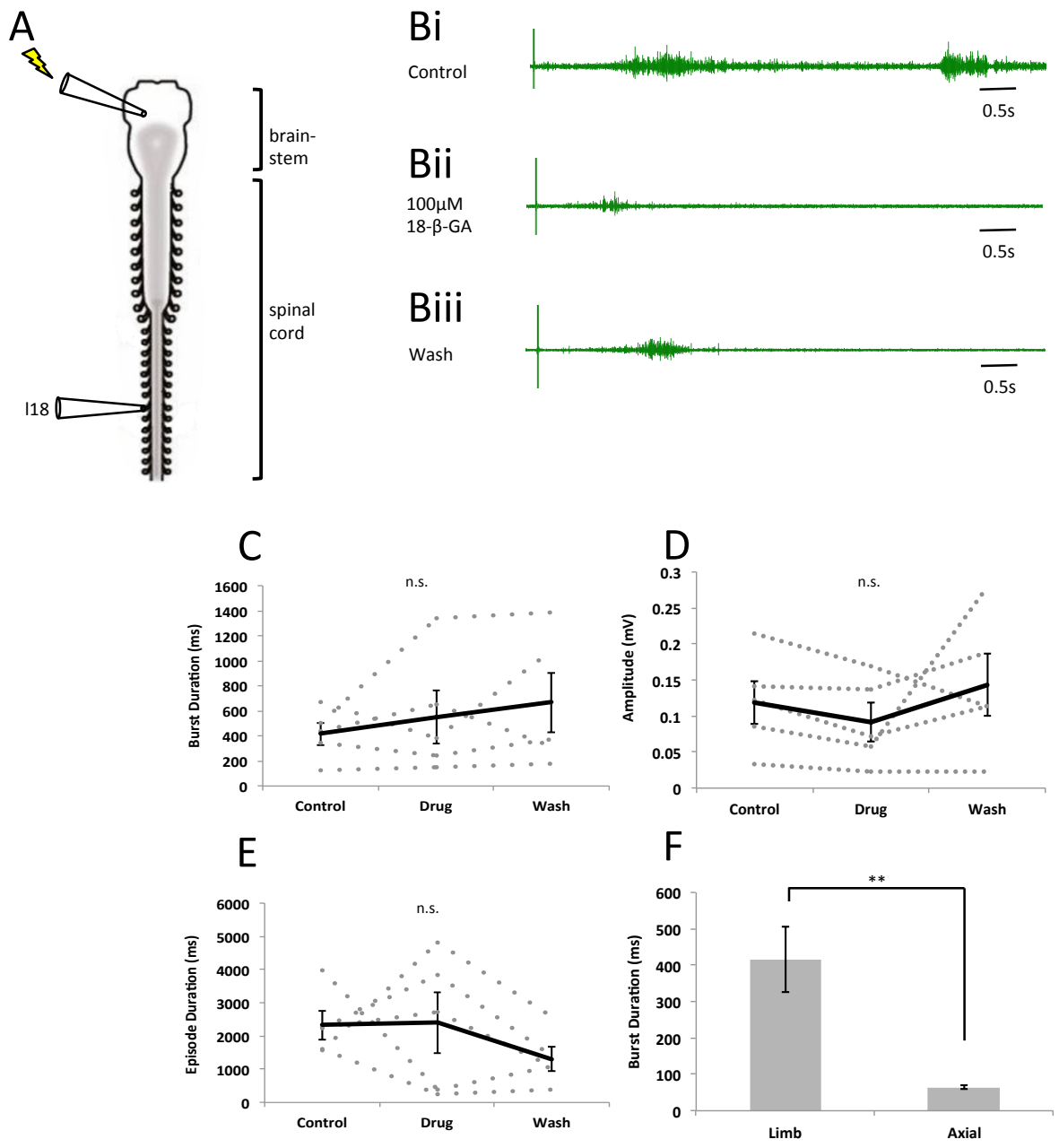

Fig. 21 Electrically elicited fictive locomotor limb response of the pro-metamorphic *Xenopus laevis* axial spinal cord in the presence of the gap junction blocker 18-β-glycyrrhetinic acid (18-β-GA; 100µM). (A) Schematic of the pro-metamorphic isolated brainstem/spinal cord preparation with a glass suction stimulating electrode (denoted by the lightning bolt) on the optic tectum, and glass suction recording electrodes on a tail ventral motor root and a limb ventral motor root. (Bi-iii) Representative extracellular recordings of a fictive locomotor limb ventral root bursting episode from a single preparation in control, drug and wash conditions. (C-E) Limb VR output parameters: grey lines represent individual preparations, and black lines represent the average of all preparations. (C) Burst duration is unaffected by gap junction blockade (n=5). (D) Amplitude is unaffected by gap junction blockade (n=5). (E) Episode duration is unaffected by gap junction blockade (n=5). (F) Limb burst duration is significantly longer than axial burst duration ($t=4.69$, $df=10$, $p<0.01$; limb n=5, axial n=7). Repeated measures ANOVA with Bonferroni correction (C-E) and paired t-test (F); error bars represent ±SEM. ** = $p<0.01$.

to Results section IIIB iii), no significant difference was found in any of the limb burst parameters here.

IIIB IX. OPTIC TECTUM-EVOKED SIMULTANEOUS AXIAL AND APPENDICULAR LOCOMOTOR EPISODE OUTPUT IS UNAFFECTED BY GAP JUNCTION BLOCKADE

Since optic tectum stimulation evokes simultaneous axial and appendicular output, the success in eliciting this simultaneous output in the presence of gap junction blockade was tested (Fig. 22). This was only testing the number of times the axial and/or limb VR produced an episode of output, and whether or not this output from both was simultaneous; burst and episode parameters have been quantified previously (Results section IIIB iii and viii) and are not discussed in this section. First, the total number of elicited episodes exhibiting simultaneous activity was unaffected by drug application (Fig. 22 B). This number was then converted into percent success in eliciting episodes in three different modalities with the addition of drug: simultaneous axial and limb output, axial output only, and limb output only (Fig. 22 C-E). This way, if there was a reduction in percent success in the drug condition with simultaneous output, it would be possible to tell if this was due to output failure from just one, or both of the axial or limb output. However, addition of 100µM 18-β-GA had no effect on percent success in eliciting an episode as a whole (axial, limb, or simultaneous) (Fig. 22 C-E): therefore, electrical stimulation of the optic tectum in the presence of a gap junction blocker was as effective at producing simultaneous axial and limb VR output as in control.

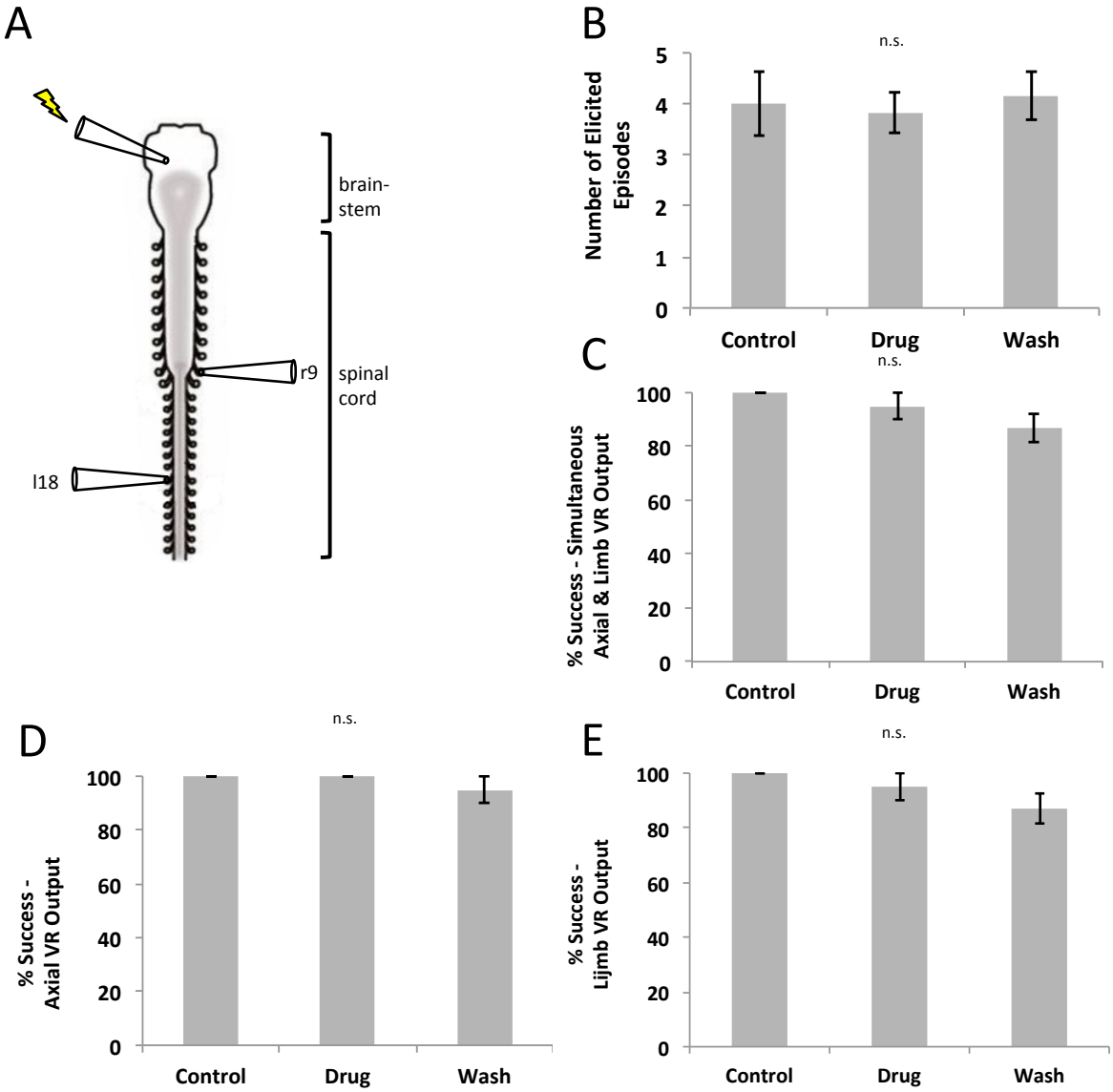

Fig. 22 Electrically elicited fictive coupled locomotor response of the pro-metamorphic *Xenopus laevis* axial and limb spinal cord in the presence of the gap junction blocker 18-β-glycyrrhetinic acid (18-β-GA; 100µM). (A) Schematic of the pro-metamorphic isolated brainstem/spinal cord preparation with a glass suction stimulating electrode (denoted by the lightning bolt) on the optic tectum, and glass suction recording electrodes on a tail ventral motor root and a limb ventral motor root. (B) Number of elicited episodes (simultaneous axial and limb response) in a 20 minute period is unaffected by gap junction blockade (n=5). (C-E) Percent success in eliciting an episode with simultaneous axial/limb VR output as well as individually axial VR only output or limb VR only output are unaffected by gap junction blockade/in the drug condition (n=5). Repeated measures ANOVA with Bonferroni correction; error bars represent ±SEM.

IIIB X. AXIAL VR-EVOKED SIMULTANEOUS AXIAL AND APPENDICULAR LOCOMOTOR EPISODE OUTPUT IS DECREASED WITH GAP JUNCTION BLOCKADE

Another way to test connectivity is to try stimulating an area other than the optic tectum. If the axial and limb systems are coupled, both should respond when either the axial VR or limb VR is stimulated. Therefore, an axial root was stimulated to see if there was a response from either another axial VR or a limb VR and/or simultaneous axial and limb VR output (Fig. 23). Indeed, in the control condition, stimulation of an axial VR could evoke a simultaneous response 82% ±8.2SEM of the time; this decreased significantly to 15% ±15SEM of the time in drug, and did not wash (5% ±5SEM) ($F=16.51$; $p<0.01$; $n=5$) (Fig. 23 Bi-Biii, E). Likewise, the total number of successful elicited episodes with simultaneous axial and limb output in a 20-minute period also decreased significantly in the drug and did not wash (control: 3.8 episodes ±0.58SEM, drug: 0.6 episodes ±0.6SEM, wash: 0.2 episodes ±0.2SEM) ($F=15.78$, $p<0.01$, $n=5$). This must be due to a failure of *both* the axial and limb VR output, as each individually decreased significantly to similar levels in the drug and neither washed (Fig. 23 F-G) (% success axial only output: control: 82% ±8.2SEM, drug: 15% ±15SEM, wash: 5% ±5SEM; $F=16.51$, $p<0.01$, $n=5$) (% success limb only output: control: 88.7% ±7.9SEM, drug: 15% ±15SEM; drug 5% ±5SEM; $F=20.09$, $p<0.01$, $n=5$). Therefore, stimulation of an axial VR in the presence of gap junction block reduced both axial and limb VR output, but when output occurred, it remained simultaneous.

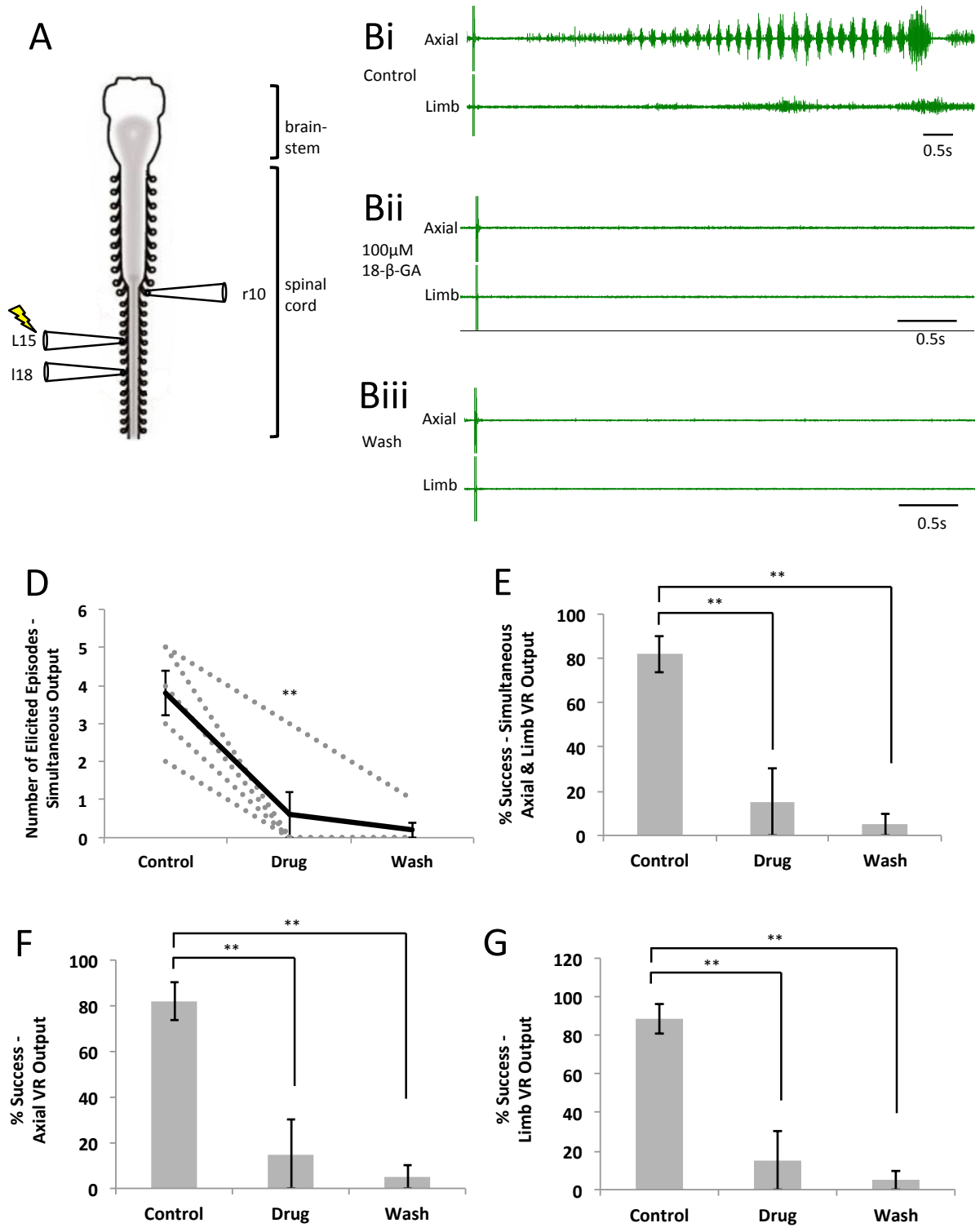

Fig. 23 Electrically evoked fictive locomotor responses of the pro-metamorphic *Xenopus laevis* axial and limb spinal cord in the presence of the gap junction blocker 18-β-glycyrrhetinic acid (18-β-GA; 100µM). (A) Schematic of the pro-metamorphic isolated brainstem/spinal cord preparation with a glass suction stimulating electrode (denoted by the lightning bolt) on the an axial ventral root, and glass suction recording electrodes on a tail ventral motor root and a limb ventral motor root. (Bi-iii) Representative extracellular recordings of a fictive locomotor ventral root (simultaneous axial and limb) activity from a single preparation in control, drug and wash conditions. (D) Number of elicited episodes (simultaneous axial and limb response) in a 20 minute period is significantly decreased by application of the gap junction blocker ($F=16.51$; $p<0.01$; $n=5$). (E-G) Percent success in eliciting an episode with simultaneous axial/limb VR output as well as individually axial VR only output or limb VR only output are significantly decreased by gap junction blockade/in the drug condition ($F=15.78$, $p<0.01$, $n=5$). Repeated measures ANOVA with Bonferroni correction; error bars represent ±SEM. ** = $p<0.01$.

IIIB XI. LIMB VR-EVOKED SIMULTANEOUS AXIAL AND APPENDICULAR LOCOMOTOR EPISODE OUTPUT IS SUCCESSFUL IN THE CONTROL CONDITION

Just as the stimulation of an axial VR can show coupling when simultaneous axial VR and limb VR output is observed, so too can the stimulation of a limb VR (Fig. 24). In all of the limb-VR stimulation attempts to elicit locomotor activity, simultaneous axial VR and limb VR output occurred on each occasion (Fig. 24 E (light grey bars; n=6)). When this is converted into percentages, simultaneous axial and limb output occurred with 100% success in all evoked episodes (Fig. 24 F (light grey bars; n=6)). To ensure this was not simply due to the stimulating electrode being located near enough to the spinal cord to stimulate it, a negative control was performed (Fig. 24 A) in which the stimulating electrode was located the same distance from the cord as in (Fig. 24 C), but the limb VR was released from the suction electrode. In this instance, as anticipated, no response occurred from either the axial VR or the limb VR (Fig. 24 B). That is, the number of evoked episodes with either axial VR, limb VR, or simultaneous output was zero (Fig. 24 E (black bars; n=6)), making the percent success in evoking episodes with either or both axial VR and limb VR response also 0% (Fig. 24 F (black bars; n=6)). This limb VR stimulation was not attempted in the drug condition due to time constraints. However, it is clear from both these stimulation attempts to the axial (Results section IIIB x) and limb VRs that there is functional coupling between the two systems in the control condition: that is, stimulation of one network recruits the other network to operate in concert.

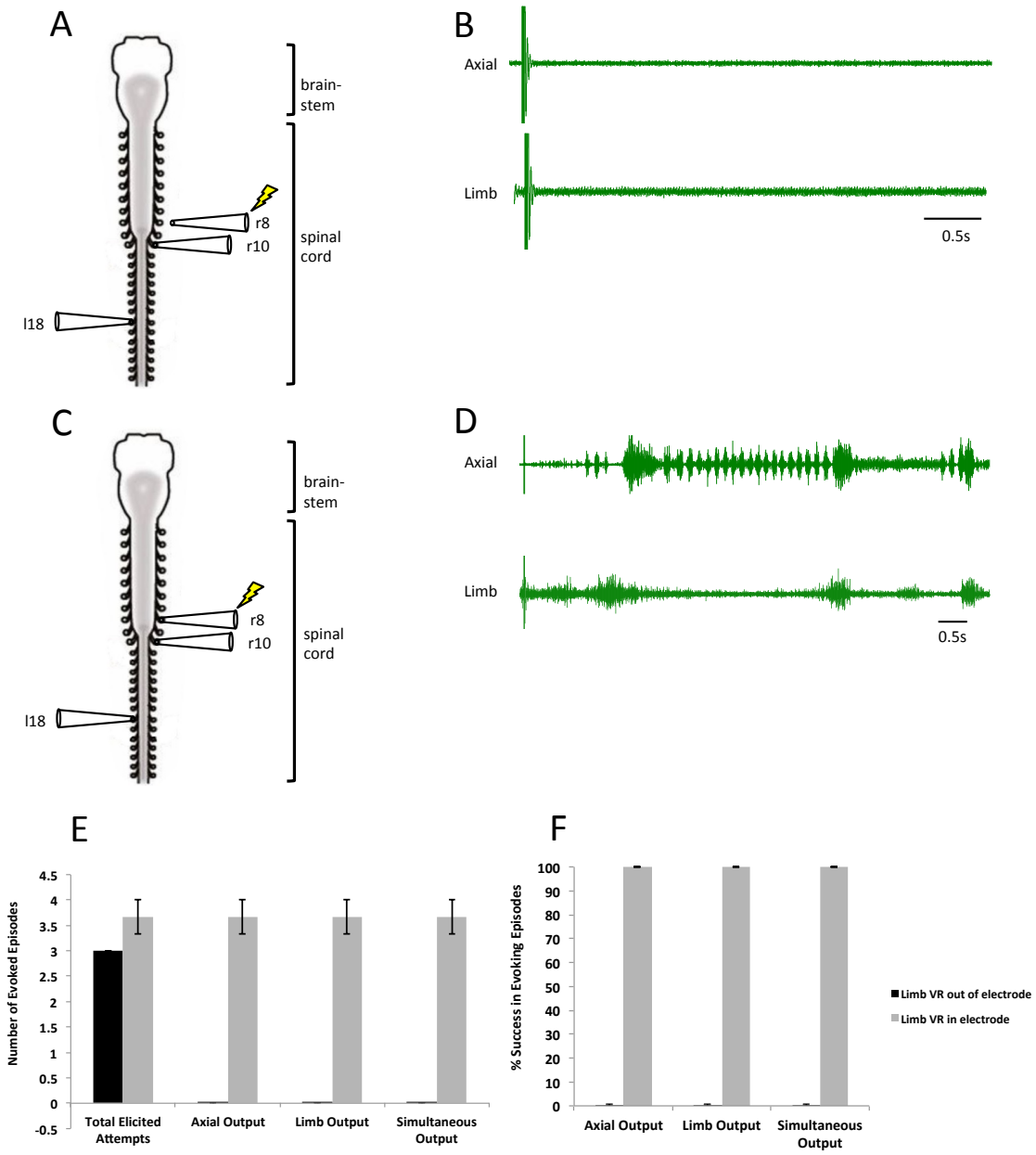

Fig. 24 Electrically elicited fictive locomotor response of the pro-metamorphic *Xenopus laevis* axial and limb (coupling) spinal cord in the control condition. (A) Schematic of the pro-metamorphic isolated brainstem/spinal cord preparation with a glass suction stimulating electrode (denoted by the lightning bolt) *outside* a limb ventral root; and glass suction recording electrodes on a tail ventral motor root and a limb ventral motor root. (B) Representative extracellular recordings of fictive locomotor ventral root activity from a single preparation in the control condition, showing both axial and limb output. (C) Schematic of the pro-metamorphic isolated brainstem/spinal cord preparation with a glass suction stimulating electrode (denoted by the lightning bolt) *on* a limb ventral root; and glass suction recording electrodes on a tail ventral motor root and a limb ventral motor root. (D) Representative extracellular recordings of fictive locomotor ventral root activity from a single preparation in the control condition, showing both axial and limb output. (E) Average number of elicited episodes per preparation in control from simultaneous axial and limb VR output, compared with the total number of attempts per preparation (n=6). (F) Percent success in eliciting an episode with simultaneous axial/limb VR output as well as individually axial VR only output or limb VR only output in the control condition (n=6). Error bars represent ±SEM.

IV. Discussion

IVa. Physiological Requirements During an Intense Metamorphic Change

Xenopus laevis is a well-established model to study vertebrate locomotion. The relatively simple neural circuitry of the spinal cord at early stages of development has allowed, especially in the past few decades, many studies decoding the basic mechanisms of locomotor physiology. Most of this work has been performed on very young hatchling larvae (~2 days old) (e.g., reviewed in Roberts, Li & Soffe, 2010; Roberts, Li & Soffe, 2012; Sillar, 1991) which exclusively use tail-based swimming. Far less is known about the extreme morphological changes and developmental transitions involved during metamorphosis, particularly with respect to the change in the locomotor strategy. While the entire *Xenopus laevis* body undergoes major morphological and biomechanical changes, those changes happening within the locomotor system are particularly intriguing, as the animal must be able to continuously locomote in and navigate through its environment throughout the entire process of tail regression, limb development and the accompanying reconfiguration of the underlying neural circuits; since the nervous system acts as an interface between an organism and its environment, this adaptability is distinctly different to many other animals undergoing metamorphosis in e.g., a cocoon (e.g., Blossman-Myer & Burggren, 2010). Due to the imperative reorganisation of the *Xenopus* tadpole CNS in the course of metamorphosis, this means that these tadpoles require significant neural plasticity and long-term adaptive and functional rewiring.

Metamorphosis necessitates that *Xenopus* tadpoles undergo a change in locomotor strategy from undulatory axial tail movements to successive bilateral appendicular flexor-extensor cycles, and this entails the desynchronisation and decoupling of axial and limb VR bursting

(Combes et al., 2004; reviewed in Sillar et al., 2008). At younger larval stages, *Xenopus* propels itself exclusively through its aqueous environment using its tail for anguilliform swimming (axial system). During metamorphosis, appendages form, and these exhibit a different rhythm (appendicular system); once metamorphosis is complete, *Xenopus* uses these limbs almost exclusively for movement, and the axial system is primarily used for postural control (Combes et al., 2004; Beyeler et al., 2008). However, during this metamorphic period, the axial and appendicular systems coexist in the spinal cord and can be utilised both individually and simultaneously (Beyeler et al., 2008). Of course the sensory afferents (e.g., new limb proprioceptive afferents) of these networks must also undergo extensive reconfiguration to be integrated with and participate in the diminishing tail swimming network and the superseding appendicular network, however that is outwith the scope of this work. This set of experiments sought to determine to what extent gap junctions (GJs) between neurons in the underlying spinal circuitry are responsible for this metamorphic change in locomotor strategy at a network level.

IVB. Discussion: Anatomy

IVB i. The Use of Dextran Dyes to Label MN Populations

Dextrans conjugated to different fluorophores were crushed into axial and appendicular muscle tissue, and travelled retrogradely via axons from the innervated muscle to mark MN somas in the spinal cord. Additionally, these molecules are amenable to fixation by paraformaldehyde, which is required for histological processing. Dextrans are hydrophilic water-soluble polysaccharides with low toxicity, and are normally quite large molecules (10,000-70,000MW). However, the smallest MW dextran dyes (under 3,000MW) were carefully chosen with the idea that it would be possible for at least some of the molecules to

pass through gap junction pores (~1,500kDa) (Sohl et al., 2005). The use of two different fluorophores, one crushed into the axial musculature and another crushed into the limb musculature, allowed for distinction of the MNs involved in axial versus limb muscle contraction.

IVB II. Location and Description of Axial and Appendicular MNs in the Spinal Cord

First it was established that the axial and appendicular MN pools which innervate post-otic myotomes 11 and 12 as well as the hindlimb flexor and extensor muscles coexist in the spinal cord at the level of the lumbar enlargement (VR 8-10) (Fig 8). Previous work (van Mier, 1986; Zhang et al., 2011) has shown that the MN somas innervating axial muscle blocks are located rostral to these myotomes they innervate, which was confirmed here; the dye can be seen travelling up the VRs to MNs located in a more rostral region of the cord (Fig. 8 and 10). Since the axial population and the limb population of MNs were filled with dextrans conjugated to different fluorophores (rhodamine, fluorescein), each population should be clearly distinguished and identified by a single colour (red or green). The axial and appendicular MN pools were found in discrete locations, with the axial pool being located medially and rostrally to the appendicular pool. The MNs from these pools also displayed different morphological characteristics: the axial MNs were larger and less numerous than the hindlimb MNs within each cluster.

However, there were some neurons which appeared as orange/yellow rather than strictly red or green, apparently caused by co-labelling of rhodamine and fluorescein within one soma (Fig. 8). That is to say, dye from both the axial and limb populations was present together in a small proportion of neurons, particularly in axial MNs. If colabelling is any

indication of coupling, it is important to note that these preparations from stages 52-58 exhibit colabelling, as this supports Combes et al. (2004) and Sillar et al.'s (2008) conclusions that extensive communication between the axial and appendicular systems occurs through to metamorphic climax which concludes at stage 63. Rauscent (2008) did not find any colabelling of axial and limb MNs using the same technique; however, the dextran conjugates used for those experiments were far larger (50-70,000MW), therefore experiments using smaller MW dextran conjugates produce novel results as one would not expect these larger MW dyes to pass through comparatively miniscule gap junction pores.

IVB III. PHYSICAL PARAMETERS: DIFFERENTIAL AXIAL AND APPENDICULAR MN SOMA SIZE AND RELATIVE LOCATION

The current findings show a significant difference between axial and appendicular MN soma size and cell number; MN somas innervating axial musculature are significantly larger but also fewer in number than MN somas innervating hindlimb musculature (Fig. 9). Several explanations could account for this.

First, the limb MNs are born after the axial MNs and are therefore more immature. Second, the roles and requirements of the axial and appendicular muscle tissue at this point in development are quite different: during this pro-metamorphic period, the animals still primarily locomote via axial undulations as opposed to hindlimb propulsions (Combes et al., 2004). In terms of the limb muscles, the types are more numerous and diverse (various flexors and extensors that comprise the whole limb and serving multiple joints). It is conceivable that finer and more variable movements are required for limb propulsion than axial undulations, and more but smaller MNs project to more numerous hindlimb muscle

fibres for the orchestration of this alternative and more complex locomotor strategy involving multiple muscles and multiple joints. That is, the muscle innervation fields of the appendicular MNs are smaller, with less metabolic demand and hence smaller somas. It would be interesting to quantify soma diameter and cell number in each population again in a later stage of development (e.g., at climax after the tail recedes) to see if these characteristics of each population have changed following the employment of a different locomotor strategy.

In characterising the physical parameters of MNs in the axial and hindlimb systems, a significant lateromedial and also rostrocaudal distance was found between the two populations (Fig. 9 c and d), meaning the 11^{th} and 12^{th} post-otic axial and appendicular MN clusters occupy a physically different space in the spinal cord, albeit adjacent to each other presumably to accommodate any interaction. Axial MN clusters were located medially in the cord to the appendicular clusters, and axial clusters were also located rostrally to the appendicular clusters. Though no difference was found in the (rostrocaudal) cluster length of either population. This means that axial clusters projecting to myotomes 11 and 12 occupy a rostral and medial position in the cord, whilst hindlimb clusters occupy a relatively lateral and caudal space in the cord. Since the cluster length is the same, but limb MNs are smaller and more numerous, it follows that the limb clusters contain a higher density of somas than the axial clusters. van Mier (1986) previously reported that axial MNs reside in the medial motor column (MMC) and appendicular MNs in the lateral motor column (LMC), which is in accord with the present findings on the lateromedial positioning of axial and limb somas in the spinal cord. These various parameters reveal that, although the axial and limb

systems are linked through colabelling, they each have their own distinct cell properties and locations to accommodate the two different locomotor strategies.

As MN somas innervating axial muscle blocks are located rostral to these myotomes, it follows that the portion of the axial network corresponding to post-otic myotomes 13 and beyond could be located more caudally and thus possess fewer interactions with the appendicular network, which is situated at the lumbar enlargement. This hypothesis should be tested in the future; indeed, the entirety of the individual axial and limb networks and the extent of their interconnectedness along the whole rostrocaudal length of the spinal cord could be probed via the same dye coupling protocol by applying one colour dye to the hindlimb and another to successively caudal axial myotomes, with the prediction that the degree of colabelling with axial myotomes located more caudally would be reduced.

In addition, if GJ pruning occurs with age, animals at the younger end of the metamorphic spectrum might display more colabelling between axial and appendicular MNs; Rauscent (2008) suggests that electrical coupling of the axial and limb systems might decrease with progressing metamorphosis due to the change in locomotor strategy. Therefore another useful experiment would be to separate the animals into smaller age groups (e.g., stages 52-54, 54-56, 56-58, and 58-60) with a high enough sample size for each, to determine any difference in the number of colabelled cells at various points in time during the switch.

Another experiment exclusively labelling the various muscles in the hindlimb could also be employed: if the flexors or extensors were labelled with different fluorophores to the axial myotomes, the differential axial and appendicular connectivity between these two distinct

limb muscles could be explored. These experiments would help to elucidate network interdependence and plasticity throughout the remarkable metamorphic period.

IVB iv. The Possibility of Using Lucifer Yellow in the Backfilling Technique

Although larger MW dyes are suitable for looking simply at the properties of the two axial and limb MN populations and soma properties in the spinal cord, their coupling would be better probed by using a dye that is more certain to pass freely through gap junctions, namely Lucifer Yellow (e.g., Piccolino et al., 1984). Lucifer yellow is more commonly used in a solution and injected directly into the soma during intracellular recording, as opposed to the dye crystals being packed into the muscle tissue and retrogradely transported via a backfilling technique. Backfilling Lucifer Yellow was attempted here with limited success, but not enough samples could be tested to perform any statistical analyses to obtain any meaningful results.

One clear example (Fig. 10 a) using only Lucifer Yellow (not in conjunction with dextran dyes) applied to the axial musculature shows both larger cells and smaller cells that have been successfully backfilled. It is unclear, however, if the smaller cells are actually part of a different (i.e., hindlimb) population, or if they are still axial cells with a smaller morphology, as there is natural variation in size. In order to determine this, the Lucifer Yellow would need to be used in conjunction with another small but differently-coloured dye, such as the small MW rhodamine-conjugated dextran dye used previously.

This was also attempted, but for some unknown reason, the appendicular axons consistently did not take up the Lucifer Yellow; however, Lucifer Yellow dye uptake was

more successful when crushed into the axial musculature. Therefore, Lucifer Yellow was applied exclusively to the axial 11th and 12th myotomes, and dextran-rhodamine to the limb (Fig. 10 b-d). One problem with this method is that the gold standard dye which permeates GJs is only applied to one of the two muscle locations (axial), and is not effective when applied to the appendicular muscles. Therefore, it would be possible to visualise Lucifer Yellow dye transfer from axial to appendicular MNs, but not the other way around. It is unclear as of yet if electrical rectification between neurons that are coupled by GJs plays a part in the bidirectional transfer of dye; if the dye carries some electrical charge, it could affect dye transfer between the two neurons.

In hindsight, an additional problem with the use of Lucifer Yellow as well as a dextran dye is that it is unclear what coupling looks like when these two dyes with different properties are mixed, as opposed to two dextran dyes simply with different conjugated fluorophores. It may not be as simple as a cell exhibiting coupling turning orange, depending on the different chemical properties of these dyes and how they mix. It is true that, while imaging on the microscope, the red and yellow channels can be turned off independently, so it would be possible to see if any given cell was filled with both dyes; however, it is potentially less straightforward than using the two dextran dyes. Future work should attempt to find a way to backfill appendicular MNs using Lucifer Yellow, and also ensure coupling is visible when pairing that dye with another dye (e.g., dextran-rhodamine).

IVB v. The Use of Gap Junction Blockers to Determine the Extent of Electrical Coupling Between and Within the Axial and Limb Systems

A natural extension of this backfilling technique to probe the extent of coupling as mediated by gap junctions would be to add gap junction blockers to the saline during the backfilling process. If gap junctions mediate the dye coupling, a decrease in the number of colabelled cells would be predicted in the presence of gap junction blockers. It is also foreseeable that spread within either the axial or appendicular system might also be hindered by blocking coupling within each system, such that fewer cells would be labelled in total.

This was performed in an undergraduate project in 2013 using fluorescein- and rhodamine-conjugated dextran dyes (not Lucifer Yellow): the addition of 200µM CBNX was found to significantly decrease the number of colabelled neurons in the cord (Wagner, 2013 unpublished). The plan for the current project was to replicate these results using Lucifer Yellow and dextran-rhodamine with a higher sample size using 200µM CBNX as well as the less "dirty" drug, 100µM 18-β-GA. As mentioned previously, a significant amount of time was spent attempting to label the appendicular MNs using Lucifer Yellow, and this proved to be unsuccessful. Twenty-six cords across three conditions (control, 200µM CBNX, 100µM 18-β-GA) were labelled, but only five produced spinal cords with both populations labelled. The gap junction blockers also seemed to degrade the tissue quite rapidly; the tissue was exposed to the drug for approximately 24 hours and became somewhat "mushy". This often resulted in cords that looked diffusely labelled but with no distinct cells; it is conceivable that the tissue integrity was compromised perhaps due to drug overexposure. Although this somehow did not seem to be an issue for the 2013 experiments, it might be worthwhile attempting less exposure time for the sake of maintaining tissue integrity.

The present attempts at gap junction block using Lucifer Yellow and dextran-rhodamine dye backfilling were therefore met with an extremely low success rate, which needs to be remedied in future attempts. It is critical to ascertain any change in the degree of coupling following the addition of gap junction blockers, with whatever dyes produce effective and reproducible results. This will make it possible to probe the anatomical coupling and functional coordination between the two separate pattern generating networks and functional rewiring which is at the root of this gradual change in locomotor strategy. Until then, it will not be possible to comment definitively on the specific role that gap junctions play in the co-labelling seen here between the axial and appendicular networks (Fig. 8 and 10). Nevertheless, these data provide evidence for dye coupling between a few members of the two motor pools, which is highly suggestive of GJ, and therefore electrical, coupling between the two systems. In addition to CBNX and 18-β-GA, other potential gap junction blockers that could be used include flufenamic acid (FFA) and Heptanol (Li et al., 2009). It is also recommended in the future to use a semi-automated (e.g., Fiji/ImageJ) software for cell counting rather than manual counting (in Zen2012).

IVB VI. THE IMPORTANCE OF ANATOMICAL COUPLING BETWEEN THE AXIAL AND LIMB SYSTEMS

The coexistence of both axial and appendicular MN networks in the lumbar region of the spinal cord and finding a link (i.e., co-labelling) between the two using anatomical evidence corroborates the circumstantial electrophysiological evidence of rhythmogenic coupling of the two systems during the metamorphic period (Combes et al., 2004). During this time, the hindlimb system adopts the rhythm of the axial system before diverging and developing its own separate rhythmic output pattern. But it is also important to note that the average number of co-labelled cells in the present study is small (5.33 axial and 2.83 limb). If this co-

labelling is due to electrical coupling, it would suggest that, perhaps not many strong electrical connections are needed for the limb CPG to adopt the axial CPG rhythm.

A precedent exists for the role of GJ coupling in rhythmic axial output in younger *Xenopus* (Li et al., 2009; Zhang et al., 2009), and GJs are even thought to exist between pMNs and sMNs of young zebrafish (reviewed in Lewis & Eisen, 2003) before they are pruned. Additionally, Song et al. (2016) have found in adult zebrafish that MN can actually play an active role in CPG output by retrogradely communicating with V2a interneurons responsible for rhythmic neural circuit activity. Thus it is conceivable that GJs would be a likely contender, or at least play some role, in the rhythmogenic coupling seen between the axial and appendicular systems during metamorphosis. However, more anatomical experiments to this effect will be required, as the critical experiments using gap junction blockers did not yield enough results.

IVB VII. OTHER IMPORTANT ANATOMICAL EXPERIMENTS FOR THE FUTURE

Aside from the continued use of backfilling to map out the rostrocaudal extent of axial-limb network interactions, as well as the use of gap junction blockers (CBNX, 18-β-GA, FFA, Heptanol) mentioned above, there are several other techniques which could be used to elucidate any role of GJs in the metamorphosing *Xenopus* spinal cord. For example, real-time calcium imaging could be a valuable tool: after backfilling these two MN pools using indicators which fluoresce with different wavelengths, it might be possible to identify if both the axial and limb MN fire simultaneously in the lumbar cord, implying an electrical connection.

In addition, immunocytochemistry could be used to identify which connexin (Cx) subunits comprising GJs are present during various stages of *Xenopus* development and metamorphosis. Cofre & Abdelhay (2007) have found a Cx43-like subunit that is present in oocytes and embryos of *Xenopus laevis*, and they believe this contributes to the establishment of the dorso-ventral axis. However, it would be important to determine if any other Cx subunits exist in the *Xenopus* spinal cord, and if and how these subunits vary across metamorphosis and ontogeny in general. The lab of Dr HongYan Zhang (University of Edinburgh) is attempting to identify the Cx subunits which exist in the NF stages 37/38 and 42 tadpole spinal cord; if these experiments are successful, attempts will then be made to identify Cx subunits in the metamorphosing animal spinal cord. This would not only establish that GJs are present in the cord, but it might also be possible to visualise if these exist in clusters, for example, near the lumbar enlargement where it is proposed the electrical connections between the axial and limb systems take place.

IVc. From Anatomy to Physiology

The anatomy described previously can give insights into morphological features of the networks and their cells, but complementary physiological studies are required to elucidate the functional properties of the coupling seen between the axial and appendicular systems. Therefore, extracellular motor ventral root electrophysiology was performed on pro-metamorphic animals (stages 55-58) using established *in vitro* isolated preparations of the *Xenopus laevis* brainstem/spinal cord (Combes et al., 2004). These preparations remain viable for hours and even days, and generate spontaneous and evoked motor output, which is similar to that normally inciting locomotion *in vivo*. This is termed “fictive locomotion”, as the ventral roots have been severed from the muscles to which they project, but these

efferent motor signals to the muscles can still be recorded via extracellular glass suction electrodes. In pro-metamorphic stages 55-58, the limbs are motile; but these stay in an extended position against the body during locomotor episodes, as the tail and torso remain the primary generators of thrust. The practical significance of this gradual change in locomotor strategy comes from the fact that the tadpole changes from a mainly sessile animal (stages ~43-45) to a filter feeder which is continuously active and swimming, meaning that the tail is more or less constantly engaged during the entirety of metamorphosis. During this transitory pro-metamorphic period, the forelimbs are just appearing from their protective skin pouches and thus are not involved in forward propulsion. It is during this period that the hindlimbs increase in power and functional independence; they eventually generate extension/flexion cycles which clearly differ from the tail-based rhythm (Fig. 20). Thus motor output from both the axial and hindlimb generators can be observed and compared by placing axial and limb VR in separate glass suction recording electrodes (Combes et al., 2004; Rauscent et al., 2006).

The physiology experiments described in this thesis first explore the role of gap junctions within the axial system itself: two gap junction blockers (100 and 200µM 18-β-GA (n=7 and n=5); 200µM CBNX (n=10)) were applied to study their effects upon both electrically-evoked and spontaneous fictive locomotor preparations with output being recorded from axial VR 17-20 (or 12-20 to measure left-right alternation and rostrocaudal delay). The lower concentration (100µM 18-β-GA) yielded differential burst parameters in the axial VR output; this in addition to the fact that 18-β-GA is considered to have fewer off-target effects than CBNX, the parameters of limb VR output and axial-limb network coupling were then also explored in the presence of 100µM 18-β-GA (n=5) only. Animals at pro-metamorphic stages

53-58 were chosen for axial-only output experiments and stages 55-58 were chosen for limb and coupling output experiments. The latter were chosen because Combes et al. (2004) proposed that spinal cords in intermediate metamorphic stages (54-63) exhibit the co-existence of two different rhythm-generating capabilities, with stage 58 being the pivotal stage at which axial and hindlimb motor bursting central pattern-generating and co-ordinating circuitry remains shared, before gradually becoming segregated. Combes et al. (2004) demonstrate that this limb VR dissection is possible at stages younger than 55, however the minuscule size of the roots and the fact that they are embedded in muscles of the small and freely moving hind limb makes dissections at stages younger than 55 too technically challenging for someone with less experience. For the coupling experiments, axial output was again measured from VR 17-20, with simultaneous limb output measured from either VR 9 or 10.

IVD. DISCUSSION: PHYSIOLOGY

IVD I. CHARACTERISATION OF LOCOMOTOR OUTPUT IN METAMORPHOSING XENOPUS TADPOLES

It is well-documented in hatchling *Xenopus* embryos (stage 37/38) that a CPG network producing rhythmic locomotor output is distributed along the hindbrain and rostral spinal cord (e.g., Roberts et al., 2008). This CPG activates MNs in a well-coordinated sequence, which, in turn innervates segmented axial swimming muscles, producing a characteristic left-right pattern across the body with a brief rostrocaudal delay, ultimately giving rise to undulations propelling the animal forward through its aqueous environment (e.g., Tunstall & Sillar, 1993). Extensive work has been done on the swimming CPGs of these younger animals (stages 37/38 – 42) and all of the types of neurons and their inter-connectivity within the network have been described, which ultimately gives rise to this type of

locomotion (described in Introduction section Ic i). The understanding of interactions giving rise to similar movements during pre-metamorphosis and metamorphosis have begun to be explored (e.g., Combes et al., 2004; Rauscent et al., 2006; reviewed in Sillar et al., 2008) but are less well-known, especially with regard to the introduction of the appendicular system during this critical period and its brief co-option of the axial rhythm before being able to generate its own independent rhythm. Electrical coupling seemed a likely candidate for the functional coupling of these two networks, as gap junctions are important in the *Xenopus* axial CPG at younger stages (Li et al., 2009; Zhang et al., 2009), and they appear to link primary and secondary MN networks in other vertebrates such as zebrafish (Saint-Amant & Drapeau, 2001). Therefore, gap junction blockers were applied to assess the possible role of electrical connections within and between pre-metamorphic *Xenopus* axial and limb networks.

IVD II. GAP JUNCTION BLOCK PRODUCES A SLOWER EVOKED AXIAL RHYTHM

Both evoked and spontaneous axial VR output display left-right alternation and a rostrocaudal delay (Figs. 11 & 16), in accordance with the current literature (Combes et al., 2004; Rauscent, 2006; Currie, 2013). Electrical stimulation of the optic tectum via a glass suction electrode was sufficient to evoke this rhythmic output (Fig. 11), as in Currie (2013). Similar stimulation techniques have been used in zebrafish (Kyriakatos et al., 2011). Intervals between the trains of optic tectum stimuli used to trigger fictive swimming were based on the fact that the preparation requires time to recover from previous network activity. This is likely due to the hyperpolarisation of the membrane potential of spinal neurons (Zhang & Sillar, 2012): CPG network activity results in neuronal firing, which leads to increased intracellular sodium. This sodium is extruded by increased Na^+/K^+ pump

activity, which leads to a hyperpolarisation of the membrane potential (ultraslow afterhyperpolarisation, termed usAHP), causing this network to become less excitable until it has recovered (this takes approximately one minute in younger animals). Currie (2013) has found in pro-metamorphic preparations, an appropriate interval for full recovery takes even longer, at least two minutes. Since the evoked rhythmic pattern here was consistent with established output for metamorphic preparations (e.g., Combes et al., 2004; Rauscent et al., 2006; Currie, 2013), gap junction blockers (100 and 200µM 18-β-GA (n=7 and n=5); 200µM CBNX (n=10)) were applied. As described by others (Li et al., 2009; Zhang et al., 2009), in stages 37/38 and 42 animals, there is a time-dependency to the effects of the gap junction blocker 18-β-GA; the block takes approximately 30-35 minutes to become stable. Therefore, the effects were quantified after a period of 35-40 minutes following drug application.

With the addition of both CBNX and the lower concentration of 18-β-GA, burst durations in evoked preparations significantly increased, meaning the rhythm slowed; this increase in burst duration was by ~32% for CBNX and ~37% for the lower concentration of 18-β-GA, which are comparable. In the case of 18-β-GA, and the cycle period significantly increased as well as the burst duration (therefore no significant change in burst proportion) (Figs. 12 & 13), whereas with CBNX, only the burst duration increased, but this was not enough to increase the burst proportion as well ($p = 0.08$) (Fig. 15). These differences are most likely accounted for by the fact that CBNX is known to have off-target effects; therefore, it is prudent to rely more on the results from 100µM 18-β-GA. A higher concentration of 18-β-GA (200µM) was then applied to assess whether the effects increase with dose. However, this concentration appeared to be exceed the upper limit to elicit any response at all in the

drug condition; no episodes could be elicited in drug to analyse burst parameters. The partial wash (Fig. 14) indicates the preparations did not experience a lethal dose of the drug at this concentration. These data suggest that metamorphic axial CPG output is in part regulated by GJs, and with a severe enough block, signal transmission to the muscles is abolished altogether. However, it is possible that this higher 200µM dose inhibited the activation pathway from the optic tectum stimulus and therefore was not affecting the CPG output directly. It would be interesting in the future to apply both 50µM and 150µM 18-β-GA to further explore the dose dependency of this particular drug. It would also be important to test a wider range of GJ blockers (e.g., flufenamic acid (FFA), heptanol, as in Li et al., 2009). Currie (2013) implemented a negative control, whereby the *in vitro* preparation was simply left in the control saline condition for several hours, and found no significant changes over time in burst or episode parameters; Combes et al. (2004) have also found this preparation to be viable for over 24 hours. This is noteworthy, since the effects of CBNX and 18-β-GA can be difficult to wash off, so it strengthens the argument that the effects seen are actually drug effects rather than simply the passage of time or the preparation degrading.

Li et al. (2009) and Zhang et al. (2009) have reported an increase in burst duration in younger (stage 37/38) *Xenopus* in the presence of GJ blockers, that is most likely due to a disruption in synchronisation of spike activity among CPG neurons, including MNs, resulting in more erratic MN firing. Specifically, Li et al. (2009) suggested the dIN-dIN connections were altered in GJ blockade at younger larval stages. The resulting activity recorded at stage 37/38 is similar to rhythmic patterns seen in the control condition of stage 42 animals, with addition of gap junction blockers at stage 42 having no further significant effects on burst

duration. This implies that pruning and/or neuromodulation of gap junctions contributes significantly to the maturation of the axial system between stages 37/38 to 42. While the burst duration in metamorphosing animals also increased with gap junction block, this may serve a different purpose than in the younger counterparts. Perhaps this is indicative of another period of extensive re-wiring and pruning, leading to a resurgence of electrical coupling in the locomotor system, namely between the axial and appendicular systems. It is not certain whether dINs play the same role at this later stage in development (although Currie (2013) presents some evidence for dINs having similar firing patterns at metamorphic stages to younger animals (n=1)); this could be determined in future by whole-cell recordings as in Li et al. (2009).

IVD III. GAP JUNCTION BLOCK SIGNIFICANTLY REDUCES OR ABOLISHES SPONTANEOUS ACTIVITY

While results from experiments on fictive swimming evoked by optic tectum stimulation provide some insight into the control of CPG output, spontaneous activity can reveal a nuanced version of similar information as this output is more naturally occurring and therefore unaffected by external input (i.e., stimulation). Specifically, supra-spinal control centres (e.g., the mesencephalic locomotor region (MLR)) are responsible for initiating locomotor episodes; so any increase or decrease in episode frequency could be due to activation or deactivation of such higher centres. This is controlled for in stimulated preparations, as episodes are elicited at regular intervals via e.g., optic tectum stimulation. Although it is not entirely clear how optic tectum stimulation initiates locomotor episodes, it could be that the optic tectum projects to the MLR or simply activates reticulospinal centres in the hindbrain directly instead (Currie, 2013).

With both the addition of CBNX and the lower concentration of 18-β-GA (100μM), spontaneous episode occurrence first sharply increased for approximately 20-25 minutes, then significantly decreased or was abolished in some instances (Fig. 17 & 18) thereafter. This same sharp increase and decrease in episode frequency has also been observed in with younger animals (Wenchang Li, personal communication, 2015). Since the increased frequency of spontaneous episodes occurs before the GJ block is fully established (~35min), this fictive locomotor behaviour cannot be attributed to the action of any GJ block; rather, this is thought to be due to undesired and more rapid off-target effects of the drug (Wenchang Li, personal communication, 2015). A partial wash off of the effects of these two drugs demonstrates that the preparations were still alive and functional with respect to locomotor rhythm generation. However, with the addition of the higher concentration of 18-β-GA, this profile of episode frequency was not the same: it actually decreased with drug application, before being abolished altogether as the drug period progressed (Fig. 19). This is likely due to the fact that 200μM 18-β-GA is too high a concentration to use (as seen with the evoked experiments), and so results from 100μM 18-β-GA should be more trusted instead. Since all concentrations of both drugs used abolished activity in most preparations, it might be useful in the future to see if lower concentrations (e.g., 50μM 18-β-GA) yield some activity in the drug condition, such that the spontaneous burst and episode parameters can be quantified in the presence of GJ block, in addition to episode occurrence.

Thus, GJ block inhibited network output by reducing the number of episodes after 35 minutes of drug exposure, and this is likely due to an inhibitory effect on supra-spinal centres; alternatively, it could be that this block reduces the excitability of the spinal CPG, such that descending inputs from supra-spinal centres are not sufficient to activate the

spinal CPG in order to produce rhythmic output. To dissect where exactly this effect originates, split-bath experiments would need to be employed, whereby the drug is applied either to either the brainstem or the spinal cord selectively. A decrease in episode occurrence when drug is applied to the brainstem would imply an effect on supra-spinal centres, whereas any effect when drug is applied to the spinal cord itself would suggest downstream CPG involvement.

IVD IV. GAP JUNCTION BLOCK HAS NO EFFECT ON EVOKED LIMB VENTRAL ROOT OUTPUT

Simultaneous axial and limb VR output was successfully evoked via optic tectum stimulation in the brainstem/spinal cord preparation of stage 56-58 animals, as described in Combes et al. (2004) (Fig. 20). The limb burst duration (416.5ms ±90.3SEM, n=5) from stages 56-58 was significantly longer than the axial burst duration already described in this thesis (64.2ms ±5.7SEM, n=7) (Figs. 13 & 21). Combes et al. (2004) have also described a slower appendicular rhythm in comparison with the axial rhythm, with these recordings being made from individual flexor and extensor MNs, whereas here a recording was made more proximally to the spinal cord before the nerve bifurcated into flexor and extensor outputs. In most cases, only one burst occurred per episode, therefore, cycle period was not able to be calculated. Limb burst duration and episode duration did not appear to be affected by gap junction block (100µM 18-β-GA) (Fig. 21); in all five preparations, the burst amplitude decreased, however this was not statistically significant, perhaps because the starting amplitudes of each preparation in control were quite variable. While amplitude is an indicator of a variety of characteristics, such as the electrical excitability of neurons, it is also an indicator of synaptic strength; so this decrease in limb VR amplitude supports the idea that there is some degree of electrical coupling between the axial and limb systems, with

the limb system coming decoupled from the axial system in the presence of gap junction blocker.

IVD V. GAP JUNCTION BLOCK DOES NOT DECOUPLE OPTIC TECTUM-EVOKED AXIAL AND LIMB VENTRAL ROOT OUTPUT

It is clear from these recordings that simultaneous output occurs from both axial and limb VRs when the optic tectum is stimulated. In intermediary stage 55/56 preparations (Fig. 20), it is evident that the limb system is not fully disengaged from the axial rhythm at this point: although there is a slower limb rhythm compared to the axial rhythm, there are shorter bursts inside this rhythm that coincide with the simultaneous axial output. This has also been seen in a stage 58 preparation in Combes et al. (2004). However, the other preparations used in the present study did not exhibit evidence of this axial rhythm still being present, although the recordings were made from stage 57-58 animals (Fig. 20). The fact that the limb exclusively displays the slower rhythm here indicates the limb CPG has already become independent from the axial CPG. Combes et al. (2004) suggest this independence occurs closer to stage 60-61, so it is unclear exactly why the stage 57-58 preparations here appear functionally more mature. During this transitional period, it is possible that there is some individual variation in the speed with which the limb CPG becomes independent from the axial CPG, as seen between the two stage 55/56 preparations; it could also suggest a difference in the accuracy of staging, with Combes et al. (2004) erring on identifying animals on the older side compared to the present study. Additionally, it is known in younger animals that rearing conditions, for example, temperature, can affect the rate of neural and circuit development: rearing in cooler conditions, for example, can allow the body to appear at stage 42, but the spinal locomotor

system can appear to operate at e.g., stage 45, as if it developed at a faster rate (Laurence Picton, personal communication, 2016). Perhaps the tadpoles in the present study were reared under slightly different conditions to those used in Combes et al. (2004), as they have put forward stage 58 being the critical stage when central pattern-generating and co-ordinating circuitry remains shared before the functional segregation of the axial and limb CPGs.

The application of gap junction blocker to the optic tectum-stimulated preparations in the current study did not appear to affect the simultaneous axial and limb VR output. This could either be due to the location of stimulation: perhaps the descending pathways from the optic tectum to the axial and limb CPGs are independent at this point and do not contain any gap junctions. Alternatively, as these preparations may already exhibit an independent limb CPG, these findings may simply confirm that the functional separation is complete and if gap junctions had been present between the systems before, they are no longer.

IVD VI. GAP JUNCTION BLOCK PREVENTS OUTPUT OF AXIAL VR-EVOKED AXIAL AND LIMB VENTRAL ROOT OUTPUT

Both axial and limb VR stimulation yielded simultaneous axial and limb VR output (Figs. 23 & 24). This alone has important implications: first, that VR stimulation (input) can activate CPG output, and second, it implies central coupling of MNs to other neurons within the spinal cord. This has been under investigation and debate recently (reviewed in O'Donovan et al., 2010). Antidromic stimulation of motor axons in the developing spinal cord of the mouse and chick embryos has also been seen to trigger ipsilateral bursting within the respective spinal (limb) CPG, likely via interneurons transmitting VR excitation to spinal

networks (Hanson & Landmesser, 2003; Wenner & O'Donovan, 1999; Wenner & O'Donovan, 2001). Although those experiments focussed mainly on chemical transmission (such as the role of ACh), rather than GJs. This series of experiments in the current project represent a major novel outcome of this current project, showing that the coupling of axial MNs is sufficient to activate a *different* CPG for the limb VR in *Xenopus*, and vice versa. Thus, this strengthens Combes et al.'s (2004) hypothesis that there is a functional link between the axial and limb MN networks, and that CPG output can be transmitted in the direction of axial to limb. Although these experiments do not elucidate if the coupling is exclusively electrical (it seems likely that mixed chemical and electrical synapses are responsible (Perrins & Roberts, 1995; reviewed in Pereda, 2014)), they do show that there must be bidirectional synaptic coupling.

Axial VR-stimulated axial and limb VR output was further tested in the presence of gap junction block (100µM 18-β-GA) (Fig. 23). Simultaneous axial and limb VR output significantly decreased in the presence of the gap junction blocker, and this was due to neither root responding; that is, when there was a response, the axial and limb VRs still responded simultaneously. But the incidence of a response simply decreased in the drug and the effect did not wash off significantly. This failure was not due to the preparation dying, as it still responded to optic tectum stimulation during this period (Fig. 22). Therefore, there must be electrical coupling at least within the axial CPG in pro-metamorphic animals, which, when blocked, prevents the rostrocaudal propagation of fictive locomotion. With this disabled due to the GJ block, it is conceivable that any further signal transmission, for example, to the limb CPG would also be impaired. Therefore, while

these results could indicate electrical coupling between the axial and limb systems that has been inhibited by GJ block, it cannot be asserted with certainty from this experiment alone.

V. Concluding Remarks

This work attempts to narrow the gap in knowledge of the way axial and limb CPGs are coupled and gradually gain independence in metamorphosing *Xenopus* tadpoles by using both anatomical and physiological techniques, with the intention of extending the results and questions posed by Combes et al. (2004). The functional coupling of these two systems via GJs is a plausible idea. GJ coupling has been shown to occur within the *Xenopus* axial CPG at various stages (e.g., Li et al., 2009; Zhang et al., 2009); in other vertebrates, GJs even appear to link sMNs to a pMN scaffold in zebrafish (Saint-Amant & Drapeau, 2001). Electrical coupling has also been documented in the adult goldfish spinal cord (Fetcho & Faber, 1988), and electrical coupling synchronises firing of MNs in the same motor pools in the neonatal mammalian spinal cord (Tresh & Kiehn, 2000). Indeed, electrical coupling is a firmly-established method of synchronisation in various CNS regions, for example in the neonatal rat brainstem to synchronise breathing rhythms (Rekling et al., 2000), as well as in a variety of regions in the adult brain: for example in the neocortex (Galarretta & Hestrin, 1999), cerebellum (Mann-Metzer & Yarom, 2000) and hippocampus (Draguhn et al., 1998). Furthermore, a novel role for gap junctions within the zebrafish CPG has even been determined very recently: rather than MNs simply being passive recipients of network signals to the muscles, GJs allow MNs and V2a interneurons to form functional ensembles which play an active part in neural circuit output (Song et al., 2016). Thus GJs perform pivotal roles in CPGs, which are integral to motor output.

While electrical coupling of the axial and limb CPGs via GJs during *Xenopus* metamorphosis remains a tantalising theory, the results shown here indicate they play only a contributory role. Although ideas for many future experiments have been suggested throughout this work, there are a few key directions: it will be critical to run more anatomical backfilling experiments using dyes that produce a reliable success, with a variety of gap junction blockers. In terms of physiology, simultaneous extracellular axial and limb VR recordings of younger pre-metamorphic (e.g., 54-56) stages will need to be explored in the presence of gap junction blockers as well, ensuring in the control condition that the limb VR output has still co-opted the axial CPG rhythm: it will be useful to observe both spontaneous output as well as output evoked from the optic tectum and axial and limb VRs. In addition, intracellular patch clamp recordings from cells in the axial and limb populations could also indicate coupling and the extent of GJ involvement and the recent development of a suitable *in vitro* preparation (Currie, 2013,) now makes this feasible.

However, there are other biological phenomena especially in developing systems that could explain how the *Xenopus* tadpole limb CPG utilises the axial CPG as a functional scaffold before segregating at the conclusion of metamorphosis, for example the switch of GABA and glycine from depolarising to hyperpolarising transmitters during ontogeny due to the differential expression of NKCC1 and KCC2 transporters (reviewed in Ben-Ari et al., 2007; refer to Introduction section Ia). Clearly, although the presence and importance of functional coupling between the axial and limb CPGs during metamorphosis is evident, and GJs likely play a contributory role, a full understanding their mode(s) of coupling and routes to independence of the limb and axial CPGs is still at an early stage.

REFERENCES

Ben-Ari Y, Gairarsa JL, Tyzio R, Khazipov R, 2007. GABA: a pioneer transmitter that excites immature neurons and generates primitive oscillations. *Physiology Review*, 87(4), 1215-84.

Bishop CD & Brandhorst BP, 2003. On nitric oxide signalling, metamorphosis, and the evolution of biphasic life cycles. *Evolution and Development*, 5(5), 542-550.

Blossman-Myer B & Burggren WW, 2010. The silk cocoon of the silkworm, *Bombyx mori*: Micro structure and transmural diffusion of oxygen and water vapor. *Comparative Biochemistry and Physiology*, 155(2), 259-263.

Brown TG, 1914. On the nature of the fundamental activity of the nervous centres; together with an analysis of the conditioning of rhythmic activity in progression, and a theory of the evolution of function in the nervous system. Journal of Physiology (London), 48, 18-46.

Clemens S, Belin-Rauscent A, Simmers J & Combes D, 2012. Opposing modulatory effects of D1- and D2-like receptor activation on a spinal central pattern generator. *Journal of Neurophysiology*, 107, 2250-2259.

Combes C, Merrywest SD, Simmers J & Sillar KT, 2004. Developmental segregation of spinal networks driving axial- and hindlimb-based locomotion in metamorphosing Xenopus laevis. *The Journal of Physiology*, 559, 17-24.

Connors BW & Long MA, 2004; Electrical synapses in the mammalian brain. *Annual Review of Neuroscience*, 27, 393-418.

Currie SP, 2013. *A behaviourally related developmental switch in nitrergic modulation of locomotor rhythmogenesis in larval Xenopus tadpoles.* PhD Thesis. University of St Andrews: United Kingdom.

Currie SP, Doherty GH, Sillar KT, 2016. Deep-brain photoreception links luminance detection to motor output in *Xenopus* frog tadpoles. PNAS 113(21), 6053-6058.

Draguhn A, Traub RD, Schmitz D & Jefferys JGR, 1998. Electrical coupling underlies high-frequency oscillations in the hippocampus *in vitro*. Nature, 394, 189-192.

Eaton RC, Bombardieri RA & Meyer DL, 1977. The Mauthner-initiated startle response in teleost fish. *Journal of Experimental Biology*, 66(1), 65-81.

Eisen JS, 1991. Motoneuronal development in the embryonic zebrafish. *Development*, 2, 141-7

Fetcho JR, 1986. The organization of the motoneurons innervating the axial musculature of vertebrates. I. Goldfish (*Carassius auratus*) and Mudpuppies (*Necturus maculosus*). *The Journal of Comparative Neurology*, 249, 521-550.

Fetcho JR & Faber DS, 1988. Identification of motoneurons and interneurons in the spinal network for escapes initiated by the mauthner cell in goldfish. Journal of Neuroscience, 8(11), 4192-4213.

Galarreta M & Hestrin S, 1999. A network of fast-spiking cells in the neocortex connected by electrical synapses. Nature, 402(6757), 72-75.

Galton VA, 1992. The role of thyroid hormone in amphibian metamorphosis. *Trends in Endocrinology and Metabolism*, 3(3), 96-100.

Goodenough DA & Paul DL, 2009. Gap Junctions. Cold Spring Harbor Perspectives in Biology.

Grillner S & Zangger P, 1979. The central generation of locomotion in the low spinal cat. Experimental Brain Research, 34(2), 241-261.

Hackett JT, Cochran SL & Brown DL, 1979. Functional properties of afferents which synapse on the Mauthner neuron in the amphibian tadpole. Brain Research, 176(1), 148.

Hanson MG & Landmesser LT, 2003. Characterization of the circuits that generate spontaneous episodes of activity in the early embryonic mouse spinal cord. Journal of Neuroscience, 23, 587-600.

Hinckley CA & Ziskind-Conhaim L, 2006. Electrical coupling between locomotor-related excitatory interneurons in the mammalian spinal cord. *Journal of Neuroscience*, 26(33), 8477-83

Kahn JA, Roberts A & Kashin SM, 1982. The neuromuscular basis of swimming movements in embryos of the amphibian *Xenopus laevis*. Journal of Experimental Biology, 99, 175-184.

Kaila K, Price TJ, Payne JA, Puskarjov M & Voipio J, 2014. Cation-chloride cotransporters in neuronal development, plasticity and disease, 15(10), 637-654.

Kiehn O & Tresch MC, 2002. Gap junctions and motor behaviour. *Trends in Neuroscience*, 25, 108–115

Kudo N, Nishimaru H & Nakayama K, 2004. Developmental changes in rhythmic spinal neuronal activity in the rat fetus. Progress in Brain Research, 143, 49-55.

Lewis KE & Eisen JS, 2003. From cells to circuits: development of the zebrafish spinal cord. *Progress in Neurobiology*, 69, 419-449.

Li W, 2015. Personal communication.

Li W, Perrins R, Soffe SR, Yoshida M, Walford A & Roberts A, 2001. Defining classes of spinal interneuron and their axonal projections in hatchling Xenopus laevis tadpoles. *Journal of Comparative Neurology*, 441, 248-265

Li W, Higashijima S, Parry DM, Roberts A & Soffe, SR, 2004. Primitive roles for inhibitory interneurons in developing frog spinal cord. *The Journal of Neuroscience*, 24(25), 5840-8

Li W, Soffe SR & Roberts A 2004. A direct comparison of whole cell patch and sharp electrodes by simultaneous recording from single spinal neurons in frog tadpoles. *Journal of Neurophysiology* , 92(1), 380-6

Li W, Soffe SR, Wolf ES & Roberts A 2006. Persistent responses to brief stimuli: feedback excitation among brainstem neurons. *The Journal of Neuroscience*, 26(15), 4026-4035

Li W, Roberts A & Soffe SR 2009. Locomotor rhythm maintenance: electrical coupling among premotor excitatory interneurons in the brainstem and spinal cord of young *Xenopus* tadpoles. *The Journal of Physiology*, 587(8), 1677-1693

Li W, Merrison-Hort R, Zhang HY & Borisyuk R, 2014. The generation of antiphase oscillations and synchrony by a rebound-based vertebrate central pattern generator. *The Journal of Neuroscience*, 34(17), 6065-77

Liddell EGT & Sherrington CS, 1925. Recruitment and some other factors of reflex inhibition. Proceedings of the Royal Society of London B, 97, 488-518.

Mann-Metzer P & Yarom Y, 2000. Electrotonic coupling synchronizes interneuron activity in the cerebellar cortex. Progress in Brain Research, 124, 115-122.

Marder E, 2009. Electrical synapses: rectification demystified. *Current Biology*, 19(1), 34-5

McDearmid JR, Scrymgeour-Wedderburn JF, Sillar KT, 1997. Aminergic modulation of glycine release in a spinal network controlling swimming in Xenopus laevis. *Journal of Physiology*, 503 pt 1, 111-7

McLean DL, Merrywest SD & Sillar KT 2000. The development of neuromodulatory systems and the maturation of motor patterns in amphibian tadpoles. *Brain Research Bulletin*, 53(5), 595-603

Nieuwkoop, P. D. *&* Faber, J., 1956*. Normal Tables for Xenopus Laevis (Daudin).* North Holland, Amsterdam.

Nishimaru H & Kudo N, 2000. Formation of the central pattern generator in the rat and mouse. *Brain Research Bulletin*, 53(5), 661-9

O'Donovan MJ, Bonnot A, Mentis GZ, Chub N, Pujala A & Alvarez FJ, 2010. Mechanisms of excitation of spinal networks by stimulation of the ventral roots. Annals of the New York Academy of Sciences, 1198, 63-71.

Oshima A, 2014. Structure and closure of connexin gap junction channels. FEBS Letters, 588(8), 1230-1237.

Pereda AE, 2014. Electrical synapses and their functional interactions with chemical synapses. *Nature Reviews Neuroscience*, 15(4), 250-63.

Pereda A, Triller A, Korn H & Faber DS, 1992. Dopamine enhances both electrotonic coupling and chemical excitatory postsynaptic potentials at mixed synapses. PNAS, 89(24), 12088-12092.

Pereda AE, Nairn AC, Wolszon LR & Faber DS. Postsynaptic modulation of synaptic efficacy at mixed synapses on the Mauthner cell. Journal of Neuroscience, 14(6), 3704-3712.

Perrins R & Roberts A, 1995. Cholinergic and electrical motoneuron-to-motoneuron synapses contribute to on-cycle excitation during swimming in Xenopus embryos. *Journal of Neurophysiology*, 73(3), 1005-12.

Perrins R & Roberts A, 1995. Cholinergic and electrical synapses between synergistic spinal motoneurones in the *Xenopus laevis* embryo. Journal of Physiology, 485(pt.1), 135-144.

Perrins R & Roberts A, 1995. Cholinergic contribution to excitation in a spinal locomotor central pattern generator in Xenopus embryos. *Journal of Neurophysiology*, 73(3), 1013-19.

Personius KE, Chang Q, Mentis GZ, O'Donovan MJ & Balice-Gordon RJ, 2007. Reduced gap junctional coupling leads to uncorrelated motor neuron firing and precocious neuromuscular synapse elimination. *PNAS*, 104(28), 11808-11813.

Piccolino M, Neyton J & Gerschenfeld HM, 1984. Decrease of gap junction permeability by dopamine and cyclic adenosine 3':5'-monophosphate in horizontal cells of turtle retina. Journal of Neuroscience, 4(10), 2477-2488.

Picton L, 2016. Personal communication.

Qu Y & Dahl G, 2002. Function of the voltage gate of gap junction channels: Selective exclusion of molecules. PNAS, 99(2), 697-702.

Ramanathan S , Combes D , Molinari M , Simmers J , Sillar KT, 2006. Developmental and regional expression of NADPH-diaphorase/nitric oxide synthase in spinal cord neurons correlates with the emergence of limb motor networks in metamorphosing Xenopus laevis. European Journal of Neurosience, 24(7)

Rauscent A, Le Ray D, Cabirol-Pol MJ, Sillar KT, Simmer J & Combes D, 2006. Development and neuromodulation of spinal locomotor networks in the metamorphosing frog. *Journal of Physiology Paris*, 100(5-6), 317-27

Rauscent A, 2008. *Remaniements fonctionnels des réseaux locomoteurs spinaux au cours du développement de l'amphibien Xenopus laevis en métamorphose*. PhD Thesis. L'Universitie Bordeaux: France.

Rauscent A, Einum J, LeRay D, Simmers J & Combes D, 2009. Opposing aminergic modulation of distinct spinal locomotor circuits and their functional coupling during amphibian metamorphosis. *Journal of Neuroscience*, 29(4), 1163-1174.

Rekling JC, Funk JG, Bayliss DA, Dong XW, Feldman JL, 2000. Synaptic control of motoneuronal excitability. Physiology Reviews, 80(2), 767-852.

Roberts A & Clarke JD, 1982. The neuroanatomy of an amphibian embryo spinal cord. *Philosophical transactions of the Royal Society of London B Biology*, 296 (1081), 195-212

Roberts A, van Mier P & Armstrong J, 1989. Development of early swimming in Xenopus laevis embryos: myotomal musculature, its innervation and activation. *Neuroscience*, 32(1), 113-26

Roberts A, Walford A, Soffe SR & Yoshida M, 1999. Motoneurons of the axial swimming muscles in hatchling *Xenopus* tadpole features, distribution, and central synapses. *The Journal of Comparative Neurology*, 411, 472-486.

Roberts A, 2000. Early functional organization of spinal neurons in developing lower vertebrates. *Brain Research Bulletin*, 53(5), 585-93

Roberts A, Li W & Soffe SR, 2010. How neurons generate behaviour in a hatchling amphibian tadpole: an outline. Frontiers of Behavioral Neuroscience, 4-16.

Roberts A, Li W, Soffe SR, 2012. A functional scaffold of CNS neurons for the vertebrates: the developing Xenopus laevis spinal cord. *Developmental Neurobiology*, 72(4), 575-84

Robertson JD, Bodenheimer TS & Stage DE, 1963. The ultrastructure of Mauthner cell synapses and nodes in goldfish brains. Journal of Cell Biology, 19, 159-199.

Rodino-Klapac LR & Beattie CE, 2004. Zebrafish *topped* is required for ventral motor axon guidance. *Developmental Biology*, 273, 308-320.

Rozental R, Giaume C & Spray DC, 2000. Gap junctions in the nervous system. Brain Research Review, 32(1), 11-15.

Saint-Amant L & Drapeau P, 2001. Synchronization of an embryonic network of identified spinal interneurons solely by electrical coupling. Neuron, 31(6), 1035-1046.

Sautois B, Soffe SR, Li W & Roberts A, 2007. Role of type-specific neuron properties in a spinal cord motor network. *Journal of Computational Neuroscience*, 23(1), 59-77

Shi YB. *From Morphology to Molecular Biology*. Wiley-Liss; New York: 2000. Amphibian metamorphosis

Shi YB, Ishizuya-Oka A, 2001. Thyroid hormone regulation of apoptotic tissue remodelling: implications from molecular analysis of amphibian metamorphosis. *Progress in Nucleic Acid Research and Molecular Biology*, 65, 53-100

Sillar KT, 1991. Spinal pattern generation and sensory gating mechanisms. Current Opinion in Neurobiology, 1(4), 583-589.

Sillar KT, Wedderburn JF, Simmers J, 1991. The development of swimming rhythmicity in post-embryonic Xenopus laevis. *Proceedings of Biological Science*, 1991, 246(1316), 147-53.

Sillar KT, Simmers J & Wedderburn JF, 1992. The post-embryonic development of cell properties and synaptic drive underlying locomotor rhythm generation in Xenopus larvae. *Proceedings of Biological Science*, 249(1324), 65-70.

Sillar KT, Wedderburn JF, Simmers J, 1992. Modulation of swimming rhythmicity by 5-hydroxytryptamine during post-embryonic development in Xenopus laevis. *Proceedings of Biological Science*, 250 (1328), 107-14.

Sillar KT, Woolston AM & Wedderburn JF, 1995. Involvement of brainstem serotonergic interneurons in the development of a vertebrate spinal locomotor circuit. *Proceedings of Biological Science*, 259(1354), 65-70.

Sillar KT, Combes D, Ramanathanan S, Molinari M & Simmers J, 2008. Neuromodulation and developmental plasticity in the locomotion of anuran amphibians during metamorphosis. *Brain Research Reviews*, 57(1), 94-102.

Sillar KT, Combes D, Simmers J, 2014. Neuromodulation in developing motor microcircuits. *Current opinion in neurobiology*, 29C, 73-81

Soffe SR, Roberts A, Li W, 2009. Defining excitatory neurons that drive the locomotor rhythm in a simple vertebrate: insights into the origin of reticulospinal control. *The Journal of Physiology*, 587, part 20, 4829-4844

Sohl G, Maxeiner S & Willeke K, 2005. Expression and functions of neuronal gap junctions. *Nature Reviews Neuroscience*, 6, 191-200

Song J, Ampatzis K, Bjornfors ER & El Manira A, 2016. Motor neurons control locomotion circuit function retrogradely via gap junctions. Nature, 529, 399-402.

Tornqvist K, Yan XL & Dowling JE, 1988. Modulation of cone horizontal cell activity in the teleost fish retina. III. Effects of prolonged darkness and dopamine on electrical coupling between horizontal cells. *Journal of Neuroscience*, 8(7), 2279-88.

Tresch MC & Kiehn O, 2000. Motor coordination without action potentials in the mammalian spinal cord. Nature Neuroscience, 3(6), 593-599.

Tunstall MJ & Sillar KT (1993). Physiological and developmental aspects of intersegmental coordination in Xenopus embryos and tadpoles. *Seminars in Neuroscience,* 5, 29–40

Tyrrell S, Schroeter S, Coulter L & Tosney KW, 1990. Distribution and projection pattern of motoneurons that innervate hindlimb muscles in the quail. *The Journal of Comparative Neurology*, 298, 413-430.

van Mier P, 1986. *The development of the motor system in the clawed toad Xenopus laevis*. PhD Thesis. Katholieke Universiteit: Belgium.

Wagner M, 2013. *The activity-dependent development of the locomotor system in Xenopus laevis larvae, and the anatomy of the axial- and limb-motoneuron networks during the metamorphic period.* Undergraduate Dissertation. The University of St Andrews: United Kingdom.

Wenner P & O'Donovan MJ, 1999. Identification of an interneuronal population that mediates recurrent inhibition of motoneurons in the developing spinal cord. Journal of Neuroscience, 19, 7557-7567.

Wenner P & O'Donovan MJ, 2001. Mechanisms that initiate spontaneous network activity in the developing chick spinal cord. Journal of Neurophysiology, 86, 1481-1498.

Westerfield M, McMurray JV & Eisen JS, 1986. Identified motoneurons and their innervation of axial muscles in the zebrafish. *The Journal of Neuroscience*, 6(8), 2267-2277.

Wilson JM, Hartley R, Maxwell DJ, Todd AJ, Lieberam I, Kaltschmidt JA, Yoshida Y, Jessell TM & Brownstone RMJ, 2005. Conditional rhythmicity of ventral spinalinterneurons defined by expression of the Hb9 homeodomain protein. *Neuroscience*, 25, 5710–5719

Zhang HY, Li W-C, Heitler WJ & Sillar KT, 2009. Electrical coupling synchronises spinal motoneuron activity during swimming in hatchling Xenopus tadpoles. *The Journal of Physiology*, 578, 4455-4466.

Zhang HY, Issberner J & Sillar KT, 2011. Development of a spinal locomotor rheostat. *PNAS*, 108(28), 11674-11679.